UNIONE EUROPEA
Fondo Sociale Europeo

Ministero dell'Università e della Ricerca

PON RICERCA E INNOVAZIONE 2014 - 2020

REACT EU

Università Ca'Foscari Venezia

PhD Program

in Environmental Science

37° Cycle

Research Thesis

Green Analytical Strategies for Integrated Screening of Emerging Contaminants

SSD: CHIM/01

PhD Coordinator
Prof. Dr. Enrico Bertuzzo

Supervisor
Prof. Dr. Andrea Gambaro

PhD Candidate
Francesco Fama
877784

La borsa di dottorato è stata cofinanziata con risorse del
Programma Operativo Nazionale Ricerca e Innovazione 2014-2020, risorse FSE REACT-EU
Azione IV.4 "Dottorati e contratti di ricerca su tematiche dell'innovazione"
e Azione IV.5 "Dottorati su tematiche Green"

Table of Contents

Abstract

The growing concern for public health and environmental protection has underscored the urgent need to develop analytical methodologies capable of monitoring environmental pollutants that enter the human body. Monitoring these compounds in biological fluids—such as urine and plasma—is particularly challenging, especially in regions with high environmental exposure, where economic, technical, and regulatory barriers hinder the implementation of systematic surveillance practices.

Although organizations such as the European Environment Agency (EEA) and the World Health Organization (WHO) have acknowledged the correlation between pollution and disease onset, analytical techniques—particularly chromatography coupled with mass spectrometry (LC-MS)—have been only occasionally applied to this understanding. In addition, the long time required for the analysis, especially due to time consuming sample pre-treatment, limit the large-scale or routine monitoring of population. On the basis of this requirement, portable sensor systems constitute an alternative approach for first screening before the application of confirmatory lab analysis only on selected samples.

This thesis addresses these challenges by proposing innovative analytical strategies for the monitoring of contaminants of emerging concerns (**CECs**) in complex biological matrices. In particular, the focus is on pesticides, namely glyphosate, and disinfection by-products, namely haloacetic acids (**HAAs**), two classes of compounds with known toxicological and environmental relevance, often associated with chronic exposure through contaminated water and food.

Chapter 1 presents a critical overview of the current state-of-the-art in sensing and chromatographic strategies for the detection of pesticides and HAAs, with a focus on the limitations of current technologies in large-scale epidemiological studies. It highlights how electrochemical sensors, while still limited in sensitivity and reproducibility compared to chromatographic techniques, offer great potential in terms of portability, miniaturization, and rapid *in situ* analysis. Integration between sensor-based and chromatographic approaches is identified as a promising path to combine rapid, low-cost screening with analytical reliability, improving the overall efficiency and accessibility of biomonitoring.

Chapter 2 describes the development of a paper-based electrochemical sensor platform based on paper for glyphosate detection in urine. The system integrates both sample pre-treatment and detection on a single support, reducing interference from further electroactive species present in solution, without the application of long pre-analytical procedures. This efficiency is ascribed to the porous structure of paper that can be exploited as a storage medium for reagents, enabling the in-situ execution of pre-treatment steps and with a minimal quantity of reagent needed. A direct comparison of advantages and disadvantages of both sensing and chromatographic method was carried out, following the White Analytical Chemistry criteria, introduced by Novak et al. in 2021.

To go deeper inside the study concerning the application of paper for the realization of chemical sensors, Chapter 3 describes the effectiveness of a sample pre-treatment strategy for protein removal, applied to paper-based analytical devices. The approach is based on the “salting-out” effect imparted by addition of ammonium sulfate, which is found to remove approximately 70% of total proteins in human urine, significantly reducing matrix effects and enhancing sensor performance. As a proof of concept of the sample pre-treatment proposed, the platform was applied to the detection of free tryptophan, a biomarker relevant to several pathological conditions.

Moving to the problems related to the analysis of disinfection by-products, Chapter 4 is dedicated to the development of effective methods for the detection of HAAs. In particular, the chapter discusses the development of a chromatographic method based on ion chromatography coupled with tandem mass spectrometry (IC-ESI-MS/MS) adapted from PM2.5 atmospheric aerosols by modifying the pre-analytical steps. Indeed, the biological matrices of interest pose several challenges such as the variability of the matrix composition or the presence of proteins and other organic molecules that can act as interferents. In parallel, a preliminary sensor-based strategy was explored, exploiting selective silver surface etched by trichloroacetic acids. Although this technique yielded promising results on bulk silver wires, its application to screen-printed silver-modified electrodes revealed significant limitations in terms of sensitivity and reproducibility, requiring further optimization for use in real biological matrices. The optimized device demonstrates good sensitivity and specificity for target analytes and matrix pretreatment in general, exemplifying its utility for potential real-time pollutant monitoring in complex biological matrices.

The thesis concludes with a reflection on the importance of sustainable analytical technologies—not only to reduce the environmental impact of laboratory activities, but also to address the growing issue of electronic waste. The integration of innovative devices and advanced pre-treatment techniques lays the foundation for scalable, efficient, and environmentally friendly biomonitoring tools. These findings can contribute to the development of more effective public health and environmental policies by providing a practical, accessible framework for pollutant detection and management.

Chapter 1: Introduction

The contents of this chapter are partially adapted from the review article "Pesticide Monitoring in Biological Fluids: Mapping the Gaps in Analytical Strategies", published in Talanta in 2023, in which I am one of the co-authors. The chapter aims to provide a comprehensive overview of the organic contaminants studied in this Thesis and of the analytical challenges associated with their detection. It critically examines how analytical methodologies — particularly consisting of chromatographic and sensor-based approaches — proposed for the analysis of environmental matrices can be adapted to enable the detection and quantification of these contaminants in biological fluids. The chapter offers a state-of-the-art perspective on available strategies and identifies key gaps that motivate the research presented in this thesis.

1.1 Emerging contaminants

The concept of *Contaminants of Emerging Concern* (**CECs**) has evolved considerably over the past few decades, driven by advancements in analytical chemistry that have enabled the detection of previously unrecognized pollutants in water, air, soil, and even biological fluids. CECs include a broad spectrum of substances such as pharmaceuticals, personal care products, industrial chemicals, microplastics, and disinfection by-products (**DBPs**) like haloacetic acids (**HAAs**). Unlike traditionally regulated pollutants, CECs present specific challenges due to their low concentrations, complex degradation pathways, potential bioaccumulation, and long-term toxicological effects [1]. The emergence of CECs as a scientific and regulatory focus can be traced back to the mid-20th century, when synthetic organic compounds began to be widely used in industrial and agricultural applications. While early regulations targeted persistent organic pollutants (**POPs**), like polychlorinated biphenyls (**PCBs**) and **DDT** (dichlorodiphenyltrichloroethane), by the 1980s researchers had begun identifying numerous unmonitored substances in the environment [2]. Over time, as industrial processes and consumer habits evolved, new classes of CECs were identified. Pharmaceuticals and personal care products emerged as significant pollutants due to their continuous release into the environment through wastewater effluents. Similarly, per- and polyfluoroalkyl substances (**PFAS**), widely used in non-stick coatings and firefighting foams, gained recognition as persistent and bio accumulative contaminants. Another major category includes microplastics, which have been

detected in marine environments, drinking water, and even human tissues, raising concerns about their long-term health implications [3]. Among these contaminants, DBPs gained prominence following the discovery of trihalomethanes (**THMs**) in chlorinated drinking water in 1974. This finding sparked widespread investigations into other potentially harmful DBPs, culminating in the identification of HAAs as the second most abundant class of DBPs in disinfected water [4]. The increasing complexity of drinking water treatment processes, combined with varying source water compositions, has led to the formation of an expanding array of DBPs, many of which remain unregulated and poorly characterized in terms of toxicity [5].

1.2 History and classification of Pesticides

In this thesis, pesticides are investigated as a first class of target compounds for the development of innovative, green analytical strategies for their detection in biological fluids. The European Commission (Directive 94/414/EEC) defines pesticides as "plant protection products." These chemical compounds (over 800), include herbicides, fungicides, insecticides, nematicides, and acaricides, and are used to control pest populations [6–9]. Since the Green Revolution of the 1950s, the application of pesticides in agriculture has been promoted to increase crop yields, as it was estimated that pest infestations could cause losses of up to 40% of total crop yields. For this reason, between the 1970s and 1990s, most governments encouraged the use of pesticides [10] without adequately monitoring their effects on the environment and human health [11]. The diversification in the mode of action and application rates of these chemicals has contributed to their global spread. The first concerns regarding pesticides toxicity arose in the early 1970s, with case studies on DDT, organophosphates, and pyrethroids, increasing public awareness of the risks associated with these chemicals [12]. As a result, regulations for presence of pesticides in the environment and in agricultural products were implemented, and maximum residue limits (**MRLs**), defined as the upper legal level allowed for a specific contaminant or its metabolite in a particular matrix, were introduced [13]. As a result, regulations for presence of pesticides in the environment and in agricultural products were implemented, and maximum residue limits (MRLs), defined as the upper legal level allowed for a specific contaminant or its metabolite in a particular matrix, were introduced [15]. MRLs in soils are determined by applying the pesticide to specific crops and evaluating their residual amount after an appropriate withdrawal period in

the harvested crop [16]. For other matrices, such as food and biological fluids, MRL levels are defined based on specific screening studies. It is important to note that pesticide MRLs are set by regional/national competent authorities and vary from country to country. Overall, the lack of common international regulation contributes to complicating pesticide pollution phenomena, diversifying their global distribution and uses [17].

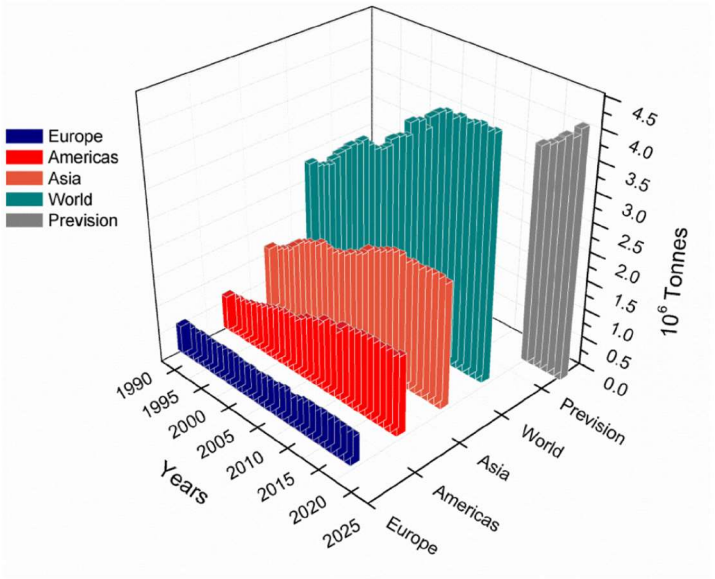

Figure. 1.1*) Trends in pesticides use in different geographical areas from 1990 to 2019. The data were acquired from the Food and Agriculture Organization Statistical Databases [14] database and PEST-CHEMGRID dataset [15].*

Figure 1.1 provides an overview of pesticide usage trends, emphasizing regional differences and growth rates in total pesticide use in different geographic regions from 1990 to 2019, showing an increase in import values by up to 261% between 2000 and 2010 [16]. Predictions regarding pesticide usage for about twenty crop-specific pesticides using the PESTGRID model suggest that the trend is approaching a plateau, but the application of these chemicals is not expected to decrease in the coming years [15]This ongoing trend highlights the urgent need to improve the sustainable use of pesticides in modern agriculture and to monitor their levels not only in the environment, but also in biological fluids for large-scale epidemiological studies [18].

Pesticides are classified into 10 main classes based on their chemical structure [19]. Despite their structural differences, all these chemicals can enter living organisms via the skin (dermal route), inhalation, or absorption through the gastrointestinal tract (oral route) [20–22]. In studies of pesticides' effects on human health, it is crucial to also consider their metabolites, which are generated both in the environment and within living organisms through various degradation pathways such as mineralization, biodegradation, and photolysis [23,24]. The chemical structure of pesticides, including their chirality, significantly influences their degradation pathways, as well as the composition of the biological environment in which they are dispersed [25]. In general, pesticide metabolites are observed to be as toxic as their parent compounds, since their toxicity is determined by the presence of functional groups that remain unaffected by degradation processes [26,27]. Among pesticide classes, organochlorines (**OCPs**), organophosphates (**OPPs**), and carbamates are the most widespread.

OCPs are a class of non-biodegradable, volatile chemicals characterized by at least one covalently bonded chlorine atom (see **Table A1, Appendix A**). Although many of these compounds are banned since classified in the group B2 of carcinogenic compound, residues of OCPs continue to be reported in various environmental matrices over the MRLs [28–30] and even biological fluids in different geographic areas [31–35]. One of the most commonly detected OCPs in the blood of oncological patients is endosulfan, whose presence has been previously correlated with an increased incidence of breast cancer and non-Hodgkin’s lymphoma.

OPPs are esters derived from phosphoric acids, initially introduced as substitutes for OCPs (see **Table A2, Appendix A**). Their most recognized neurological effect is the inhibition of acetylcholine activity, resulting in various symptoms of intoxication [36,37]. One of the most widely used and recognized pesticides in this class is glyphosate (**GLY**), an herbicide primarily applied to transgenic crops engineered to tolerate its effects [38]. GLY degrades primarily via mineralization, but also by immobilization or leaching, leading to the production of aminomethylphosphonic acid (**AMPA**), methylphosphonic acid, glycine, and sarcosine. AMPA can undergo further mineralization, resulting in methylamine and phosphate [39]. The presence of GLY and AMPA have been widely investigated in various matrices (soil, water, plant products) as well as their impact on animals, humans, and microorganisms [40].

Carbamates are derivatives of dimethyl/methyl/dithio-N-methyl carbamic acid (see **Table A3**, **Appendix A**). Examples of this class of pesticides include carbaryl, propoxur, and carbofuran. They serve as alternatives to OPPs and OCPs due to their lower persistence. However, they share similar modes of action with OPPs (acetylcholinesterase inhibition) and resistance patterns, resulting in similar health effects in humans. Carbamate pesticides undergo conversion into various products through different pathways, such as oxidation, hydrolysis, biotransformation, photolysis, and metabolic reactions within living organisms [41,42].

Another alternative to OPPs are synthetic pyrethroids, such as permethrin and cypermethrin [43]. Derived from ketoalcoholic esters of chrysanthemic and pyrethroic acids, they show lower neurotoxicity compared to OPPs. However, exposure to high levels of pyrethroids, e.g. permethrin, can lead to symptoms such as headache, vomiting, muscle twitching, dizziness, and even loss of consciousness [44]. These chemicals mainly affect sodium channels, and prolonged exposure to permethrin has been linked to immune system suppression and endocrine disruption in animals [45,46]. Although pyrethroids exhibit slightly lower mammalian toxicity compared to OPPs and have faster biodegradation capabilities, they still pose a risk to individuals routinely exposed to them.

Further classes of pesticides are summarized in **Table A4, Appendix A**. They include phenylamide derivatives of aniline, primarily used as fungicides [47–49], phenoxyalkonates, which are widely used herbicides with a phenoxyacetic acid structure [50,51], and triazines, consisting of a six-membered heterocyclic ring. Triazines are used as herbicides to control unwanted plants by inhibiting photosynthesis [52], but they are highly toxic due to their ability to disrupt endocrine function [53–55]. Phthalimides include three fungicides (captan, folpet, and captafol) that are among the most used in American agriculture. The toxicity associated with these compounds is mainly attributed to the imide rings, which are retained in degradation products [56]. These compounds undergo various degradation routes such as hydrolysis, thiol reactions, photooxidation, and enzymatic reactions. Dipyridyl herbicides, including paraquat (**PQ**) and diquat (**DQ**), contain a functionalized dipyridyl ring and were introduced in the late 1960s. These are among the most toxic pesticides in use today. Biomonitoring pesticides in the human body is crucial to reduce their incidence and collect new guidelines to implement regulations on their use. Overall,

the adverse clinical effects of pesticides exposure are investigated measuring the concentrations of themselves (uptake) and of their metabolites in biological samples (serum, fat, urine, blood, or breast milk) and/or following the changes in the levels of specific biomarkers (i.e., genotoxic effects testing) to correlate these values with the incidence of specific pathologies/diseases/symptoms.

1.3 Haloacetic acids as contaminants of emerging concerns

Disinfection by-products (**DBPs**) are a broad class of chemical compounds formed during water treatment processes when disinfectants - such as chlorine, chloramine, or chlorine dioxide - react with natural organic matter (**NOM**) and halide ions present in the source water [57]. Among these, HAAs are one of the most prevalent and concerning groups of contaminats, generated primarily through the halogenation of organic precursors such as humic and fulvic acids. HAAs account for over than 25% of total halogenated DBPs in chlorinated drinking water, and are of growing concern due to their widespread occurrence, chemical stability, and potential health effects [58].[58] The U.S. Environmental Protection Agency (**EPA**) currently regulates only five of the most common HAAs, namely-monochloroacetic acid (**MCAA**), dichloroacetic acid (**DCAA**), trichloroacetic acid (**TCAA**), monobromoacetic acid (**MBAA**), and dibromoacetic acid (**DBAA**). They are collectively known as **HAA5** [59]. However, several other HAAs, including brominated and iodinated derivatives, remain unregulated despite evidence suggests that they may be even more toxic than their regulated counterparts (see **Table A5**, **Appendix A**) [60].

Numerous studies have demonstrated that exposure to HAAs can lead to mutagenic, genotoxic, cytotoxic, and teratogenic effects, with some compounds also exhibiting carcinogenic and endocrine-disrupting properties [61]. For example, DCAA and TCAA have been shown to induce oxidative stress and liver toxicity while brominated HAAs, such as DBAA, display even higher levels of mutagenicity. Additionally, HAAs interfere with metabolic pathways, such as pyruvate dehydrogenase activity, and disrupt endocrine functions [62]. Long-term epidemiological studies have suggested potential links between chronic HAAs exposure and adverse pregnancy outcomes, liver toxicity, and developmental disorders [63]. Human exposure to HAAs occurs primarily through ingestion of treated drinking water, but also via dermal absorption and inhalation during activities such as showering and swimming in chlorinated pools. Biomonitoring studies

have demonstrated that urinary TCAA levels remain stable over time, reflecting cumulative ingestion exposure, whereas MCAA peaks after showering, indicating rapid absorption via the skin and lungs [64]. These findings highlight the need for comprehensive exposure assessments beyond traditional drinking water compliance testing.

Despite growing evidence of HAAs toxicity, their regulation varies significantly across countries. In the United States, the EPA established a maximum contaminant level (**MCL**) of **60 µg L^{-1} for HAA5** in drinking water. Similarly, Directive (EU) 2020/2184 introduced this limit for the first time in the European Union, requiring monitoring when chlorine-based disinfectants are used. However, unregulated HAAs, such as BCAA, remain a concern due to their high toxicity and lack of established safety thresholds. The challenge in monitoring HAAs stems from their variable concentrations, which depend on factors such as source water composition, seasonal changes, and disinfectant type. Studies have shown that HAAs levels can fluctuate significantly within a single water distribution system, complicating compliance-based risk assessments. Additionally, current regulations focus on drinking water concentrations rather than biomonitoring data, leading to potential underestimation of real human exposure. In the last years research on HAAs has expanded, driven by advances in high-resolution mass spectrometry (**HRMS**), sensor technologies, and biomonitoring approaches. Furthermore, the identification of urinary HAAs as potential biomarkers of exposure has opened new avenues for epidemiological studies investigating associations between HAAs and adverse health outcomes, including low birth weight and intrauterine growth restriction. Despite these advances, key gaps remain. The need for harmonized international regulations, improved detection methodologies, and long-term epidemiological studies is critical for fully understanding and mitigating the risks associated with HAAs. Moving forward, a combination of chromatographic validation, sensor-based pre-screening, and biomonitoring efforts will be essential to developing a more accurate risk assessment framework for these ubiquitous contaminants.

1.4 Biological fluids and Matrix effect

1.4.1 Introduction to the Matrix Effect

Biological fluids such as urine, blood, and saliva are widely used matrices for assessing human exposure to environmental contaminants. However, their complex and variable composition poses significant analytical challenges. In particular, these fluids contain a wide range of endogenous substances, including proteins, salts, phospholipids, and metabolites which can interfere with the detection and quantification of target analytes since they can partially binds target analytes. This phenomenon, known as the **matrix effect (ME)**, can cause signal suppression or enhancement, thus compromising accuracy, precision, and reproducibility in both chromatographic and sensor-based analyses [65,66]. The ME in chromatography was first identified in the 1990s, showing how electrolyte concentrations and biological matrices influence peak intensity [67].

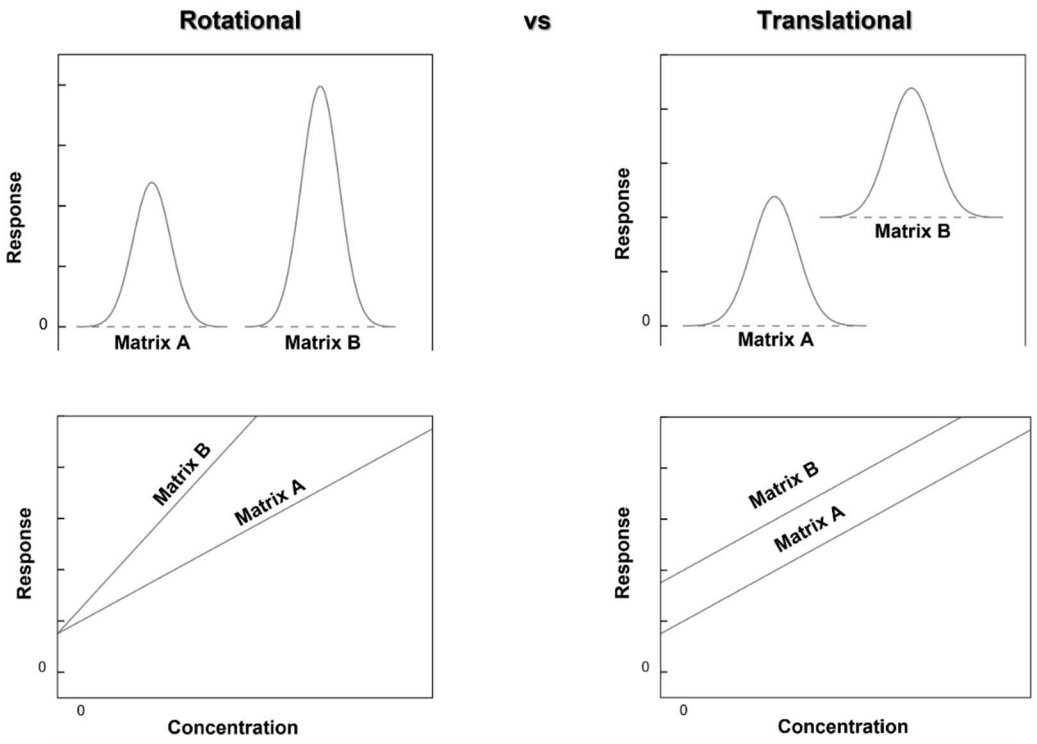

Figure 1.2) *Graphical comparison between rotational and translational matrix effect on the analytical signal (above) and on the calibration line (below). Plots adapted from Ellison et al. [68].*

Still considering the issues related to the analysis of CECs, proteins in biological fluids can bind hydrophobic chemicals like pesticides, so partition equilibria must be carefully

evaluated to ensure accurate quantification of target analytes. Several validation procedures were developed to quantify and/or control ME, but there are still some controversies about regulations that need to be bridged, starting from giving a unique definition for his quantification.

ME should be distinguished in absolute, i.e. related to a certain sample, and relative, depending on the sample source [69]. Absolute ME represents the ratio between signal responses of the same amount of analyte when present in a pure solvent sample or in the sample after suitable pretreatment. Relative ME can be estimated by comparing the signal collected in different lots of samples spiked with the same amount of analyte [70,71]. ME is classified also as translational and/or rotational ME [68], as summarized in ***Figure 1.2***. Transitional ME consists of a shift of the signal baseline, which affects the intercept of a calibration curve independently from the analyte presence and concentration. Rotational ME affects the intensity of the signal due to the analyte and, thus, the slope of the curve and are related to the analyte concentration. These latter can be corrected with standard addition methods, unlike transitional ME.

1.4.2 The Matrix Effect on Sensor-Based Analysis

Electrochemical sensors, due to their direct contact with unprocessed or minimally treated biological samples, are particularly vulnerable to MEs. In sensors, matrix interference often manifests through non-specific adsorption (**NSA**), where biomolecules, specially proteins, adhere to the sensor surface, leading to signal drift, reduced sensitivity, and compromised reproducibility [72]. Biological fluids are rich in proteins, lipids, and other macromolecules that can interact non-specifically with sensor surfaces. Proteins like albumin, globulins, and fibrinogen possess a high affinity for sensor materials, forming unwanted layers that reduce the effective interaction between the analyte and the sensor's recognition element. This phenomenon can obscure the actual signal, making it difficult to distinguish between specific and non-specific responses. Hydrophobic interactions, electrostatic forces, and covalent bonding further exacerbate NSA, ultimately affecting sensor performance [73]. To minimize NSA, strategies such as multiple washing/rinsing steps and protective layers (e.g., polymeric films) are employed, as well as suitable sample pretreatment. In recent decades, Vörös et al. have devoted significant effort to elucidating NSA physisorption

mechanisms through various methods, following its kinetics and demonstrating how introducing surface-active copolymers or peptide-based arrays can mitigate the phenomenon [74–76]. One common approach is surface passivation, where sensor surfaces are modified with materials such as polyethylene glycol (**PEG**) coatings, bovine serum albumin (**BSA**) blocking agents, or self-assembled monolayers (**SAMs**). These materials act as protective barriers, preventing non-specific protein binding while maintaining the sensor's ability to detect target analytes. Additionally, sample pre-treatment methods such as centrifugation, filtration, and affinity separation are often employed to reduce matrix complexity before analysis, enhancing the overall reliability of sensor-based detection [77]. Another important aspect to consider in sensor-based methods is the partitioning effect, where analytes are differentially distributed between the biological matrix and the sensor interface. In cases where the analyte has a strong affinity for matrix components, such as proteins or lipids, its availability for detection is reduced, leading to an underestimation of its concentration. This is particularly problematic for hydrophobic pesticides and pharmaceuticals, which tend to bind preferentially to plasma proteins rather than remaining in the free phase.

1.4.3 The Matrix Effect on Chromatographic Analysis

Unlike sensors, where surface interactions dominate ME, chromatographic techniques such as LC-MS and ion chromatography (**IC**) experience matrix interference primarily in the form of ion suppression or enhancement. This occurs when co-eluting compounds compete with the target analyte during ionization, reducing or amplifying its signal and leading to significant quantification errors [78]. In LC-MS, matrix components such as salts, phospholipids, and endogenous metabolites can negatively affect ionization efficiency by altering the charge distribution in the electrospray ionization (**ESI**) process. Ion suppression is particularly problematic in biological samples, where the presence of high concentrations of competing ions can reduce the formation of analyte ions, thereby decreasing detection sensitivity. Conversely, ion enhancement occurs when matrix components facilitate the ionization of the target analyte, artificially inflating its signal and leading to overestimated concentrations [79]. To minimize these issues, several strategies have been developed. Internal standards, particularly isotopically labeled analogs of the analyte, are commonly used to correct

for signal variations caused by matrix effects. Additionally, sample preparation methods such as solid-phase extraction (**SPE**) and liquid-liquid extraction (**LLE**) help remove interfering substances before chromatographic analysis. Another important approach involves post-column infusion experiments, where a continuous stream of analyte is introduced alongside the sample to evaluate the extent of ion suppression and adjust chromatographic conditions accordingly [80]. IC plays a pivotal role in the detection of ionic contaminants, including HAAs, which are frequently monitored in water and biological fluids. However, IC is not immune to matrix effects, which can arise from high ionic strength samples that disrupt ion exchange equilibria, leading to peak broadening and reduced resolution [81]. Unlike LC-MS, where matrix effects primarily affect ionization efficiency, IC faces challenges related to excessive background conductivity and interference from endogenous electrolytes. High concentrations of sodium, potassium, and chloride ions can overwhelm the ion-exchange process, causing poor separation of target analytes. To overcome these challenges, several approaches have been adopted, including dilution of high-ionic-strength samples, selection of appropriate ion-exchange resins, and the use of gradient elution techniques to optimize analyte resolution [82]. A particularly effective strategy in IC is the use of suppressed conductivity detection, where an ion-suppressor device removes background ions post-separation, enhancing the signal-to-noise ratio and improving analyte quantification. This method has proven invaluable in minimizing the impact of high ionic strength matrices, making IC a powerful tool for analyzing complex biological and environmental samples [83].

1.4.4 Comparative Analysis of Matrix Effects on Sensors and Chromatography

Understanding these fundamental differences is essential when selecting the most suitable analytical approach, as it allows for a more targeted and efficient methodology based on the specific needs of the analysis. Factors such as the complexity of the sample, the required detection limits, and operational constraints, including time, cost, and portability, all play a significant role in this decision-making process. While sensor-based methods excel in offering rapid, on-site detection, they often face challenges in terms of reproducibility and interference from complex biological matrices. In contrast, chromatographic methods, although more time-consuming and requiring more

intensive sample preparation, provide a level of precision and sensitivity that is difficult to match.

Future advancements in analytical chemistry should aim to bridge the gap between these two approaches, leveraging the strengths of both. Integrating sensor-based pre-screening methods with chromatographic validation could allow for a more streamlined and versatile workflow, where sensors provide initial detection and rapid quantification, and chromatography ensures accuracy and reliability in the final analysis. Such hybrid methodologies could offer a more comprehensive, multi-faceted approach to contaminant analysis, particularly in complex biological samples, improving both efficiency and overall performance. Furthermore, the development of novel materials and technologies for sensors, as well as innovations in chromatographic techniques, holds the potential to address the current limitations of each approach, making them more complementary and effective in various analytical applications. This convergence could lead to the creation of more robust, cost-effective, and reliable solutions for the detection of emerging contaminants in biological fluids, advancing the field of environmental and public health monitoring.

1.5 Chromatographic Methods for the analysis of CECs in biological fluids

Chromatographic strategies, particularly gas chromatography (**GC**) and liquid chromatography (**LC**), rely on different approaches for the detection of CECs. GC is typically employed for volatile and thermally stable compounds, taking advantage of their physico-chemical properties to achieve separation and quantification. In contrast, LC is more suitable for thermolabile and non-volatile analytes, allowing the detection of a broader range of compounds, including those with high polarity. In both techniques, selectivity and sensitivity can be enhanced through various strategies, such as derivatization, the use of selective stationary phases, or coupling with high-resolution detectors. Mass spectrometry (**MS**) is often integrated with both GC and LC to improve specificity and provide structural information about the analytes. However, each technique presents intrinsic strengths and limitations. Gas chromatography coupled with mass spectrometry (**GC-MS**) is characterized by high resolution and sensitivity, particularly for volatile compounds, but requires extensive sample preparation, including derivatization for polar analytes. On the other hand, LC-MS is more versatile

in handling complex biological matrices without derivatization, yet it may suffer from matrix effects and lower resolution compared to GC. When dealing with biological matrices, both techniques face significant challenges due to the presence of proteins and endogenous compounds that can interfere with the analysis. As already underlined, ME can lead to signal suppression or enhancement, affecting the accuracy and reproducibility of the results. Strategies such as SPE, LLE, or protein precipitation are commonly employed to minimize these interferences. In the last decades, researchers have extensively investigated ways to mitigate matrix effects in chromatographic analyses, highlighting the importance of an optimized sample pretreatment and stationary phase selection to improve method robustness. Given the complexity of biological matrices, we reviewed the main chromatographic approaches applied in recent years for pesticide and HAAs determination, evaluating which techniques and strategies are the most effective in addressing these analytical challenges. Regarding pesticides, glyphosate (**GLY**) served as a representative compound, as it can be detected using both GC and LC, depending on the employed derivatization and detection strategy.

1.5.1 Liquid Chromatographic Methods for Pesticides detection

LC-MS/MS has become the preferred method for quantifying highly polar pesticides. However, the presence of endogenous polar components in biological matrices often interferes with the analysis, leading to issues such as co-elution, ion suppression, or isobaric interferences in MS detection. Traditional reversed-phase LC is often unsuitable for direct analysis of polar pesticides in biological samples, requiring alternative chromatographic approaches like IC or hydrophilic interaction liquid chromatography (**HILIC**). To improve the selectivity and sensitivity of LC-based pesticide analysis, researchers have developed various sample preparation techniques and novel stationary phases. For instance, Quick Polar Pesticides Extraction (**QuPPE**) combined with ultra-performance liquid chromatography (**UPLC-MS/MS**) using a zwitterionic HILIC column has proven highly effective for separating GLY from human blood samples without the need for derivatization [84]. The SeQuant ZIC-pHILIC column, with its densely bonded zwitterionic functional groups, offers excellent peak shapes and chromatographic resolution across a broad pH range, effectively minimizing ME when used with appropriate buffer solutions [85]. Another notable LC-MS/MS method, developed by A. Covaci et al., uses a SPE procedure to

determine 13 pesticides and their main metabolites in human urine [86]. This method, adapted from a previous technique [87] replaces acetone and hexane with methanol for the final purification step, significantly reducing ME. The method was designed to analyze compounds that ionize in both positive and negative polarity modes. By optimizing dynamic multiple reaction monitoring (**MRM**) mode, the authors were able to overcome the sensitivity limitations typically associated with frequent polarity switching in standard monitoring modes. Furthermore, parent compounds such as fipronil, bifenthrin, and prothioconazole were detected in urine samples for the first time using this approach. A simpler LC-high resolution mass spectrometry (**LC-HRMS**) method for the direct determination of GLY and AMPA in human urine was also reported, utilizing a new adsorbent based on amide-modified silica [88]. The separation was carried out using an Obelisc column with Separation Cell technology LiSC™, which introduces a novel chemical modification to the silica gel pores, creating a liquid separation cell with unique charge characteristics, ionic strength, and hydrophobic properties. This column functions similarly to HILIC columns, maintaining an equilibrium with the mobile phase much like living cells do with their environment. Chen et al. further demonstrated the determination of GLY and AMPA using a Thermo Q-Exactive HRMS (Bremen, Germany) in single ion monitoring mode at a mass resolving power of 70,000 [89]. Since the selected-reaction monitoring mode was insufficient to overcome background noise in low-resolution MS, HRMS in full scan mode was applied after a solid-phase extraction step, enhancing the method's sensitivity. By analyzing only 200 µL of urine, they were able to achieve limits of detection (LODs) of 3 µg L^{-1} for GLY and 1 µg L^{-1} for AMPA, which is suitable for clinical applications in poisoning studies. A microLC-MS/MS method was also developed to quantify GLY, AMPA, N-acetyl AMPA, and N-acetyl glyphosate in multiple biological matrices without the need for derivatization [90]. The method allows for very short chromatographic runs (about 3 minutes) while achieving limit of quantification (LOQ) values that are thousands of times lower than the EU-EFSA standards for serum and urine samples (around 0.05 µg L^{-1}) [91]. The use of micro-LC with low flow helps reduce background noise and improves the overall sensitivity of the analysis. Several IC methods have been developed to quantify pesticides in complex matrices, and while they are primarily used for environmental and food samples, new approaches have recently been proposed for analyzing human urine and serum. Schütze et al. presented an IC-MS/MS method for the online quantification of GLY and six OPPs in human urine,

achieving a LOD of 0.2 µg L^{-1} for GLY [92]. This method, which combines a clean-up and an analytical separation column, could be extended to biomonitoring pesticides and offers a simple and fast sample preparation process that includes dilution followed by a 20-minute chromatographic run. More recently, a non-conventional IC-MS/MS method for quantifying GLY and AMPA in serum was developed [93]. Unlike traditional IC-MS/MS methods that use a hydroxide eluent and suppressor, which require long elution times (>30 minutes), this approach uses a non-suppressed IC-MS/MS method that shortens the elution time and can be performed on standard LC-MS/MS systems without any modifications. The mobile phase consists of a mixture of methylamine and acetonitrile, and EDTA solution is used as an anticoagulant in the pretreatment of plasma to prevent interference with GLY and AMPA.IC-MS/MS has also been successfully used to analyze GLY in feed, saliva, urine, and feces from cattle farms [94]. This analytical method, initially developed for environmental samples, enables the quantification of 14 polar pesticides with high sensitivity and low LOD values, such as 5 ng L^{-1} for GLY. The method involves a simple extraction process using an ultrasonic bath, eliminating the need for further purification.

1.5.2 Gas Chromatographic Methods for Pesticides detection

Gas chromatography (**GC**) techniques have long been used to analyze a wide range of pesticides in environmental samples, depending on the chemical and physical characteristics of the compounds, such as their volatility. Various GC-based methods have been reported, often incorporating different detectors such as the electron capture detector [95], flame photometric detector [96], nitrogen-phosphorus detector [97], and flame ionization detector [98]. The application of GC-MS and GC-MS/MS for pesticide residue analysis is well-documented in several pesticide analytical manuals. Numerous studies have focused on the simultaneous determination of nearly 400 pesticides using GC equipped with quadrupole mass filters and two-dimensional GC techniques [99]. GC techniques are particularly useful for analyzing pesticide classes that do not require derivatization, such as OCPs, OPPs, triazines, and chloroacetanilides, as well as their transformation products. In fact, some transformation products of OPPs and phenoxyacid herbicides are also amenable to GC analysis. The use of GC-MS detectors capable of performing Selected Reaction Monitoring (**SRM**) is becoming increasingly popular in pesticide detection because they enhance the signal-to-noise ratio, improving sensitivity [100]. However, GC-MS and

GC-MS/MS techniques still have limitations. For instance, they require analytes to be volatile and thermally stable, meaning that polar analytes must often undergo derivatization to increase their volatility. A variety of extraction techniques are employed prior to GC analysis, including Super-Critical Fluid Extraction, Matrix Solid-Phase Dispersion, Solid Phase Extraction, Solid-Phase Microextraction, Single Drop Microextraction, Stir Bar Sorptive Extraction, and Pressurized Liquid Extraction, among others [101]. Solid SPE is a common pre-analytical procedure, though it often requires a moderate to large consumption of organic solvents and can be time-consuming. Gao et al. proposed a more efficient approach for analyzing pyrethroids, using Ultrasound-Assisted Dispersive Liquid-Liquid Microextraction (**USA-DLLME**), followed by GC-MS/MS analysis [102]. This method takes only about 40 minutes and uses a very small amount of sample (approximately 1 µL), achieving LODs between 0.01 and 0.1 µg L^{-1}. Other extraction techniques based on liquid extraction, such as Pressurized Liquid Extraction and Microwave-Assisted Extraction, have also shown good performance with relatively fast protocols [103]. Several studies have developed methods for analyzing OCPs in biological fluids. For instance, a C18 Solid Phase Extraction cartridge is commonly used for their extraction. Cazorla-Reyes et al. presented a multiresidue method for the simultaneous extraction of various pesticide classes, including carbamates, organochlorines, organophosphates, pyrethroids, herbicides, and insecticides, from urine samples using Solid Phase Extraction [104]. The method could achieve LODs ranging from 0.001 to 1.452 µg L^{-1} for GC-amenable pesticides. Other techniques, using Sep-Pak® C18 cartridges, have been tested on blood samples [105], showing good selectivity for certain OPPs, which were then analyzed using GC-MS. The LOQ for these analytes were established at 50 µg L^{-1}. Another innovative method, developed by Naksen et al., uses a combination of Freezing-Lipid Precipitation, Liquid-Liquid Separation, and NH2-Solid Phase Extraction for measuring OP pesticide residues in human plasma and breast milk [106]. GC-MS/MS analysis enabled the detection of residues with LODs ranging from 0.18 to 1.36µg L^{-1}. More recently, a novel approach using Atmospheric Pressure Gas Chromatography has been proposed for quantifying various OCPs in human serum [107]. In previous studies, the authors found that classic chemical ionization failed to generate molecular ions for certain compounds, such as hexachlorocyclohexane [108]. By coupling GC with MS/MS, however, they achieved LODs between 0.022 and 0.090 µg L^{-1}, successfully applying the method to human blood samples for ultra-trace level OCP

analysis. One of the latest methods for multiresidue detection using GC-MS/MS involves a modified **QuEChERS** (Quick, Easy, Cheap, Effective, Rugged, and Safe) extraction procedure, which is compatible with both polar and non-polar compounds. This method has been applied to the analysis of pesticides in human blood and urine, as well as in food and environmental matrices [109]. It offers a relatively short analytical time (14 minutes), excellent recovery (>90%), and a consistent LOD of around 10 μg L^{-1} for all nine analytes, which represent a variety of pesticide classes [110]. Overall, chromatographic methods coupled with MS are essential for robust clinical biomonitoring. These methods continue to improve year after year, thanks to the introduction of innovative strategies, and are attracting increasing attention from the scientific community. However, only a small fraction of the full potential of this technology has been realized in pesticide biomonitoring. Widespread application of this technology will require further development, particularly in the area of quantitative results. Moving forward, a common protocol for data representation—such as linearity range, accuracy, trueness, LOD, LOQ, and ME—should be adopted to allow for better comparison of the analytical performance achieved by different methods. **Table A6 in Appendix A** reassume the methods presented in **sections 1.5.1** and **1.5.2**.

1.5.3 Liquid Chromatographic Methods for HAAs detection

LC, particularly when coupled with tandem mass spectrometry, has emerged as a powerful approach for HAAs analysis in biological samples. Unlike GC, LC-MS/MS eliminates the need for derivatization, simplifying sample preparation and reducing potential losses associated with chemical modification steps. High-performance liquid chromatography (**HPLC**) with reverse-phase or ion-exchange separation is commonly employed, utilizing electrospray ionization ESI for enhanced ionization efficiency. However, ME such as ion suppression or enhancement remain critical challenges, requiring the implementation of stable isotope dilution techniques and matrix-matched calibration to ensure analytical accuracy. Exposure to DBPs in drinking water and chlorinated swimming pools has been associated with adverse health outcomes, though the biological mechanisms remain poorly understood. In the PISCINA-II study (part of the EXPOsOMICS project), 60 volunteers swam for 40 minutes in a chlorinated pool, and levels of the most common DBPs were measured in water and exhaled breath before and after swimming [111]. Blood samples were collected before and two hours after swimming for metabolic profiling using liquid chromatography coupled with

high-resolution mass spectrometry. Multivariate normal models were used to evaluate metabolome-wide associations between DBP exposure and metabolic features. Sensitivity analyses and compound annotation were conducted. Following the experiment, levels of DBPs in exhaled breath were higher, and 6,471 metabolic features were detected. Of these, 293 features were associated with DBPs in breath, and 333 features were linked to DBPs in water or urine. After adjusting for physical activity and DBP exposure, 20 identified metabolites were related to the tryptophan metabolism pathway. This study identified numerous molecular changes in response to swimming in a chlorinated pool, highlighting the complex interaction between exposure to DBPs and physical activity on metabolic profiles. A simple, high-throughput, and sensitive method was developed for measuring trace levels of TCAA in human urine using SPE followed by isotope dilution HPLC-MS/MS [112]. For sample preparation, Oasis-HLB columns are conditioned and used to extract TCAA from urine. After adding isotopically labeled working solutions or standards to the urine samples, the diluted urine is passed through the SPE column. Residual salts are removed, and TCAA is eluted with a 20% methanol/water solution. The total preparation time per sample is around 8 minutes, and samples can be stored for up to one month at 4 °C without degradation. The analytical step uses an Agilent 1100 liquid chromatograph coupled with an API 3000 triple quadrupole mass spectrometer. TCAA is separated from urine components on a Prism RP HPLC column, and negative ion electrospray ionization is used for detection. The method offers high sensitivity with a limit of detection of 0.5 ng/mL in 1 mL of urine, and the analysis run is completed in about 8 minutes. The high-throughput nature of the process ensures that the method is both rapid and reliable for monitoring trace levels of TCAA in biological samples. Urinary TCAA has been proposed as a biomarker for ingested DBPs, but its validity in cancer epidemiology remains unclear. A study By Salas *et al* evaluates urinary TCAA as a biomarker of DBP exposure in a colorectal cancer case-control study [113]. Urinary TCAA and creatinine levels were measured in 120 control samples using LC-MS/MS, alongside nine TAAs and four THMs. The geometric mean urinary TCAA excretion rate was 17.3 pmol/min (95% CI: 14.0–21.3), increasing with TCAA ingestion but decreasing with total tap water consumption, external water intake, plasmatic volume, smoking. No association was found between urinary TCAA and lifetime THMs exposure. These findings indicate that urinary TCAA is not a reliable biomarker for DBP exposure in adult cancer studies, as several physiological and lifestyle factors

significantly influence its levels. IC represents another viable approach for HAAs determination in biological fluids, leveraging the ionic nature of these compounds for effective separation using anion-exchange columns. IC coupled with conductivity detection has been widely used in environmental studies, though its application in biological matrices has gained attention due to advancements in IC-MS technology. However, the presence of competing anions in biological samples, such as chloride, sulfate, and phosphate, can interfere with HAAs detection, necessitating careful optimization of mobile phase composition and sample preparation strategies such as desalination via ion-exchange resins or selective membrane filtration.

1.5.4 Gas Chromatographic Methods for HAAs

GC remains a widely used technique for HAAs analysis due to its superior separation efficiency. However, given the non-volatile nature of most HAAs, a derivatization step is often required to convert them into more volatile and thermally stable forms suitable for GC analysis. The most common derivatization approaches involve methyl esterification using acidic methanol or diazomethane [3,4]. Electron capture detection (**ECD**) has historically been preferred for its high sensitivity to halogenated compounds, yet it suffers from interference from other halogenated species in complex biological matrices. GC-MS provides structural confirmation and improved selectivity, making it an invaluable tool for biological monitoring. Nevertheless, extensive sample preparation, including SPE and LLE, is required to isolate HAAs from plasma, urine, and tissue samples prior to derivatization and analysis [5,6]. After oral exposure, HAAs are rapidly absorbed and excreted in urine. Traditional methods for their detection in urine, primarily developed for rodents, often lack sensitivity for human samples and require complex, manual preparation. This study presents a static headspace gas chromatography-mass spectrometry (**HS-GC-MS**) method for the detection of nine HAAs in human urine [64]. Key derivatization and extraction parameters were optimized to enhance sensitivity, achieving LODs between 0.01 and 0.1 μg L^{-1} with relative standard deviations ranging from 6 to 11%. The method was applied to urine samples from swimmers and non-swimmers. No HAAs were detected in non-swimmers or in pre-exposure samples, whereas post-swim urine contained MCAA, DCAA, and TCAA, correlating with their levels in pool water. This HS-GC-MS approach provides a precise and sensitive tool for assessing HAAs exposure through urinary analysis. A rapid headspace solid-phase microextraction gas chromatography

(**SPME-GC-ECD**) method was optimized for the detection of HAAs in urine and blood using micro-volume samples (0.1 mL) [114]. The procedure includes liquid–liquid microextraction (**LLME**), derivatization to methyl esters with sulfuric acid and methanol, followed by SPME-GC-ECD analysis. The optimized method achieved detection limits of 1 μg L^{-1} for most HAAs, with higher values for MBAA (3 μg L^{-1}) and MCAA (16 μg L^{-1}). The ME for urine and blood was found to be negligible. HAAs were separated in under 13 min for biological samples, with total preparation and analysis time under 50 min. This method provides a sensitive and efficient approach for HAAs analysis in biological fluids, requiring minimal sample volume while maintaining precision comparable to standard methods using larger volumes. A cross-sectional study was conducted in Wuhan, China, to explore the relationship between exposure to DBPs, specifically TCAA, and newborn birth weight [115]. A total of 398 women who had given birth to live singleton infants were recruited. Urinary creatinine-adjusted TCAA served as an exposure biomarker. TCAA concentrations in urine were measured using a modified version of the EPA method 552.2, involving extraction with methyl-tert-butyl ether, conversion to the methyl ester, and analysis by gas chromatography with an electron capture detector The study did not find statistically significant results in the linear regression models. However, the analysis showed that birth weight was lower in women with higher urinary TCAA concentrations, especially in the third and top quartiles. A summary of the methods presented in this section is reported in **Table A7 in Appendix A**. These findings suggest that elevated exposure to DBPs may influence fetal growth, though further research is needed to confirm the potential impact of DBPs on birth weight during pregnancy. Despite significant advancements in chromatographic methodologies, several challenges remain in the accurate quantification of HAAs in biological samples. The low concentrations at which these compounds occur necessitate highly sensitive analytical techniques, while MEs introduce variability in detection and quantification. The integration of HRMS and emerging automated sample preparation techniques is expected to further enhance the reliability and applicability of HAAs analysis in biological exposure assessment. Future research should focus on improving method sensitivity, reducing sample preparation complexity, and developing standardized protocols for routine clinical and epidemiological studies.

1.6 Sensor-based screening strategies

Chemical sensors and biosensors have emerged as promising tools for the detection of CECs in various matrices in the last years. A typical biosensor comprises two main components: a recognition element (receptor) and a signal transducer. The receptor is responsible for the selective interaction with the target analyte, while the transducer converts this interaction into a measurable signal, mainly optical or electrochemical. Sensing strategies for detection of various CECs rely on either direct or indirect methods. In direct methods, the physico-chemical properties of the target compound are exploited to generate the analytical signal, such as its electrochemical oxidation or reduction. In contrast, for indirect methods the signal derives from species that are affected by the presence of the analyte itself. In both cases, selectivity can be provided and/or enhanced by using suitable molecular recognition layers. They normally consist of bioreceptors (such as antibodies, aptamers, enzymes, peptides, etc.), biomimetic films, carbonaceous or inorganic nano-modifiers, hybrid materials, and more. In recent years, various molecular recognition layers have been successfully applied in the design of (bio)sensing platforms for the detection of organic contaminants in environmental and food matrices [116]. However, only a limited number of these systems have been further applied in biological matrices. Indeed, biological matrices are rich in proteins and various endogenous/exogenous small molecules not only impacting the equilibrium, but also inducing ME. Additionally, they are prone to cause NSA on the transducer surface, as previously discussed [117]. A comprehensive review of how NSA has been characterized and addressed in sensor and biosensor development over the last fifty years was recently published, highlighting that NSA continues to be a bottleneck in realizing analytical devices, not only for pesticide detection but also for assessing emerging pollutants [118]. Considering these challenges, the bibliographic research was focused on the most recent surface modifiers and sensor architecture designed for pesticide and HAA detection in any matrix, to evaluate their potential for overcoming these obstacles and the possibility to apply such strategies to biological matrices. Due to the target of the research activities of this Thesis, the discussion include mostly sensors exploiting electrochemical transduction.

1.7 Electrochemical Sensing Strategies for Pesticide Detection

1.7.1 From direct detection to the formation of pesticide-metal complexes

Electrochemical sensors enable the quantitative or semi-quantitative identification of specific electroactive pesticides by leveraging their distinct electrochemical signals. For instance, GLY undergoes an irreversible oxidation process, which has been investigated using various voltammetric techniques on both unmodified and graphite oxide (**GO**)-modified carbon paste electrodes. These studies span multiple matrices, including milk, orange juice, agricultural formulations, groundwater, soybean extracts, and lettuce extracts. The adsorption of the GLY anionic form onto carbon paste/GO surfaces enhances analyte accumulation and selective oxidation at potentials ≥0.95 V vs. Ag/AgCl [119]. This adsorption capability can be further optimized through thermal or chemical treatments that enrich surface functional groups, as demonstrated with activated biochar [120]. Activated biochar derived from waste biomass has recently been applied to detect methyl parathion in water and PQ in various matrices, including water, coconut water, honey, lemon, and lettuce [121]. De Oliveira et al. emphasized the significance of incorporating a pre-concentration step into the analytical protocol to maximize spontaneous adsorption processes. Carbon-based nanomaterials (e.g., single/multi-walled carbon nanotubes, carbon black) have also been combined with organometallic compounds and/or metal oxide nanoparticles (**NPs**) to enhance mechanical stability, electrical conductivity, active surface area, and adsorption efficiency [122]. Material selection is often dictated by the analytical context. For example, a pencil graphite electrode integrating hollow fiber with a multi-walled carbon nanotubes-ionic liquid composite and copper oxide NPs (***Figure 1.3a***) was specifically designed for GLY detection, with copper being chosen due to its frequent association with GLY in fungicide formulations [123]. This hybrid modifier enabled GLY oxidation monitoring over a broad concentration range (5 nM to 1.1 µM) with a LOD of 1.3 nM. A comparable LOD (1 nM) was achieved using a copper-aluminum hydrotalcite doped with graphene for GLY determination in water [124]. In this case (***Figure 1.3b***), the electrochemical response did not originate from direct GLY oxidation but rather from its ability to chelate copper, thereby reducing the copper redox signal. Copper-organophosphate pesticide complexes have been extensively utilized in pesticide detection using strategies analogous to those demonstrated for GLY [125,126]. Many of these approaches involve a decrease in the copper oxidation peak

($E_{p.a}$ = +0.3 V vs. Ag/AgCl) due to copper-pesticide complex formation [127–129]. Conversely, some studies have reported a linear increase in the copper oxidation signal with increasing GLY concentrations when using porous copper nanowire electrodes or electrodeposited copper, likely due to progressive metal dissolution [130,131].

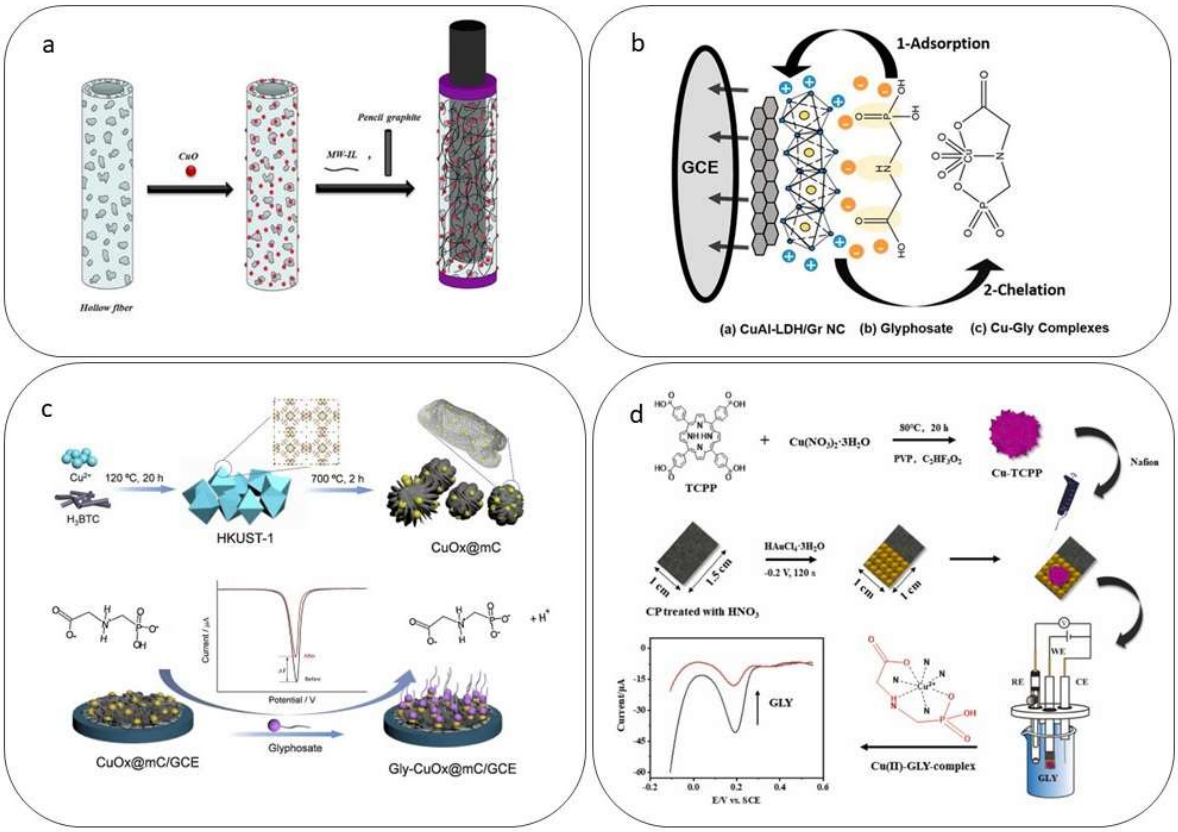

Figure 1.3 a) *Main preparation steps of a graphite pencil electrode integrated in a hollow fiber with a MWCNTS-ionic liquid composite decorated with copper oxide NPs for GLY direct detection adapted from [123];* ***b)*** *Architecture of the copper-aluminium hydrotalcite doped graphene nanoprobe sensor for the indirect detection of GLY adapted from [124];* ***c)*** *Schematic description of the mesoporous carbon composite formation and the following analytical protocol used for the indirect detection of GLY adapted from [132] ;* ***d)*** *Synthesis of copper porphyrin metal organic framework decorated with NPs for GLY indirect detection via the formation of copper-GLY complexes adapted from [122].*

Recently, sensing strategies based on organometallic complex formation have incorporated metal-organic frameworks (**MOFs**) and their derivatives, which are promising hybrid organic/inorganic materials [133]. In GLY detection, copper benzene-1,3,5-tricarboxylate MOFs were initially employed as simple electrode modifiers and

later combined with other two-dimensional nanomaterials to improve conductivity limitations [134]. Both Cu-BTC-based sensors demonstrated ultra-low GLY detection levels (LOD ≤ 0.1 pM) in various aqueous matrices, such as water and soybean extracts. An even lower LOD (≈77 fM) was reported using MOF-derived copper oxide@mesoporous carbon materials (***Figure 1.3c***), obtained via pyrolysis to enhance adsorption capacity [132]. Additionally, copper porphyrin MOFs combined with gold NPs (***Figure 1.3d***), immobilized on carbon paper surfaces, exhibited a synergistic electrocatalytic effect, delivering high performance and broad applicability in real samples (water, soybean, carrot, and wheat extracts) [122]. Designed for disposability, these carbon paper electrodes show potential for large-scale production and in-situ monitoring. MOF-based and carbonaceous modifiers derived from waste biomass appear particularly promising for developing electrochemical screening platforms for pesticide monitoring, employing both direct and indirect detection strategies. These approaches could be extended to other electroactive pesticides. GLY complexes with various transition metals—including cadmium, lead, zinc, calcium, cobalt, iron, magnesium, manganese, chromium, nickel, gold, and silver—have been explored for different sensing applications [135]. Additionally, metal-pesticide complexes have been incorporated into colorimetric assays, primarily utilizing copper, gold, and silver NPs, as recently reviewed [136]. These findings underscore the adaptability of metal-based sensing strategies beyond electrochemical detection. Despite the high selectivity, sensitivity, and reproducibility demonstrated in environmental and food matrices, none of the reported electrochemical sensors for pesticide detection have been applied to biological fluids. Future studies should focus on assessing the feasibility of adapting these strategies in biological samples, addressing NSA minimization and integrating appropriate sample pretreatment steps. Without such measures, the highly functionalized and porous nature of electrode modifiers could facilitate undesired interactions with matrix-related compounds, including partially unfolded proteins and exogenous or endogenous small molecules.

1.7.2. Biosensing strategies

In the late 1980s, ecotoxicological studies began exploring the mechanisms behind pesticide-enzyme inhibition, revealing that the activity of several enzymes is significantly impacted by exposure to pesticides, particularly OPPs [137]. These findings contributed to the development of biosensing technologies, employing

different transduction mechanisms. Early strategies focused on the indirect detection of pesticide concentrations by monitoring the enzymatic inhibition of enzymes such as horseradish peroxidase (**HRP**), acetylcholinesterase (**AChE**), urease, and acid phosphatase in response to increasing GLY concentrations [138–140]. These techniques were later combined with screen-printed electrodes (**SPEs**), particularly origami paper-based designs, which offer a portable, miniaturized, and cost-effective solution for pesticide detection [141,142]. Despite their advantages, these portable biosensing platforms often exhibit lower performance compared to traditional analytical methods conducted in solutions, as demonstrated in a recent comparative study on GLY detection using HRP inhibition [143].

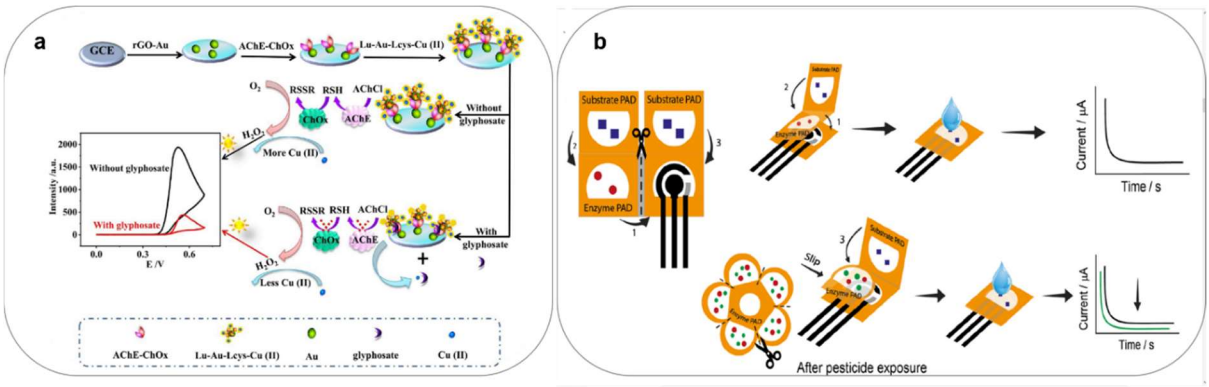

Figure 1.4) *Schematic representation of:* ***a)*** *An electrochemical luminescence sensor adapted from Ref [144];* ***b)*** *Flower-like origami biosensor for multiple pesticides detection adapted from Ref [145].*

One approach to improve the sensitivity of these biosensors is to design systems that utilize dual inhibition mechanisms, where the analyte, in this case GLY, inhibits both the enzymatic reaction and the catalytic action of HRP towards a secondary system [144]. This electrochemical/luminescence hybrid platform shows promising results; however, it presents a complex architecture (***Figure 1.4a***). On the other hand, double inhibition strategies are particularly useful for detecting pesticides in biological fluids, where high selectivity is essential. An option for enhancing the sensitivity of these dual-detection platforms involves increasing the electroactive area before immobilizing the enzyme, which can be achieved using nanomaterials, as demonstrated in the development of GLY sensors based on acid phosphatase or urease inhibition [146]. A comprehensive understanding of the inhibition mechanisms is critical for the development of hybrid photoelectrochemical systems [147]. For example, the inhibition of AChE by GLY was studied using an extended-gate field-effect transistor sensor with

an AChE-modified indium tin oxide (**ITO**) electrode, enabling real-time monitoring of GLY in vegetables and potentially in biological fluids. However, the scalability of such electrochemiluminescent and photoelectrochemical platforms is hindered by their complexity and production costs. As a result, simpler origami SPEs configurations are often preferred. A recent advancement in multianalyte detection has been the development of a platform capable of simultaneously measuring GLY, paraxon, and 2,4-dichlorophenoxyacetic acid at parts per billion (mg/Kg) levels, by correlating their inhibitory effects on specific enzymes such as HRP, butyrylcholinesterase, and alkaline phosphatase [145]. The use of wax-printed paper pads loaded with enzymes or substrate, combined with chronoamperometric measurements, allows for the detection of pesticide concentrations through enzymatic activity changes (***Figure 1.4b***). To facilitate the use of these sensors in biological fluids, an additional paper pad for sample pretreatment could be introduced to avoid NSA. Moreover, the inclusion of specific biological targets for each pesticide can enhance detection. For instance, the enzyme 5-enolpyruvyl-shikimate-3-phosphate synthase has been utilized to develop an optical sensor specific to GLY [148]. The need for highly specific enzymes for pesticide detection is critical, especially considering the complexity and variability of biological fluids, which often contain a range of interfering compounds that can inhibit common enzymes like peroxidases. Pesticides may also act as antigens, making pesticide-specific antibodies viable candidates for use in affinity immunosensors. Recent studies have shown the application of electrochemical and optical immunosensors for detecting GLY and other OPPs [149,150]. These bioreceptors can be selected both for single-target recognition (e.g., GLY) or for broader classes of molecules (e.g., OPPs), and integrated with various sensor platforms, such as gold nanoparticles and Prussian Blue in electrochemical immunosensors, or colorimetric platforms for OPP screening. Recently, a label-free immunoassay-based sensing strategy for GLY detection in human urine was reported [151]. The immunosensor was developed by anchoring GLY antibody at the gold electrode surface using a thiol-based cross-linker and the signal variations upon antigen binding was followed via chronoamperometry and by non-faradic EIS (***Figure 1.5a***). The biosensor architecture described is rather simple compared to other immunosensors, such as the competitive electrochemical assay for imidacloprid detection [152] illustrated in **Figure 1.5b**. One noteworthy advancement in immunosensing for GLY detection in human urine involves

a label-free strategy, in which GLY antibodies are anchored to the gold electrode surface using a thiol-based cross-linker [152].

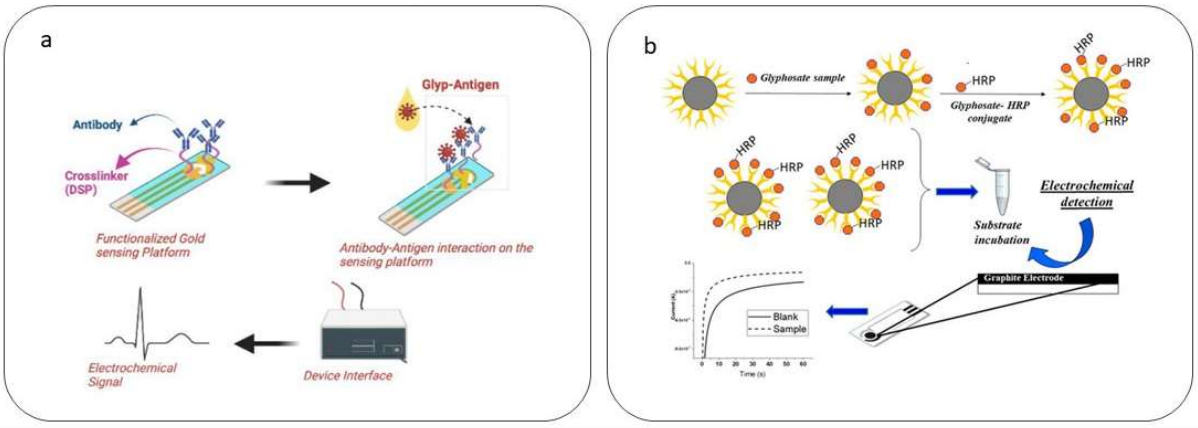

Figure 1.5) *Comparing different immunosensor architectures with the biorecognition layer immobilized* ***(a)*** *at the electrode surface adapted from Ref. [151] or* ***(b)*** *at the surface of magnetic beads adapted from Ref [152].*

The signal variations upon antigen binding are tracked using chronoamperometry and electrochemical impedance spectroscopy (**EIS**) [151]. One significant advantage of using immunosensing strategies is the ability to prevent NSA phenomena by immobilizing antibodies on magnetic beads (**MB**). This approach involves incubating the functionalized MB with the sample to "capture" the analyte, followed by removal with a magnet and washing to eliminate NSA. The analyte concentration is then correlated with the current generated by HRP-labeled MBs. In addition to enzyme-based immunosensors, aptasensors are increasingly being used for pesticide detection, offering benefits such as high stability, selectivity, and cost-effectiveness, without the need for labeling. The recyclability of aptamers further enhances the practical application of these sensors. Recent developments in aptamer-based strategies for pesticide detection include amperometric aptasensors, where the presence of the analyte leads to a reduction in the electrochemical signal of a redox probe due to conformational changes in the target, as seen with OPPs [153].

1.7.3. Biomimetic receptors for indirect sensing strategies

Molecularly imprinted polymers (**MIPs**) are inspired by enzyme-based recognition systems, offering a cost-effective, stable, and easy-to-fabricate alternative to bioreceptors. MIPs have the added advantage of long shelf life and the ability to recognize small molecules with high selectivity, even among structurally similar

analytes like pesticides [154]. Initially applied in separation processes, MIPs are now being integrated with various types of transducers, providing enhanced long-term stability compared to biomolecular receptors. A widely used integration strategy in electrochemical MIP-based sensors involves direct electropolymerization of a monomer-target/template mixture on the transducer surface. For example, a label-free GLY-MIP sensor was developed by electro-synthesizing chitosan biopolymer at gold microelectrodes. EIS was used to monitor changes in impedance as the MIP cavities filled with the target analyte, showing good selectivity for GLY in the presence of other pesticides such as glufosinate chlorpyrifos, and phosmet [155]. Though this platform has not yet been tested on biological samples, promising results were observed in spiked river water samples.

MIPs can also be deposited on nanostructured surfaces. This approach enhances sensor performance in terms of selectivity and sensitivity due to the synergy of different modifiers. A common example involves the combination of MIPs with gold nanoparticles (**Au-NPs**), which have been widely used in colorimetric assays and surface-enhanced Raman spectroscopy (**SERS**)-based sensors for pesticide detection. Recently, a dual colorimetric/SERS platform was reported for atrazine detection in food samples, allowing both instrument-free detection and instrument-based quantification [156]. Another notable example involved the use of cysteine-functionalized Au-NPs in combination with ortho-phenylenediamine MIP for ethephon sensing [195]. This approach demonstrated good selectivity and cross-selectivity when tested against other pesticides (e.g., chlorothalonil, GLY, trichlorfon) and their mixtures. In conclusion, MIP-based sensing platforms offer a promising approach for the large-scale and rapid screening of pesticides in biological fluids, such as urine and blood. Despite the wide variety of sensors available for pesticide monitoring in water and food, only a few have reached the market, highlighting the ongoing challenges in scaling up these technologies.

1.8 Electrochemical Sensing Strategies for Haloacetic Acid Detection

Electrochemical sensing strategies for HAAs rely on direct and indirect detection approaches. In direct detection, the intrinsic electrochemical properties of HAAs are exploited to generate an analytical signal, such as their reduction behavior at an electrode surface. In contrast, indirect detection methods exploit intermediate species

or molecular recognition elements to transduce the presence of HAAs into a measurable signal. Selectivity is improved using modified electrodes with bioreceptors (e.g., enzymes, redox proteins), biomimetic layers, or nanomaterials, as already described for pesticide detection. These molecular recognition elements have been successfully integrated into biosensing platforms for environmental monitoring of HAAs in water systems [157–162].

1.8.1 Molecular Recognition Strategies

The most common molecular recognition elements in electrochemical HAAs biosensors include redox proteins such as hemoglobin (**Hb**) and myoglobin (**Mb**), which contain electroactive heme groups that facilitate electron transfer at electrode interfaces. While these proteins have demonstrated effective catalytic activity for HAA detection, their electroactive centers are often shielded by polypeptide structures, leading to limitations in sensitivity and selectivity [163]. To address this challenge, alternative recognition elements such as metal complexes, including porphyrins and phthalocyanines, have been employed. These synthetic analogs of heme proteins offer enhanced stability and improved catalytic performance in HAAs detection [164,165]. Enzyme-based recognition strategies have also been widely explored. HRP, for example, has been employed in electrochemical biosensors for HAAs by catalyzing reduction reactions that generate an electrochemical signal [161,166]. However, enzymes require precise environmental conditions to maintain stability, and pH variations or high temperatures can lead to denaturation, compromising sensor performance. To mitigate this issue, biocompatible film-forming agents such as chitosan and Nafion have been used to create protective microenvironments that stabilize enzyme activity and enhance biosensor longevity [167,168].

1.8.2 Molecularly Imprinted Polymers for HAAs

MIPs represent a promising alternative to biological recognition elements also for this class of analytes, offering high selectivity, long shelf life, and resistance to environmental fluctuations. Kibechu et al. developed an MIP-based electrochemical sensor incorporating reduced graphene oxide (**rGO**) for the selective detection of TCAA, achieving enhanced sensitivity and selectivity [169]. Similarly, Cetó et al. employed an MIP strategy using methacrylic acid and electropolymerized pyrrole for

the detection of HAAs in water, demonstrating improved detection limits and reduced cross-reactivity [170].

1.8.3 Electrode Modifications and Signal Amplification

Electrochemical sensors for HAA detection by direct electrochemical reduction rely on electrode modifications to enhance sensitivity, stability, and signal transduction efficiency. Two main classes of electrodes have been employed: metal electrodes and carbon-based electrodes. Among metal electrodes, silver-based materials have demonstrated exceptional efficiency in HAA detection due to their high conductivity, catalytic properties, and strong affinity for halogenated compounds. Silver electrodes have been used in combination with chemometric analysis techniques, such as principal component analysis and artificial neural networks, to achieve selective electrochemical detection of HAAs [171]. Silver nanoparticles (**AgNPs**) have also emerged as key components in electrochemical biosensing, serving as signal amplifiers that enhance electron transfer and improve detection sensitivity. In one study, a glassy carbon electrode functionalized with AgNPs and malic acid was developed for TCAA detection, demonstrating superior stability and reproducibility [172]. The use of AgNPs in conjunction with biomolecules such as hemoglobin has further improved the selectivity and sensitivity of electrochemical HAA sensors. A core-shell Au@Ag nanorod-based sensor, modified with hemoglobin and polyelectrolytes, achieved significantly enhanced detection limits for TCAA [173]. Beyond silver, other metal-based electrodes, including gold, have been explored for HAA detection. A miniaturized gold electrochemical sensor integrated with polydimethylsiloxane microfluidics was developed for the detection of DBAA and TBAA, demonstrating exceptional sensitivity with detection limits in the part-per-trillion range [174]. Carbon-based electrodes, including glassy carbon electrodes (**GCE**) and carbon paste electrodes (**CPE**), offer an alternative to metal electrodes due to their lower cost, ease of fabrication, and enhanced surface area for electrochemical reactions [164,172,175,176]. To further improve sensor performance, carbon-based electrodes have been modified with graphene and carbon nanotubes (**CNTs**), which provide superior electrical conductivity and increased surface area for analyte adsorption [177]. Hybrid graphene-CNT composite electrodes have shown significant improvements in

the detection of TCAA, achieving detection limits as low as 15.3 μM [159]. Additional electrode modifications have incorporated metal oxides and conductive polymers to enhance signal transduction. Metal oxides such as TiO_2, ZnO, and CuS have been integrated into electrode surfaces to provide catalytic activity for HAA reduction reactions [158,178–181]. Despite the significant advancements in electrochemical sensing of HAAs, several challenges remain. Many current sensing platforms are optimized for laboratory conditions and require further adaptation for real-world applications, including long-term stability in complex environmental matrices and scalability for widespread deployment. Furthermore, while direct electrochemical detection has shown promise, the development of hybrid sensing strategies incorporating molecular imprinting, nanomaterial-based enhancements, and multi-analyte detection capabilities will be critical in advancing HAA monitoring technologies. Future research should focus on integrating portable and cost-effective electrochemical biosensors into existing water quality monitoring frameworks. The incorporation of real-time data acquisition and wireless communication technologies could further enhance the practicality of electrochemical sensors for HAAs, enabling rapid response to contamination events. Ultimately, the continued refinement of electrode materials, recognition elements, and signal amplification techniques will drive the development of next-generation electrochemical biosensors for the accurate and reliable detection of HAAs in drinking water and environmental systems.

1.9 Conclusions

In the broader context of biological fluids monitoring, the discussion provides an overview of analytical methods proposed by the recent literature for the determination of CECs. Currently, screening tests based on optical or electrochemical sensors applicable in urine, saliva, or plasma are still limited, while chromatographic methods require simplification in sample pre-treatment stages. To address these gaps, we have analyzed recent advancements, emphasizing the importance of adapting existing sensor strategies and developing new chromatographic approaches. **Figure 1.6** provides a visual evaluation and comparison, which indirectly highlights the advantages of combining both approaches. From this comparison, we observe that sensing strategies can provide rapid, in-situ screening allowing the fast analysis of a large number of samples and to further analyze only the ones testing positive.

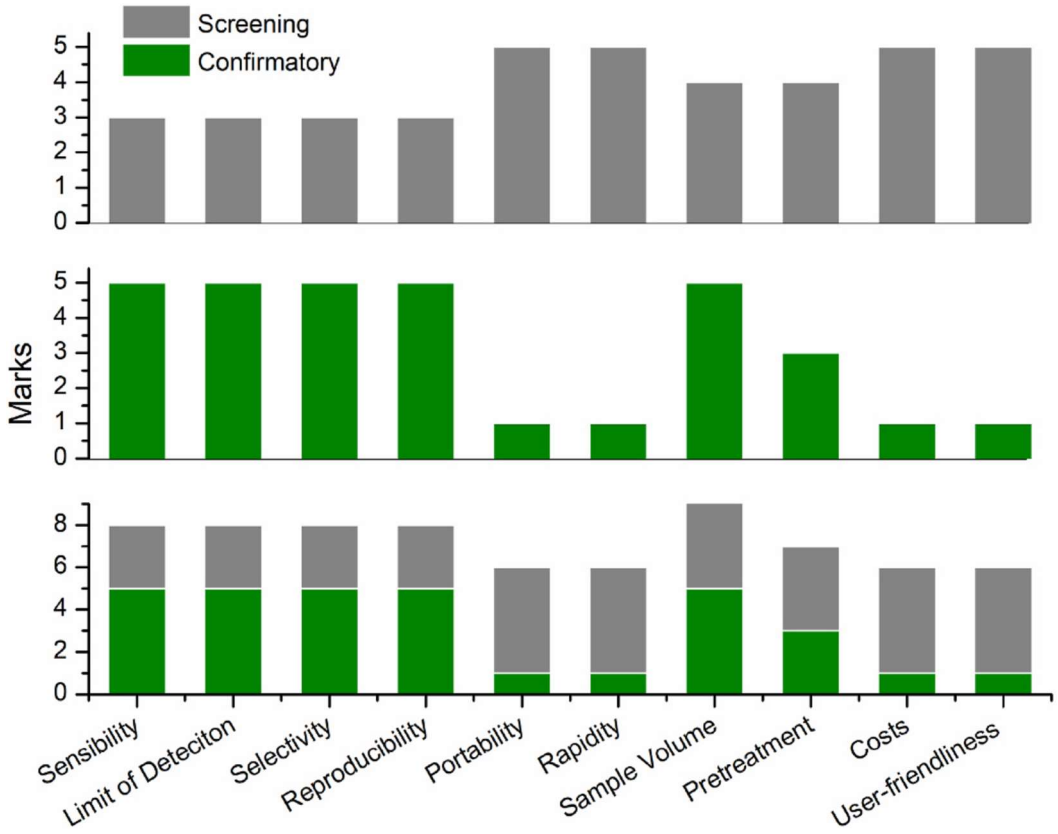

Figure 1.6) *Comparison of the discussed techniques in terms of sensitivity, selectivity, reproducibility, portability, rapidity, costs, amount of sample required, sample pretreatment and user-friendliness. Both screening and chromatographic methods have been evaluated with a grading scale from 1 to 5, where 1 corresponds to the poorest performance and 5 to best one. The lowest graph represents the complementary of the two approaches.*

Sensors can be miniaturized, coupled with microfluidic systes and automatized, reducing the overall costs and resulting in user-friendly devices. However, their performance in terms of sensitivity, LOD, selectivity and reproducibility, are lower compared to chromatographic methods, which are always needed for quantification. To design fully complementary sensing and chromatographic strategies for pesticides biomonitoring we need to identify common guidelines, to minimize the sample pre-treatments steps and to improve the regulation.

References

[1] S. Polesello, I. Cnr Brugherio, I CONTAMINANTI EMERGENTI NELLE ACQUE POTABILI: NUOVI APPROCCI NELLA LEGISLAZIONE EUROPEA E NEL MONITORAGGIO, n.d.

[2] A. Gogoi, P. Mazumder, V.K. Tyagi, G.G. Tushara Chaminda, A.K. An, M. Kumar, Occurrence and fate of emerging contaminants in water environment: A review, Groundw Sustain Dev 6 (2018) 169–180. https://doi.org/10.1016/j.gsd.2017.12.009.

[3] F.H. Frimmel, J.B. Jahnel, Formation of Haloforms in Drinking Water, in: A.D. Nikolaou (Ed.), Haloforms and Related Compounds in Drinking Water, Springer Berlin Heidelberg, Berlin, Heidelberg, 2003: pp. 1–19. https://doi.org/10.1007/978-3-540-44997-3_1.

[4] U.S. Environmental Protection Agency, National Primary Drinking Water Regulations, (2024). https://www.epa.gov/ground-water-and-drinking-water/national-primary-drinking-water-regulations (accessed March 9, 2025).

[5] World Health Organization, Guidelines for Drinking-water Quality FOURTH EDITION INCORPORATING THE FIRST ADDENDUM, 2017.

[6] C.J. Jack, J.D. Ellis, Integrated Pest Management Control of Varroa destructor (Acari: Varroidae), the Most Damaging Pest of (Apis mellifera L. (Hymenoptera: Apidae)) Colonies, Journal of Insect Science 21 (2021). https://doi.org/10.1093/jisesa/ieab058.

[7] S.O. Duke, Interaction of Chemical Pesticides and Their Formulation Ingredients with Microbes Associated with Plants and Plant Pests, J Agric Food Chem 66 (2018) 7553–7561. https://doi.org/10.1021/acs.jafc.8b02316.

[8] M.S. Tixier, Predatory mites (Acari: Phytoseiidae) in agro-ecosystems and conservation biological control: A review and explorative approach for forecasting plant-predatory mite interactions and mite dispersal, Front Ecol Evol 6 (2018). https://doi.org/10.3389/fevo.2018.00192.

[9] L.H. Swanepoel, C.M. Swanepoel, P.R. Brown, S.J. Eiseb, S.M. Goodman, M. Keith, F. Kirsten, H. Leirs, T.A.M. Mahlaba, R.H. Makundi, P. Malebane, E.F. Von Maltitz, A.W. Massawe, A. Monadjem, L.S. Mulungu, G.R. Singleton, P.J. Taylor, V. Soarimalala, S.R. Belmain, A systematic review of rodent pest research in Afro-Malagasy small-holder farming systems: Are we asking the right questions?, PLoS One 12 (2017). https://doi.org/10.1371/journal.pone.0174554.

[10] W.R. Reeves, M.K. McGuire, M. Stokes, J.L. Vicini, Assessing the Safety of Pesticides in Food: How Current Regulations Protect Human Health, Advances in Nutrition 10 (2019) 80–88. https://doi.org/10.1093/advances/nmy061.

[11] A. Sharma, V. Kumar, B. Shahzad, M. Tanveer, G.P.S. Sidhu, N. Handa, S.K. Kohli, P. Yadav, A.S. Bali, R.D. Parihar, O.I. Dar, K. Singh, S. Jasrotia, P. Bakshi, M. Ramakrishnan, S. Kumar, R. Bhardwaj, A.K. Thukral, Worldwide pesticide usage and its impacts on ecosystem, SN Appl Sci 1 (2019). https://doi.org/10.1007/s42452-019-1485-1.

[12] L.G. Costa, Toxicology of Pesticides: A Brief History, in: L.G. Costa, C.L. Galli, S.D. Murphy (Eds.), Toxicology of Pesticides, Springer Berlin Heidelberg, Berlin, Heidelberg, 1987: pp. 1–10.

[13] C.R. Fleming, V. Gartner, P. Valverde-Garcia, P. Geurs, C. Tiu, Comprehensive Analysis of the Value of Single Versus Multiple Year (Season) Crop Residue Data for Establishment of Maximum Residue Levels (MRLs), J Agric Food Chem 65 (2017) 1784–1791. https://doi.org/10.1021/acs.jafc.6b05106.

[14] R. FAOSTAT, FAOSTAT Database, Food and Agriculture Organization of the United Nations (FAO) (2017). https://www.fao.org/faostat/en/#home (accessed March 9, 2025).

[15] F. Maggi, F.H.M. Tang, D. la Cecilia, A. McBratney, PEST-CHEMGRIDS, global gridded maps of the top 20 crop-specific pesticide application rates from 2015 to 2025, Sci Data 6 (2019). https://doi.org/10.1038/s41597-019-0169-4.

[16] I. Shaw, R. Vannoort, 10 - Pesticides, in: D.H. Watson (Ed.), Food Chemical Safety, Woodhead Publishing, 2001: pp. 218–237. https://doi.org/https://doi.org/10.1533/9781855736320.2.218.

[17] D.J. MacLachlan, D. Hamilton, Estimation methods for Maximum Residue Limits for pesticides, Regulatory Toxicology and Pharmacology 58 (2010) 208–218. https://doi.org/https://doi.org/10.1016/j.yrtph.2010.05.012.

[18] M. Lykogianni, E. Bempelou, F. Karamaouna, K.A. Aliferis, Do pesticides promote or hinder sustainability in agriculture? The challenge of sustainable use of pesticides in modern agriculture, Science of the Total Environment 795 (2021). https://doi.org/10.1016/j.scitotenv.2021.148625.

[19] R. Kaur, G.K. Mavi, S. Raghav, I. Khan, Pesticides Classification and its Impact on Environment, Int J Curr Microbiol Appl Sci 8 (2019) 1889–1897. https://doi.org/10.20546/ijcmas.2019.803.224.

[20] Z. Singh, Toxic Effects of Organochlorine Pesticides: A Review, American Journal of BioScience 4 (2016) 11. https://doi.org/10.11648/j.ajbio.s.2016040301.13.

[21] L. Rani, K. Thapa, N. Kanojia, N. Sharma, S. Singh, A.S. Grewal, A.L. Srivastav, J. Kaushal, An extensive review on the consequences of chemical pesticides on human health and environment, J Clean Prod 283 (2021). https://doi.org/10.1016/j.jclepro.2020.124657.

[22] K.H. Kim, E. Kabir, S.A. Jahan, Exposure to pesticides and the associated human health effects, Science of the Total Environment 575 (2017) 525–535. https://doi.org/10.1016/j.scitotenv.2016.09.009.

[23] A.S.R.L. Brajesh Kumar Singh Ramesh Chander Kuhad, K.K. Tripathi, Biochemical and Molecular Basis of Pesticide Degradation by Microorganisms, Crit Rev Biotechnol 19 (1999) 197–225. https://doi.org/10.1080/0738-859991229242.

[24] K. Fenner, S. Canonica, L.P. Wackett, M. Elsner, Evaluating Pesticide Degradation in the Environment: Blind Spots and Emerging Opportunities, n.d. www.sciencemag.org.

[25] G.P. Satish, D.M. Ashokrao, S.K. Arun, Microbial degradation of pesticide: A review, Afr J Microbiol Res 11 (2017) 992–1012. https://doi.org/10.5897/ajmr2016.8402.

[26] S. Mishra, W. Zhang, Z. Lin, S. Pang, Y. Huang, P. Bhatt, S. Chen, Carbofuran toxicity and its microbial degradation in contaminated environments, Chemosphere 259 (2020). https://doi.org/10.1016/j.chemosphere.2020.127419.

[27] J.P.K. Gill, N. Sethi, A. Mohan, S. Datta, M. Girdhar, Glyphosate toxicity for animals, Environ Chem Lett 16 (2018) 401–426. https://doi.org/10.1007/s10311-017-0689-0.

[28] M. Attaullah, M.J. Yousuf, S. Shaukat, S.I. Anjum, M.J. Ansari, I.D. Buneri, M. Tahir, M. Amin, N. Ahmad, S.U. Khan, Serum organochlorine pesticides residues and risk of cancer: A case-control study, Saudi J Biol Sci 25 (2018) 1284–1290. https://doi.org/10.1016/j.sjbs.2017.10.023.

[29] Á.G. Polanco Rodríguez, M.I. Riba López, T.Á. DelValls Casillas, J.A. Araujo León, O. Mahjoub, A.K. Prusty, Monitoring of organochlorine pesticides in blood of women with uterine cervix cancer, Environmental Pollution 220 (2017) 853–862. https://doi.org/10.1016/j.envpol.2016.10.068.

[30] M. Koureas, F. Karagkouni, V. Rakitskii, C. Hadjichristodoulou, A. Tsatsakis, A. Tsakalof, Serum levels of organochlorine pesticides in the general population of Thessaly, Greece, determined by HS-SPME GC-MS method, Environ Res 148 (2016) 318–321. https://doi.org/10.1016/j.envres.2016.04.015.

[31] R. Haque, T. Inaoka, M. Fujimura, A.S. Ahmad, D. Ueno, Intake of DDT and its metabolites through food items among reproductive age women in Bangladesh, Chemosphere 189 (2017) 744–751. https://doi.org/10.1016/j.chemosphere.2017.09.041.

[32] A. Philbert, S.L. Lyantagaye, G. Pradel, C.J. Ngwa, G. Nkwengulila, Pyrethroids and DDT tolerance of Anopheles gambiae s.l. from Sengerema District, an area of intensive pesticide usage in north-western Tanzania, Tropical Medicine and International Health 22 (2017) 388–398. https://doi.org/10.1111/tmi.12850.

[33] J. Ma, L. bo Pan, X. yang Yang, X. ling Liu, S. yang Tao, L. Zhao, X. peng Qin, Z. jin Sun, H. Hou, Y. zhang Zhou, DDT, DDD, and DDE in soil of Xiangfen County, China: Residues, sources, spatial distribution, and health risks, Chemosphere 163 (2016) 578–583. https://doi.org/10.1016/j.chemosphere.2016.08.050.

[34] M. Aamir, S. Khan, J. Nawab, Z. Qamar, A. Khan, Tissue distribution of HCH and DDT congeners and human health risk associated with consumption of fish collected from Kabul River, Pakistan, Ecotoxicol Environ Saf 125 (2016) 128–134. https://doi.org/10.1016/j.ecoenv.2015.12.005.

[35] J. Beard, DDT and human health, Science of the Total Environment 355 (2006) 78–89. https://doi.org/10.1016/j.scitotenv.2005.02.022.

[36] P.J.E. Quintana, R.J. Delfino, S. Korrick, A. Ziogas, F.W. Kutz, E.L. Jones, F. Laden, E. Garshick, Adipose tissue levels of organochlorine pesticides and polychlorinated biphenyls and risk of non-Hodgkin's lymphoma, Environ Health Perspect 112 (2004) 854–861. https://doi.org/10.1289/ehp.6726.

[37] N.R. Reed, L.O. Lim, Organophosphate Insecticides: Neurodevelopmental Effects, n.d. http://www.cdpr.ca.gov.

[38] S.O. Duke, The history and current status of glyphosate, Pest Manag Sci 74 (2018) 1027–1034. https://doi.org/10.1002/ps.4652.

[39] M. Kwiatkowska, B. Huras, B. Bukowska, The effect of metabolites and impurities of glyphosate on human erythrocytes (in vitro), Pestic Biochem Physiol 109 (2014) 34–43. https://doi.org/10.1016/j.pestbp.2014.01.003.

[40] S.H. Bai, S.M. Ogbourne, Glyphosate: environmental contamination, toxicity and potential risks to human health via food contamination, Environmental Science and Pollution Research 23 (2016) 18988–19001. https://doi.org/10.1007/s11356-016-7425-3.

[41] M. Cycoń, A. Mrozik, Z. Piotrowska-Seget, Bioaugmentation as a strategy for the remediation of pesticide-polluted soil: A review, Chemosphere 172 (2017) 52–71. https://doi.org/10.1016/j.chemosphere.2016.12.129.

[42] Z. Cai, J. Wang, J. Ma, X. Zhu, J. Cai, G. Yang, Anaerobic Degradation Pathway of the Novel Chiral Insecticide Paichongding and Its Impact on Bacterial Communities in Soils, J Agric Food Chem 63 (2015) 7151–7160. https://doi.org/10.1021/acs.jafc.5b02645.

[43] A. Chrustek, I. Hołyńska-Iwan, I. Dziembowska, J. Bogusiewicz, M. Wróblewski, A. Cwynar, D. Olszewska-Słonina, Current research on the safety of pyrethroids used as insecticides, Medicina (Lithuania) 54 (2018). https://doi.org/10.3390/medicina54040061.

[44] A. Goel, P. Aggarwal, Terms and conditions Privacy policy Pesticide poisoning, 2007. https://www.scopus.com/inward/record.uri?eid=2-s2.0-38649085051&partnerID=40&md5=a00295c8ec3d3170a45ee3da582544.

[45] M.K. Morgan, Children's exposures to pyrethroid insecticides at home: a review of data collected in published exposure measurement studies conducted in the United States., Int J Environ Res Public Health 9 (2012) 2964–2985. https://doi.org/10.3390/ijerph9082964.

[46] S. Ferland, J. Côté, M. Ratelle, R. Thuot, M. Bouchard, Detailed Urinary Excretion Time Courses of Biomarkers of Exposure to Permethrin and Estimated Exposure in Workers of a Corn Production Farm in Quebec, Canada, Ann Occup Hyg 59 (2015) 1152–1167. https://doi.org/10.1093/annhyg/mev059.

[47] P. Iwaniuk, A. Borusiewicz, B. Lozowicka, Fluazinam and its mixtures induce diversified changes of crucial biochemical and antioxidant profile in leafy vegetable, Sci Hortic 298 (2022). https://doi.org/10.1016/j.scienta.2022.110988.

[48] Y. Song, L. Li, C. Li, Z. Lu, X. Men, F. Chen, Evaluating the sensitivity and efficacy of fungicides with different modes of action against botryosphaeria dothidea, Plant Dis 102 (2018) 1785–1793. https://doi.org/10.1094/PDIS-01-18-0118-RE.

[49] J. Liao, L. Luo, L. Zhang, L. Wang, X. Shi, H. Yang, S. Tan, L. Tan, X. Liu, D. Wang, Z. Mao, Comparison of the effects of three fungicides on clubroot disease of tumorous stem mustard and soil bacterial community, J Soils Sediments 22 (2022) 256–271. https://doi.org/10.1007/s11368-021-03073-z.

[50] M.A. Peterson, S.A. McMaster, D.E. Riechers, J. Skelton, P.W. Stahlman, 2,4-D Past, Present, and Future: A Review, Weed Technology 30 (2016) 303–345. https://doi.org/10.1614/wt-d-15-00131.1.

[51] M.D. Reuber, CARCINOGENICITY AND TOXICITY OF 2,4-DICHLOROPHENOXY-ACETIC ACID, 1983.

[52] B. Zhang, C. Li, Y. Zhang, M. Yuan, J. Wang, J. Zhu, J. Ji, Y. Ma, Improved photocatalyst: Elimination of triazine herbicides by novel phosphorus and boron co-doping graphite carbon nitride, Science of the Total Environment 757 (2021). https://doi.org/10.1016/j.scitotenv.2020.143810.

[53] X. Yu, R. Zhang, H. Liu, Z. Zhang, X. Shi, A. Sun, J. Chen, Highly-selective complex matrices removal via a modified QuEChERS for determination of triazine herbicide residues and risk assessment in bivalves, Food Chem 347 (2021). https://doi.org/10.1016/j.foodchem.2021.129030.

[54] J.T. Sun, L.L. Pan, Y. Zhan, D.C.W. Tsang, L.Z. Zhu, X.D. Li, Atrazine contamination in agricultural soils from the Yangtze River Delta of China and associated health risks, Environ Geochem Health 39 (2017) 369–378. https://doi.org/10.1007/s10653-016-9853-x.

[55] S. Singh, V. Kumar, A. Chauhan, S. Datta, A.B. Wani, N. Singh, J. Singh, Toxicity, degradation and analysis of the herbicide atrazine, Environ Chem Lett 16 (2018) 211–237. https://doi.org/10.1007/s10311-017-0665-8.

[56] V. Cutillas, F. Jesús, C. Ferrer, A.R. Fernández-Alba, Overcoming difficulties in the evaluation of captan and folpet residues by supercritical fluid chromatography coupled to mass spectrometry, Talanta 223 (2021). https://doi.org/10.1016/j.talanta.2020.121714.

[57] European Union, Directive (EU) 2020/2184 of the European Parliament and of the Council of 16 December 2020 on the quality of water intended for human consumption, 2020. https://eur-lex.europa.eu/eli/dir/2020/2184/oj/eng (accessed March 9, 2025).

[58] J.A. Pals, J.K. Ang, E.D. Wagner, M.J. Plewa, Biological Mechanism for the Toxicity of Haloacetic Acid Drinking Water Disinfection Byproducts, Environ Sci Technol 45 (2011) 5791–5797. https://doi.org/10.1021/es2008159.

[59] S. Llana-Belloch, J.I. Priego Quesada, P. Pérez-Soriano, Á.G. Lucas-Cuevas, A. Salvador-Pascual, G. Olaso-González, Y. Moliner-Martinez, J. Verdú-Andres, P. Campins-Falco, M.C. Gómez-Cabrera, Disinfection by-products effect on swimmers oxidative stress and respiratory damage, Eur J Sport Sci 16 (2016) 609–617. https://doi.org/10.1080/17461391.2015.1080306.

[60] I.R. Schultz, J.L. Merdink, A. Gonza-Lez-Leon, R.J. Bull, Comparative Toxicokinetics of Chlorinated and Brominated Haloacetates in F344 Rats, 1999. http://www.idealibrary.com.

[61] M.G. Narotsky, L.S. Fuentes, O. Ola, T.L. Willoughby, K. Lucas, Developmental Toxicity of Disinfection Byproducts in F344 Rats: Effects on Pregnancy Maintenance and Eye Development, Birth Defects Res 117 (2025) e2427. https://doi.org/https://doi.org/10.1002/bdr2.2427.

[62] R.J. Nathanael, L.N. Adyanis, K. Oginawati, The last decade epidemiologic concern of drinking water contaminants of emerging concern (CECs) in Asian Countries: A scoping review, Heliyon 10 (2024). https://doi.org/10.1016/j.heliyon.2024.e39236.

[63] W. Zhang, L. Wang, Y. Yang, P. Gaskin, K.S. Teng, Recent Advances on Electrochemical Sensors for the Detection of Organic Disinfection Byproducts in Water, ACS Sens 4 (2019) 1138–1150. https://doi.org/10.1021/acssensors.9b00272.

[64] M.J. Cardador, M. Gallego, Determination of haloacetic acids in human urine by headspace gas chromatography–mass spectrometry, Journal of Chromatography B 878 (2010) 1824–1830. https://doi.org/https://doi.org/10.1016/j.jchromb.2010.05.022.

[65] F. S. Ligler, C. R. Taitt, Optical Biosensors: Present and Future, 2000.

[66] E. Bakker, Electrochemical Sensors, Anal Chem 76 (2004) 3285–3298. https://doi.org/10.1021/ac049580z.

[67] P. Kebarle, L. Tang, From ions in solution to ions in the gas phase - the mechanism of electrospray mass spectrometry, Anal Chem 65 (1993) 972A-986A. https://doi.org/10.1021/ac00070a001.

[68] S.L.R. Ellison, M. Thompson, Standard additions: Myth and reality, Analyst 133 (2008) 992–997. https://doi.org/10.1039/b717660k.

[69] B.K. Matuszewski, M.L. Constanzer, C.M. Chavez-Eng, Strategies for the Assessment of Matrix Effect in Quantitative Bioanalytical Methods Based on HPLC−MS/MS, Anal Chem 75 (2003) 3019–3030. https://doi.org/10.1021/ac020361s.

[70] B.K. Matuszewski, Standard line slopes as a measure of a relative matrix effect in quantitative HPLC–MS bioanalysis, Journal of Chromatography B 830 (2006) 293–300. https://doi.org/https://doi.org/10.1016/j.jchromb.2005.11.009.

[71] I. Fu, E.J. Woolf, B.K. Matuszewski, Effect of the sample matrix on the determination of indinavir in human urine by HPLC with turbo ion spray tandem mass spectrometric detection1Presented in part at the 8th International Symposium on Pharmaceutical and Biomedical Analysis, Orlando, Florida, May 4–8, 1997. Abstracts M-L9 and M/P-A9.1, J Pharm Biomed Anal 18 (1998) 347–357. https://doi.org/https://doi.org/10.1016/S0731-7085(98)00048-X.

[72] R. Ulber, J.-G. Frerichs, S. Beutel, Optical sensor systems for bioprocess monitoring, Anal Bioanal Chem 376 (2003) 342–348. https://doi.org/10.1007/s00216-003-1930-1.

[73] J.Y. Lichtenberg, Y. Ling, S. Kim, Non-specific adsorption reduction methods in biosensing, Sensors (Switzerland) 19 (2019). https://doi.org/10.3390/s19112488.

[74] F. Höök, J. Vörös, M. Rodahl, R. Kurrat, P. Böni, J.J. Ramsden, M. Textor, N.D. Spencer, P. Tengvall, J. Gold, B. Kasemo, A comparative study of protein adsorption on titanium oxide surfaces using in situ ellipsometry, optical waveguide lightmode spectroscopy, and quartz crystal microbalance/dissipation, Colloids Surf B Biointerfaces 24 (2002) 155–170. https://doi.org/https://doi.org/10.1016/S0927-7765(01)00236-3.

[75] M. Beyer, T. Felgenhauer, F. Ralf Bischoff, F. Breitling, V. Stadler, A novel glass slide-based peptide array support with high functionality resisting non-specific protein adsorption, Biomaterials 27 (2006) 3505–3514. https://doi.org/https://doi.org/10.1016/j.biomaterials.2006.01.046.

[76] S. VandeVondele, J. Vörös, J.A. Hubbell, RGD-grafted poly-L-lysine-graft-(polyethylene glycol) copolymers block non-specific protein adsorption while promoting cell adhesion, Biotechnol Bioeng 82 (2003) 784–790. https://doi.org/10.1002/bit.10625.

[77] G. Liu, Grand Challenges in Biosensors and Biomolecular Electronics, Front Bioeng Biotechnol 9 (2021). https://doi.org/10.3389/fbioe.2021.707615.

[78] Y. Fu, W. Li, F. Picard, Assessment of matrix effect in quantitative LC-MS bioanalysis, Bioanalysis 16 (2024) 631–634. https://doi.org/10.4155/bio-2024-0047.

[79] T.M. Annesley, Ion Suppression in Mass Spectrometry, Clin Chem 49 (2003) 1041–1044. https://doi.org/10.1373/49.7.1041.

[80] O. González, A.C. Dubbelman, T. Hankemeier, Postcolumn Infusion as a Quality Control Tool for LC-MS-Based Analysis, J Am Soc Mass Spectrom 33 (2022) 1077–1080. https://doi.org/10.1021/jasms.2c00022.

[81] R.B. Costa, P.R. Camiloti, C.A. Sabatini, C.E.D. dos Santos, P.C.F. Lima Gomes, M.Â.T. Adorno, Matrix Effect Assessment of an Ion Chromatographic Method to Determine Inorganic Anions in Wastewater, Water Air Soil Pollut 229 (2018) 212. https://doi.org/10.1007/s11270-018-3863-5.

[82] J. Pang, Y. Huang, Y. Liu, W. Huang, Applications of ion chromatography in urine analysis: A review, J Chromatogr A 1706 (2023) 464231. https://doi.org/https://doi.org/10.1016/j.chroma.2023.464231.

[83] F. Raposo, D. Barceló, Challenges and strategies of matrix effects using chromatography-mass spectrometry: An overview from research versus regulatory viewpoints, TrAC Trends in Analytical Chemistry 134 (2021) 116068. https://doi.org/https://doi.org/10.1016/j.trac.2020.116068.

[84] Y. Han, L. Song, P. Zhao, Y. Li, N. Zou, Y. Qin, X. Li, C. Pan, Residue determination of glufosinate in plant origin foods using modified Quick Polar Pesticides (QuPPe) method and liquid chromatography coupled with tandem mass spectrometry, Food Chem 197 (2016) 730–736. https://doi.org/https://doi.org/10.1016/j.foodchem.2015.11.021.

[85] M. Montemurro, L. Pinto, G. Véras, A. de Araújo Gomes, M.J. Culzoni, M.C. Ugulino de Araújo, H.C. Goicoechea, Highly sensitive quantitation of pesticides in fruit juice samples by modeling four-way data gathered with high-performance liquid chromatography with fluorescence excitation-emission detection, Talanta 154 (2016) 208–218. https://doi.org/https://doi.org/10.1016/j.talanta.2016.03.078.

[86] B. Gao, G. Poma, G. Malarvannan, C. Dumitrascu, M. Bastiaensen, M. Wang, A. Covaci, Development of an analytical method based on solid-phase extraction and LC-MS/MS for the monitoring of current-use pesticides and their metabolites in human urine, Journal of Environmental Sciences 111 (2022) 153–163. https://doi.org/https://doi.org/10.1016/j.jes.2021.03.029.

[87] A.J. Li, M.P. Martinez-Moral, K. Kannan, Variability in urinary neonicotinoid concentrations in single-spot and first-morning void and its association with oxidative stress markers, Environ Int 135 (2020). https://doi.org/10.1016/j.envint.2019.105415.

[88] D. Chen, H. Miao, Y. Zhao, Y. Wu, A simple liquid chromatography-high resolution mass spectrometry method for the determination of glyphosate and aminomethylphosphonic acid in human urine using cold-induced phase separation and hydrophilic pipette tip solid-phase extraction, J Chromatogr A 1587 (2019) 73–78. https://doi.org/https://doi.org/10.1016/j.chroma.2018.11.030.

[89] D. Chen, H. Miao, Y. Zhao, Y. Wu, A simple liquid chromatography-high resolution mass spectrometry method for the determination of glyphosate and aminomethylphosphonic acid in human urine using cold-induced phase separation and hydrophilic pipette tip solid-phase extraction, J Chromatogr A 1587 (2019) 73–78. https://doi.org/10.1016/j.chroma.2018.11.030.

[90] N.P. Nørskov, S.K. Jensen, M.T. Sørensen, Robust and highly sensitive micro liquid chromatography–tandem mass spectrometry method for analyses of polar pesticides (glyphosate, aminomethylphosfonic acid, N-acetyl glyphosate and N-acetyl aminomethylphosfonic acid) in multiple biological matrices, J Chromatogr A 1605 (2019). https://doi.org/10.1016/j.chroma.2019.06.064.

[91] Review of the existing maximum residue levels for glyphosate according to Article 12 of Regulation (EC) No 396/2005, EFSA Journal 16 (2018). https://doi.org/10.2903/j.efsa.2018.5263.

[92] A. Schütze, P. Morales-Agudelo, M. Vidal, A.M. Calafat, M. Ospina, Quantification of glyphosate and other organophosphorus compounds in human urine via ion chromatography isotope dilution tandem mass spectrometry, Chemosphere 274 (2021). https://doi.org/10.1016/j.chemosphere.2020.129427.

[93] H. Zhang, X. Liu, Z. Huo, H. Sun, F. Zhang, B. Zhu, An ion chromatography tandem mass spectrometry (IC-MS/MS) method for glyphosate and amino methyl phosphoric acid in serum of occupational workers, Microchemical Journal 170 (2021) 106614. https://doi.org/https://doi.org/10.1016/j.microc.2021.106614.

[94] M.S.R.P.C.B. Matteo Feltracco Elena Barbaro, A. Gambaro, Detection of glyphosate residues in feed, saliva, urine and faeces from a cattle farm: a pilot study, Food Additives & Contaminants: Part A 39 (2022) 1248–1254. https://doi.org/10.1080/19440049.2022.2066194.

[95] E.A. Moawed, A.M. Radwan, Application of acid modified polyurethane foam surface for detection and removing of organochlorine pesticides from wastewater, Journal of Chromatography B 1044–1045 (2017) 95–102. https://doi.org/https://doi.org/10.1016/j.jchromb.2016.12.041.

[96] Z. Xiao, M. He, B. Chen, B. Hu, Polydimethylsiloxane/metal-organic frameworks coated stir bar sorptive extraction coupled to gas chromatography-flame photometric detection for the determination of organophosphorus pesticides in environmental water samples, Talanta 156–157 (2016) 126–133. https://doi.org/https://doi.org/10.1016/j.talanta.2016.05.001.

[97] A. Salemi, R. Rasoolzadeh, M.M. Nejad, M. Vosough, Ultrasonic assisted headspace single drop micro-extraction and gas chromatography with nitrogen-phosphorus detector for determination of organophosphorus pesticides in soil, Anal Chim Acta 769 (2013) 121–126. https://doi.org/https://doi.org/10.1016/j.aca.2013.01.054.

[98] A. Samsidar, S. Siddiquee, S.M. Shaarani, A review of extraction, analytical and advanced methods for determination of pesticides in environment and foodstuffs, Trends Food Sci Technol 71 (2018) 188–201. https://doi.org/https://doi.org/10.1016/j.tifs.2017.11.011.

[99] A.M. Muscalu, T. Górecki, Comprehensive two-dimensional gas chromatography in environmental analysis, TrAC Trends in Analytical Chemistry 106 (2018) 225–245. https://doi.org/https://doi.org/10.1016/j.trac.2018.07.001.

[100] P. He, D.S. Aga, Comparison of GC-MS/MS and LC-MS/MS for the analysis of hormones and pesticides in surface waters: advantages and pitfalls, Analytical Methods 11 (2019) 1436–1448. https://doi.org/10.1039/C8AY02774A.

[101] V.C. Fernandes, V.F. Domingues, C. Delerue-Matos, N. Mateus, Determination of Pesticides in Fruit and Fruit Juices by Chromatographic Methods. An Overview, J Chromatogr Sci 49 (2011) 715–730. https://doi.org/10.1093/chrsci/49.9.715.

[102] J.M. Kokosa, Advances in solvent-microextraction techniques, TrAC Trends in Analytical Chemistry 43 (2013) 2–13. https://doi.org/https://doi.org/10.1016/j.trac.2012.09.020.

[103] M. Anastassiades, S.J. Lehotay, D. Štajnbaher, F.J. Schenck, Fast and Easy Multiresidue Method Employing Acetonitrile Extraction/Partitioning and “Dispersive Solid-Phase Extraction” for the Determination of Pesticide Residues in Produce, J AOAC Int 86 (2003) 412–431. https://doi.org/10.1093/jaoac/86.2.412.

[104] R. Cazorla-Reyes, J.L. Fernández-Moreno, R. Romero-González, A.G. Frenich, J.L.M. Vidal, Single solid phase extraction method for the simultaneous analysis of polar and non-polar pesticides in urine samples by gas chromatography and ultra high pressure liquid chromatography coupled to tandem mass spectrometry, Talanta 85 (2011) 183–196. https://doi.org/https://doi.org/10.1016/j.talanta.2011.03.048.

[105] N.I.P. Valente, S. Tarelho, A.L. Castro, A. Silvestre, H.M. Teixeira, Analysis of organophosphorus pesticides in whole blood by GC-MS-μECD with forensic purposes, J Forensic Leg Med 33 (2015) 28–34. https://doi.org/https://doi.org/10.1016/j.jflm.2015.03.006.

[106] W. Naksen, T. Prapamontol, A. Mangklabruks, S. Chantara, P. Thavornyutikarn, M.G. Robson, P.B. Ryan, D.B. Barr, P. Panuwet, A single method for detecting 11 organophosphate pesticides in human plasma and breastmilk using GC-FPD, Journal of Chromatography B 1025 (2016) 92–104. https://doi.org/https://doi.org/10.1016/j.jchromb.2016.04.045.

[107] J. Fang, H. Zhao, Y. Zhang, Y. He, Q. Sun, S. Xu, Z. Cai, Performance of atmospheric pressure gas chromatography-tandem mass spectrometry for the analysis of organochlorine pesticides in human serum, Anal Bioanal Chem 411 (2019) 4185–4191. https://doi.org/10.1007/s00216-019-01822-1.

[108] J. Fang, Q. Wu, Y. Zhao, H. Zhao, S. Xu, Z. Cai, Comparison of different mass spectrometric approaches coupled to gas chromatography for the analysis of organochlorine pesticides in serum samples, Journal of Chromatography B 1040 (2017) 180–185. https://doi.org/https://doi.org/10.1016/j.jchromb.2016.12.001.

[109] M. Anastassiades, ; D I Kolberg, ; D Mack, ; A Barth, C. Wildgrube, ; D Roux, EU Reference Laboratory for pesticides requiring Single Residue Methods (EURL-SRM) Quick Method for the Analysis of Residues of numerous Highly Polar Pesticides in Food Commodities involving Simultane-ous Extraction with Methanol and Determination via LC-MS/MS (QuPPe-AO-Method) II. Food of Animal Origin, n.d.

[110] S. Iqbal, M.M. Iqbal, M. Javed, A. Bahadur, S. Yasien, Najam-ud-din, A. Hurr, N. Ahmad, M. Raheel, G. Liu, Modified QuEChERS extraction method followed by simultaneous quantitation of nine multi-class pesticides in human blood and urine by using GC-MS, Journal of Chromatography B 1152 (2020) 122227. https://doi.org/https://doi.org/10.1016/j.jchromb.2020.122227.

[111] K. van Veldhoven, P. Keski-Rahkonen, D.K. Barupal, C.M. Villanueva, L. Font-Ribera, A. Scalbert, B. Bodinier, J.O. Grimalt, C. Zwiener, J. Vlaanderen, L. Portengen, R. Vermeulen, P. Vineis, M. Chadeau-Hyam, M. Kogevinas, Effects of exposure to water disinfection by-products in a swimming pool: A metabolome-wide association study, Environ Int 111 (2018) 60–70. https://doi.org/10.1016/j.envint.2017.11.017.

[112] Z. Kuklenyik, D.L. Ashley, A.M. Calafat, Quantitative detection of trichloroacetic acid in human urine using isotope dilution high-performance liquid chromatography - Electrospray ionization tandem mass spectrometry, Anal Chem 74 (2002) 2058–2063. https://doi.org/10.1021/ac011250g.

[113] L.A. Salas, E. Gracia-Lavedan, F. Goñi, V. Moreno, C.M. Villanueva, Use of urinary trichloroacetic acid as an exposure biomarker of disinfection by-products in cancer studies, Environ Res 135 (2014) 276–284. https://doi.org/10.1016/j.envres.2014.09.018.

[114] F. Wu, W. Gabryelski, K. Froese, Improved gas chromatography methods for micro-volume analysis of haloacetic acids in water and biological matrices, Analyst 127 (2002) 1318–1323. https://doi.org/10.1039/b204574e.

[115] W.-S. Zhou, L. Xu, S.-H. Xie, Y.-L. Li, L. Li, Q. Zeng, Y.-K. Du, W.-Q. Lu, Decreased birth weight in relation to maternal urinary trichloroacetic acid levels, Science of The Total Environment 416 (2012) 105–110. https://doi.org/https://doi.org/10.1016/j.scitotenv.2011.10.073.

[116] L.A. Zambrano-Intriago, C.G. Amorim, J.M. Rodríguez-Díaz, A.N. Araújo, M.C.B.S.M. Montenegro, Challenges in the design of electrochemical sensor for glyphosate-based on new materials and biological recognition, Science of The Total Environment 793 (2021) 148496. https://doi.org/https://doi.org/10.1016/j.scitotenv.2021.148496.

[117] H.Y.K. Chuang, W.F. King, R.G. Mason, Interaction of plasma proteins with artificial surfaces: protein adsorption isotherms, J Lab Clin Med 92 (1978) 483–496. https://doi.org/10.5555/uri:pii:0022214378900185.

[118] A. Frutiger, A. Tanno, S. Hwu, R.F. Tiefenauer, J. Vörös, N. Nakatsuka, Nonspecific Binding—Fundamental Concepts and Consequences for Biosensing Applications, Chem Rev 121 (2021) 8095–8160. https://doi.org/10.1021/acs.chemrev.1c00044.

[119] J.S. Santos, M.S. Pontes, E.F. Santiago, A.R. Fiorucci, G.J. Arruda, An efficient and simple method using a graphite oxide electrochemical sensor for the determination of glyphosate in environmental samples, Science of The Total Environment 749 (2020) 142385. https://doi.org/https://doi.org/10.1016/j.scitotenv.2020.142385.

[120] Q. Kong, X. Shi, W. Ma, F. Zhang, T. Yu, F. Zhao, D. Zhao, C. Wei, Strategies to improve the adsorption properties of graphene-based adsorbent towards heavy metal ions and their compound pollutants: A review, J Hazard Mater 415 (2021) 125690. https://doi.org/https://doi.org/10.1016/j.jhazmat.2021.125690.

[121] P.C. Oliveira, E.M. Maximiano, P.A. Oliveira, J.S. Camargo, A.R. Fiorucci, G.J. Arruda, Direct electrochemical detection of glyphosate at carbon paste electrode and its determination in samples of milk, orange juice, and agricultural formulation, Journal of Environmental Science and Health, Part B 53 (2018) 817–823. https://doi.org/10.1080/03601234.2018.1505081.

[122] R. Jiang, Y.-H. Pang, Q.-Y. Yang, C.-Q. Wan, X.-F. Shen, Copper porphyrin metal-organic framework modified carbon paper for electrochemical sensing of glyphosate, Sens Actuators B Chem 358 (2022) 131492. https://doi.org/https://doi.org/10.1016/j.snb.2022.131492.

[123] M.-B. Gholivand, A. Akbari, L. Norouzi, Development of a novel hollow fiber- pencil graphite modified electrochemical sensor for the ultra-trace analysis of glyphosate, Sens Actuators B Chem 272 (2018) 415–424. https://doi.org/https://doi.org/10.1016/j.snb.2018.05.170.

[124] C. Zhang, X. Liang, Y. Lu, H. Li, X. Xu, Performance of CUAL-LDH/GR nanocomposite-based electrochemical sensor with regard to trace glyphosate detection in water, Sensors (Switzerland) 20 (2020) 1–16. https://doi.org/10.3390/s20154146.

[125] J. Sheals, P. Persson, B. Hedman, IR and EXAFS Spectroscopic Studies of Glyphosate Protonation and Copper(II) Complexes of Glyphosate in Aqueous Solution, Inorg Chem 40 (2001) 4302–4309. https://doi.org/10.1021/ic000849g.

[126] T. Undabeytia, E. Morillo, C. Maqueda, FTIR Study of Glyphosate−Copper Complexes, J Agric Food Chem 50 (2002) 1918–1921. https://doi.org/10.1021/jf010988w.

[127] F. Pino, C.C. Mayorga-Martinez, A. Merkoçi, High-performance sensor based on copper oxide nanoparticles for dual detection of phenolic compounds and a pesticide, Electrochem Commun 71 (2016) 33–37. https://doi.org/https://doi.org/10.1016/j.elecom.2016.08.001.

[128] P. Sakdarat, J. Chongsuebsirikul, C. Thanachayanont, S. Prichanont, P. Pungetmongkol, Development of a Nonenzymatic Electrochemical Sensor for Organophosphate Pesticide Detection Using Copper (II) Oxide Nanorod Electrodes, J Nanomater 2021 (2021) 6623668. https://doi.org/https://doi.org/10.1155/2021/6623668.

[129] M. del C. Aguirre, S.E. Urreta, C.G. Gomez, A Cu2+-Cu/glassy carbon system for glyphosate determination, Sens Actuators B Chem 284 (2019) 675–683. https://doi.org/https://doi.org/10.1016/j.snb.2018.12.124.

[130] Y.I. Moharram, I.S. El-Hallag, S.M. Selim, Quantitative Evaluation of Generic Glyphosate Using Carbon Paste Electrode Electrochemically Modified with Copper Ions, Russian Journal of Electrochemistry 57 (2021) 644–653. https://doi.org/10.1134/S1023193520120150.

[131] S. Poorahong, C. Thammakhet, P. Thavarungkul, P. Kanatharana, One-step preparation of porous copper nanowires electrode for highly sensitive and stable amperometric detection of glyphosate, 69 (2015) 385–394. https://doi.org/doi:10.1515/chempap-2015-0038.

[132] C. Gu, Q. Wang, L. Zhang, P. Yang, Y. Xie, J. Fei, Ultrasensitive non-enzymatic pesticide electrochemical sensor based on HKUST-1-derived copper oxide @ mesoporous carbon composite, Sens Actuators B Chem 305 (2020) 127478. https://doi.org/https://doi.org/10.1016/j.snb.2019.127478.

[133] J.M. Gonçalves, P.R. Martins, D.P. Rocha, T.A. Matias, M.S.S. Julião, R.A.A. Munoz, L. Angnes, Recent trends and perspectives in electrochemical sensors based on MOF-derived materials, J Mater Chem C Mater 9 (2021) 8718–8745. https://doi.org/10.1039/d1tc02025k.

[134] X. Shi, J. Sun, Y. Yao, H. Liu, J. Huang, Y. Guo, X. Sun, Novel electrochemical aptasensor with dual signal amplification strategy for detection of acetamiprid, Science of The Total Environment 705 (2020) 135905. https://doi.org/https://doi.org/10.1016/j.scitotenv.2019.135905.

[135] D. Heineke, S.J. Franklin, K.N. Raymond, Coordination Chemistry of Glyphosate: Structural and Spectroscopic Characterization of Bis(glyphosate)metal(III) Complexes, Inorg Chem 33 (1994) 2413–2421. https://doi.org/10.1021/ic00089a017.

[136] J.S. Noori, M. Dimaki, J. Mortensen, W.E. Svendsen, Detection of glyphosate in drinking water: A fast and direct detection method without sample pretreatment, Sensors (Switzerland) 18 (2018). https://doi.org/10.3390/s18092961.

[137] C. Peillex, M. Pelletier, The impact and toxicity of glyphosate and glyphosate-based herbicides on health and immunity, J Immunotoxicol 17 (2020) 163–174. https://doi.org/10.1080/1547691X.2020.1804492.

[138] P. Butmee, G. Tumcharern, C. Songsiriritthigul, M.J. Durand, G. Thouand, M. Kerr, K. Kalcher, A. Samphao, Enzymatic electrochemical biosensor for glyphosate detection based on acid phosphatase inhibition, Anal Bioanal Chem 413 (2021) 5859–5869. https://doi.org/10.1007/s00216-021-03567-2.

[139] C. Vaghela, M. Kulkarni, S. Haram, R. Aiyer, M. Karve, A novel inhibition based biosensor using urease nanoconjugate entrapped biocomposite membrane for potentiometric glyphosate detection, Int J Biol Macromol 108 (2018) 32–40. https://doi.org/https://doi.org/10.1016/j.ijbiomac.2017.11.136.

[140] Z. Aydin, M. Keleş, A reaction-based system for the colorimetric detection of glyphosate in real samples, Spectrochim Acta A Mol Biomol Spectrosc 267 (2022) 120501. https://doi.org/https://doi.org/10.1016/j.saa.2021.120501.

[141] F. Arduini, S. Cinti, V. Caratelli, L. Amendola, G. Palleschi, D. Moscone, Origami multiple paper-based electrochemical biosensors for pesticide detection, Biosens Bioelectron 126 (2019) 346–354. https://doi.org/10.1016/j.bios.2018.10.014.

[142] N. Colozza, V. Caratelli, D. Moscone, F. Arduini, Origami paper-based electrochemical (Bio)sensors: State of the art and perspective, Biosensors (Basel) 11 (2021). https://doi.org/10.3390/BIOS11090328.

[143] S. V Kergaravat, S.N. Fabiano, A.R. Soutullo, S.R. Hernández, Comparison of the performance analytical of two glyphosate electrochemical screening methods based on peroxidase enzyme inhibition, Microchemical Journal 160 (2021) 105654. https://doi.org/https://doi.org/10.1016/j.microc.2020.105654.

[144] H. Liu, P. Chen, Z. Liu, J. Liu, J. Yi, F. Xia, C. Zhou, Electrochemical luminescence sensor based on double suppression for highly sensitive detection of glyphosate, Sens Actuators B Chem 304 (2020) 127364. https://doi.org/https://doi.org/10.1016/j.snb.2019.127364.

[145] V. Caratelli, G. Fegatelli, D. Moscone, F. Arduini, A paper-based electrochemical device for the detection of pesticides in aerosol phase inspired by nature: A flower-like origami biosensor for precision agriculture, Biosens Bioelectron 205 (2022). https://doi.org/10.1016/j.bios.2022.114119.

[146] C.T. Thanh, N.H. Binh, P.N.D. Duoc, V.T. Thu, P. Van Trinh, N.N. Anh, N. Van Tu, N.V. Tuyen, N. Van Quynh, V.C. Tu, B.T.P. Thao, P.D. Thang, H. Abe, N. Van Chuc, Electrochemical Sensor Based on Reduced Graphene Oxide/Double-Walled Carbon Nanotubes/Octahedral Fe3O4/Chitosan Composite for Glyphosate Detection, Bull Environ Contam Toxicol 106 (2021) 1017–1023. https://doi.org/10.1007/s00128-021-03179-7.

[147] J. Yu, J. Lin, J. Li, A photoelectrochemical sensor based on an acetylcholinesterase-CdS/ZnO-modified extended-gate field-effect transistor for glyphosate detection, Analyst 146 (2021) 4595–4604. https://doi.org/10.1039/d1an00797a.

[148] D. Rettke, J. Döring, S. Martin, T. Venus, I. Estrela-Lopis, S. Schmidt, K. Ostermann, T. Pompe, Picomolar glyphosate sensitivity of an optical particle-based sensor utilizing biomimetic interaction principles, Biosens Bioelectron 165 (2020) 112262. https://doi.org/https://doi.org/10.1016/j.bios.2020.112262.

[149] D. Capoferri, F. Della Pelle, M. Del Carlo, D. Compagnone, Affinity sensing strategies for the detection of pesticides in food, Foods 7 (2018). https://doi.org/10.3390/foods7090148.

[150] E.C. Reynoso, E. Torres, F. Bettazzi, I. Palchetti, Trends and perspectives in immunosensors for determination of currently-used pesticides: The case of glyphosate, organophosphates, and neonicotinoids, Biosensors (Basel) 9 (2019). https://doi.org/10.3390/bios9010020.

[151] D.C. Poudyal, V.N. Dhamu, M. Samson, S. Muthukumar, S. Prasad, Portable Pesticide Electrochem-sensor: A Label-Free Detection of Glyphosate in Human Urine, Langmuir 38 (2022) 1781–1790. https://doi.org/10.1021/acs.langmuir.1c02877.

[152] B. Pérez-Fernández, J. V Mercader, B.I. Checa-Orrego, A. de la Escosura-Muñiz, A. Costa-García, A monoclonal antibody-based immunosensor for the electrochemical detection of imidacloprid pesticide, Analyst 144 (2019) 2936–2941. https://doi.org/10.1039/C9AN00176J.

[153] J. Fu, X. An, Y. Yao, Y. Guo, X. Sun, Electrochemical aptasensor based on one step co-electrodeposition of aptamer and GO-CuNPs nanocomposite for organophosphorus pesticide detection, Sens Actuators B Chem 287 (2019) 503–509. https://doi.org/https://doi.org/10.1016/j.snb.2019.02.057.

[154] A.A. Lahcen, A. Amine, Recent Advances in Electrochemical Sensors Based on Molecularly Imprinted Polymers and Nanomaterials, Electroanalysis 31 (2019) 188–201. https://doi.org/https://doi.org/10.1002/elan.201800623.

[155] F. Zouaoui, S. Bourouina-Bacha, M. Bourouina, I. Abroa-Nemeir, H. Ben Halima, J. Gallardo-Gonzalez, N. El Alami El Hassani, A. Alcacer, J. Bausells, N. Jaffrezic-Renault, N. Zine, A. Errachid, Electrochemical impedance spectroscopy determination of glyphosate using a molecularly imprinted chitosan, Sens Actuators B Chem 309 (2020) 127753. https://doi.org/https://doi.org/10.1016/j.snb.2020.127753.

[156] B. Zhao, S. Feng, Y. Hu, S. Wang, X. Lu, Rapid determination of atrazine in apple juice using molecularly imprinted polymers coupled with gold nanoparticles-colorimetric/SERS dual chemosensor, Food Chem 276 (2019) 366–375. https://doi.org/https://doi.org/10.1016/j.foodchem.2018.10.036.

[157] M. Najafi, S. Darabi, A. Tadjarodi, M. Imani, Determination of Trichloroacetic Acid (TCAA) Using CdO Nanoparticles Modified Carbon Paste Electrode, Electroanalysis 25 (2013) 487–492. https://doi.org/https://doi.org/10.1002/elan.201200462.

[158] W. Sun, Y. Guo, X. Ju, Y. Zhang, X. Wang, Z. Sun, Direct electrochemistry of hemoglobin on graphene and titanium dioxide nanorods composite modified electrode and itselectrocatalysis, Biosens Bioelectron 42 (2013) 207–213. https://doi.org/https://doi.org/10.1016/j.bios.2012.10.034.

[159] W. Sun, L. Cao, Y. Deng, S. Gong, F. Shi, G. Li, Z. Sun, Direct electrochemistry with enhanced electrocatalytic activity of hemoglobin in hybrid modified electrodes composed of graphene and multi-walled carbon nanotubes, Anal Chim Acta 781 (2013) 41–47. https://doi.org/https://doi.org/10.1016/j.aca.2013.04.010.

[160] W. Sun, Y. Guo, Y. Lu, A. Hu, F. Shi, T. Li, Z. Sun, Electrochemical biosensor based on graphene, Mg2Al layered double hydroxide and hemoglobin composite, Electrochim Acta 91 (2013) 130–136. https://doi.org/https://doi.org/10.1016/j.electacta.2012.12.088.

[161] W. Sun, Y. Guo, T. Li, X. Ju, J. Lou, C. Ruan, Electrochemistry of horseradish peroxidase entrapped in graphene and dsDNA composite modified carbon ionic liquid electrode, Electrochim Acta 75 (2012) 381–386. https://doi.org/https://doi.org/10.1016/j.electacta.2012.05.018.

[162] W. Sun, F. Hou, S. Gong, L. Han, W. Wang, F. Shi, J. Xi, X. Wang, G. Li, Direct electrochemistry and electrocatalysis of hemoglobin on three-dimensional graphene modified carbon ionic liquid electrode, Sens Actuators B Chem 219 (2015) 331–337. https://doi.org/https://doi.org/10.1016/j.snb.2015.05.015.

[163] E. V Suprun, V. V Shumyantseva, A.I. Archakov, Protein Electrochemistry: Application in Medicine. A Review, Electrochim Acta 140 (2014) 72–82. https://doi.org/https://doi.org/10.1016/j.electacta.2014.03.089.

[164] W. Tu, J. Lei, H. Ju, Functionalization of Carbon Nanotubes with Water-Insoluble Porphyrin in Ionic Liquid: Direct Electrochemistry and Highly Sensitive Amperometric Biosensing for Trichloroacetic Acid, Chemistry – A European Journal 15 (2009) 779–784. https://doi.org/https://doi.org/10.1002/chem.200801758.

[165] M. Kurd, A. Salimi, R. Hallaj, Highly sensitive amperometric sensor for micromolar detection of trichloroacetic acid based on multiwalled carbon nanotubes and Fe(II)–phtalocyanine modified glassy carbon electrode, Materials Science and Engineering: C 33 (2013) 1720–1726. https://doi.org/https://doi.org/10.1016/j.msec.2012.12.085.

[166] W. Zheng, W. Chen, W. Weng, L. Liu, G. Li, J. Wang, W. Sun, Direct electron transfer of horseradish peroxidase at Co3O4–graphene nanocomposite modified electrode and

electrocatalysis, Journal of the Iranian Chemical Society 14 (2017) 925–932. https://doi.org/10.1007/s13738-016-1042-4.

[167] S. Kang, W. Zhao, X. Li, Z. Wen, X. Niu, B. He, L. Li, W. Sun, Electrochemical Behaviors of Myoglobin on Ionic Liquid-Graphene-Cobalt Oxide Nanoflower Composite Modified Electrode and Its Electrocatalytic Activity, Int J Electrochem Sci 12 (2017) 2184–2193. https://doi.org/https://doi.org/10.20964/2017.03.64.

[168] L. Kong, Z. Du, Z. Xie, R. Chen, S. Jia, R. Dong, Z. Sun, W. Sun, Electrochemistry of Hemoglobin-Ionic Liquid-Graphene-SnO2 Nanosheet Composite Modified Electrode and Electrocatalysis, Int J Electrochem Sci 12 (2017) 2297–2305. https://doi.org/https://doi.org/10.20964/2017.03.66.

[169] R.W. Kibechu, M.A. Mamo, T.A.M. Msagati, S. Sampath, B.B. Mamba, Synthesis and application of reduced graphene oxide and molecularly imprinted polymers composite in chemo sensor for trichloroacetic acid detection in aqueous solution, Physics and Chemistry of the Earth, Parts A/B/C 76–78 (2014) 49–53. https://doi.org/https://doi.org/10.1016/j.pce.2014.09.008.

[170] X. Cetó, C.P. Saint, C.W.K. Chow, N.H. Voelcker, B. Prieto-Simón, Electrochemical detection of N-nitrosodimethylamine using a molecular imprinted polymer, Sens Actuators B Chem 237 (2016) 613–620. https://doi.org/https://doi.org/10.1016/j.snb.2016.06.136.

[171] X. Cetó, C. Saint, C.W.K. Chow, N.H. Voelcker, B. Prieto-Simón, Electrochemical fingerprints of brominated trihaloacetic acids (HAA3) mixtures in water, Sens Actuators B Chem 247 (2017) 70–77. https://doi.org/https://doi.org/10.1016/j.snb.2017.02.179.

[172] R.M. Bashami, M.T. Soomro, A.N. Khan, E.S. Aazam, I.M.I. Ismail, M.S. El-Shahawi, A highly conductive thin film composite based on silver nanoparticles and malic acid for selective electrochemical sensing of trichloroacetic acid, Anal Chim Acta 1036 (2018) 33–48. https://doi.org/https://doi.org/10.1016/j.aca.2018.06.084.

[173] D. Qian, W. Li, F. Chen, Y. Huang, N. Bao, H. Gu, C. Yu, Voltammetric sensor for trichloroacetic acid using a glassy carbon electrode modified with Au@Ag nanorods and hemoglobin, Microchimica Acta 184 (2017) 1977–1985. https://doi.org/10.1007/s00604-017-2175-6.

[174] Z. Li, M. Yu, Y. Chu, X. Wu, J. Huang, W. Tao, 1 part per trillion level detection of disinfection byproducts in drinking water using miniaturized sensor, J Mater Chem A Mater 5 (2017) 4842–4849. https://doi.org/10.1039/C6TA09904A.

[175] H. Dai, H. Xu, X. Wu, Y. Lin, M. Wei, G. Chen, Electrochemical behavior of thionine at titanate nanotubes-based modified electrode: A sensing platform for the detection of trichloroacetic acid, Talanta 81 (2010) 1461–1466. https://doi.org/https://doi.org/10.1016/j.talanta.2010.02.052.

[176] B. Liu, Y. Deng, X. Hu, Z. Gao, C. Sun, Electrochemical sensing of trichloroacetic acid based on silver nanoparticles doped chitosan hydrogel film prepared with controllable electrodeposition, Electrochim Acta 76 (2012) 410–415. https://doi.org/https://doi.org/10.1016/j.electacta.2012.05.046.

[177] X.-F. Li, W.A. Mitch, Drinking Water Disinfection Byproducts (DBPs) and Human Health Effects: Multidisciplinary Challenges and Opportunities, Environ Sci Technol 52 (2018) 1681–1689. https://doi.org/10.1021/acs.est.7b05440.

[178] W. Sun, S. Gong, Y. Deng, T. Li, Y. Cheng, W. Wang, L. Wang, Electrodeposited nickel oxide and graphene modified carbon ionic liquid electrode for electrochemical myglobin biosensor, Thin Solid Films 562 (2014) 653–658. https://doi.org/https://doi.org/10.1016/j.tsf.2014.05.002.

[179] W. Zhao, X. Li, Z. Wen, X. Niu, Q. Shen, Z. Sun, R. Dong, W. Sun, Application of Ionic Liquid-Graphene-NiO Hollowsphere Composite Modified Electrode for Electrochemical Investigation on Hemoglobin and Electrocatalysis to Trichloroacetic Acid, Int J Electrochem Sci 12 (2017) 4025–4034. https://doi.org/https://doi.org/10.20964/2017.05.06.

[180] Z. Wen, W. Zhao, X. Li, X. Niu, X. Wang, L. Yan, X. Zhang, G. Li, W. Sun, Electrodeposited ZnO@three-dimensional Graphene Composite Modified Electrode for Electrochemistry and Electrocatalysis of Myoglobin, Int J Electrochem Sci 12 (2017) 2306–2314. https://doi.org/https://doi.org/10.20964/2017.03.09.

[181] F. Shi, W. Zheng, W. Wang, F. Hou, B. Lei, Z. Sun, W. Sun, Application of graphene–copper sulfide nanocomposite modified electrode for electrochemistry and electrocatalysis of hemoglobin, Biosens Bioelectron 64 (2015) 131–137. https://doi.org/https://doi.org/10.1016/j.bios.2014.08.064.

Chapter 2: Electrochemical screening strategies for pesticides biomonitoring: the case of glyphosate

2.1 Introduction

Monitoring glyphosate (**GLY**) levels in biological matrices, particularly urine, is crucial for assessing exposure in both occupational and environmental contexts. However, the barriers associated with traditional methods necessitate the development of innovative approaches that combine cost-effectiveness, ease of use, and environmental sustainability. As previously introduced in Chapter 1, traditional chromatographic methods such as liquid chromatography coupled with mass spectrometry (LC-MS), provide reliable detection of a great variety of analytes, but are often constrained by extensive sample preparation and limited portability. These limitations pose significant challenges in large-scale epidemiological studies, particularly in resource-constrained settings. To address these gaps, the work presented in this chapter explores the development of a low-cost, compostable electrochemical sensors specifically designed for GLY detection in human urine. This platform leverages the multifunctional properties of paper to integrate rapid screening capabilities with the high sensitivity of confirmatory analytical methods. By overcoming the bottlenecks of conventional techniques, the proposed device offers a transformative approach to pesticide monitoring, with potential applications in public health surveillance. The content presented in Chapter Two is derived from the research findings detailed in the article *"A paper-based device for glyphosate electrochemical detection in human urine: A case study to demonstrate how the properties of the paper can solve analytical issues"*, published in *Green Analytical Chemistry*, Volume 7, 2023, of which I am one of the co-authors.

2.1.1 Glyphosate

As introduced in Chapter 1, biomonitoring of pesticides in human biological matrices represents a critical aspect of environmental health research and occupational exposure assessment. Among the many pesticides in use nowadays, GLY (***Figure 2.1***) has raised significant health concerns due to its potential toxic and carcinogenic effects. GLY was first synthetized in 1950 by a pharmaceutical company named Cilag. However, the molecule was swiftly abandoned as no viable pharmaceutical applications could be found. It was only after the company's acquisition by Aldrich

Chemicals in 1966 that GLY began to be tested to evaluate its applicability potential beyond the pharmaceutical sector. In 1964 it was first patented as a metal chelating and descaling agent. At the time, Monsanto was focused on synthesizing water-softening agents. When Dr. Phil Hamm tested these compounds as potential herbicides, he discovered that organophosphates exhibited herbicidal activity against perennial weeds [1]. Together with Dr. John Franz, they decided to further investigate the herbicidal potential of organophosphate derivatives. In May 1970, GLY was synthesized, and by July of that same year, it was tested in greenhouse trials. This led to the patenting of GLY as an herbicide in 1971 (US Patent No. 3,799,758) and its commercial launch in 1974 under the trade name "Roundup®." Upon its introduction, GLY rapidly became the dominant herbicide on the market. Its market position was further solidified when Monsanto's original patent expired in 1991, leading to a price reduction and a surge in the sale of generic glyphosate-based herbicides [2].

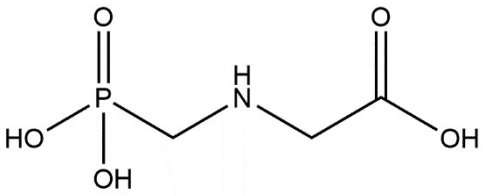

Figure 2.1) *Chemical structure the structure of glyphosate.*

The widespread use of GLY has been driven by its effectiveness, its resistance to many pests, and its application in genetically modified crops. The development of GLY-resistant crops, such as GLY-tolerant soybeans and corn, greatly contributed to this rise, allowing farmers to apply this product without harming their crops, thus simplifying weed management and increasing agricultural productivity. However, the rise in the use of this pesticide has sparked numerous legal and environmental concerns. The ubiquitous presence of GLY in water, air and, virtually, everywhere in the food chain means that it is regularly ingested. For this reason, in recent decades, Monsanto Company (acquired by Bayer in 2018) had to face a multitude of lawsuits related to the alleged carcinogenicity of this species, with thousands of claims filed by farmers and consumers. Notably, in 2018, a California jury found Monsanto responsible for the cancer of a man who had used Roundup, marking the beginning of a series of legal battles and settlement agreements. After 2018, following the mounting legal cases and

investigations into Monsanto regarding the potential risks of glyphosate, there was a significant increase in the number of research studies focused on detecting glyphosate in various environments. These investigations, driven by growing public concern over the herbicide's safety and potential links to cancer, led to a surge in the development and publication of analytical methods for GLY detection (***Figure 2.2***). Chromatographic techniques, particularly high-performance liquid chromatography (HPLC) and gas chromatography (GC), became more commonly employed, alongside innovative sensor technologies for real-time monitoring. **Figure 2.2** interestingly shows that the development of sensors for GLY detection only started very recently in respect to chromatographic methods. The increase in publications in the field reflects a heightened need for more reliable and accurate detection methods to assess GLY residues in agricultural products, water, soil, and even in human samples. Researchers have focused the attention in improving the sensitivity and selectivity of the new methods developed to ensure more effective regulation and risk assessment.

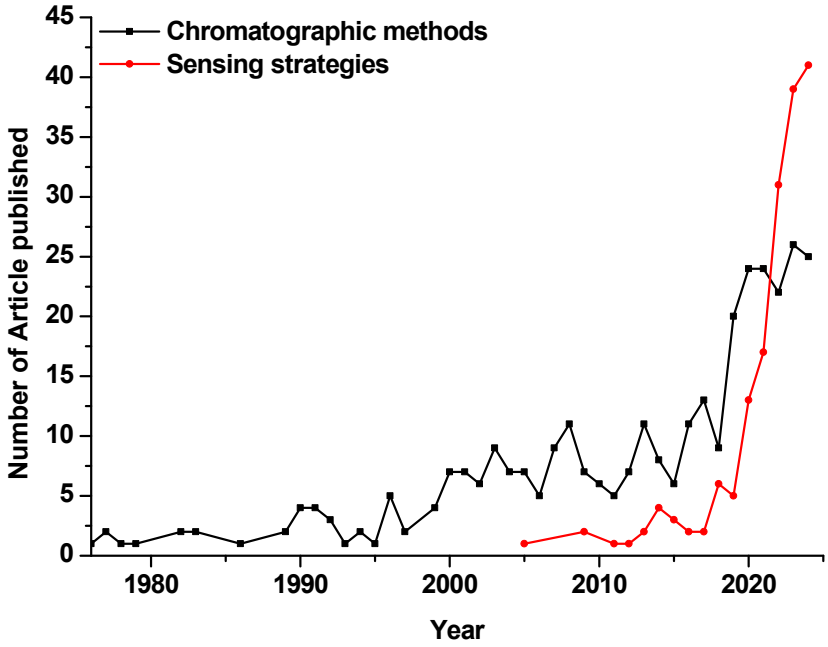

Figure 2.2) *Number of publications regarding GLY detection by sensors (**red**) and by chromatographic methods (**black**) according to Scopus Analyzer (last accessed 5/02/2025).*

This surge in the scientific output has been driven by both the legal pressure on GLY manufacturers and a broader social demand for safer and more transparent agricultural practices. Despite these controversies, GLY continues to be widely used,

particularly in agriculture. The U.S. National Nutrition Examination Survey found that GLY remains the most widely used pesticide in the U.S. Therefore, its presence detected in many urine samples, as a demonstration of the huge issue affecting the population [3]. Even in Europe, GLY was found in urine samples especially among individuals who are frequently exposed to pesticides [4]. The global annual consumption of GLY approximating 800,000 tons [5].

2.1.2 Paper-based sensors

Paper-based analytical devices have been widely used in the sensing field for various applications, as they offer an innovative approach to tackle the complexity of real-world matrices while addressing the growing demand for sustainability [6–8]. Over the past decade, the principle of sustainability has been incorporated into the analytical chemistry sector, defining new criteria for evaluating sustainable analytical methods [9]. One such approach, Green Analytical Chemistry [10] emphasizes eco-friendly principles, such as simplifying sample pre-treatment, reducing sample volumes, using miniaturized sensors, minimizing waste, and avoiding toxic reagents. White Analytical Chemistry [11] further expanded the focus to include also analytical efficiency (e.g., maximizing the number of detectable analytes, applicability, and compatibility with various sample types) as well as practical and economic considerations (e.g., cost-effectiveness, time efficiency, simplicity, and minimal need for advanced equipment, infrastructure, or specialized personnel, promoting portability and ease of use). Designing new sensing strategies that meet all these criteria is challenging, but paper-based platforms offer promising solutions.

From a sustainability and biomonitoring perspective, paper-based devices provide competitive analytical results, being cost-effective, disposable, easily destroyed (e.g., via incineration), and ideal for screening applications [12]. Cellulose structure possesses intrinsic microfluidic properties that can be exploited for different purposes: storage of reagents, manage sample solutions by capillarity, and promote reactions in a confined space [13]. This versatility was first demonstrated in a pioneering study by C.S. Henry's group, which used paper microfluidics to realize screen-printed electrochemical cells for multiplexed detection of glucose, lactate, and uric acid in human serum [14]. This enzymatic biosensor used glucose oxidase, lactate oxidase, and uricase to catalyse the oxidation of their respective substrates, measuring the

enzymatic by-product H_2O_2 through chronoamperometry with Prussian Blue as an electrochemical mediator. This innovative approach demonstrated the potential of paper for developing ready-to-use microfluidic devices with promising analytical performance, even in complex biological matrices like human serum. Starting from this initial study, numerous investigations explored the use of paper-based devices for the analysis of biological samples [8,15] and for environmental monitoring [7,16], often incorporating origami-like designs [17]. A recent example from Arduini et al. [9] involved the use of paper-based devices to detect three classes of pesticides: organophosphorus insecticides, phenoxy-acid herbicides, and triazine herbicides. Specifically, paraoxon, 2,4-dichlorophenoxyacetic acid, and atrazine were detected in aqueous solutions with these devices, showing linear ranges in the order of tens of mg L^{-1}. The detection relied on enzyme inhibition assays, using specific enzymes namely butyrylcholinesterase, alkaline phosphatase, and tyrosinase, respectively. In the following, the same group developed a flower-like paper-based biosensor for detecting pesticides in aerosol form [18], using butyrylcholinesterase, alkaline phosphatase, and horseradish peroxidase (**HRP**) enzymes to detect paraoxon, 2,4-dichlorophenoxyacetic acid, and GLY.

Using this latter work as the starting point of our research activities, I aimed at translating the use of the sensor for the quantification of GLY in the aerosol, in a similar device for the analysis of the same analyte in urine samples. In the following sections it will be presented the main challenges that I had to overcome to translate the detection strategy from environmental samples to a complex biological matrix and how paper has served as an optimal substrate, both in terms of the electrode platform and for performing preliminary sample pretreatment to minimize the matrix interference.

2.1.3 Strategy for the Electrochemical Detection of GLY by enzymatic inhibition

HRP is a heme-containing enzyme widely employed in biosensing for the ability to catalyze the oxidation of various substrates in the presence of H_2O_2 thanks to the presence of a Fe^{2+} redox active center. Among the possible substrates, 3,3',5,5'-tetramethylbenzidine (TMB) offers excellent redox and electrochemical properties, allowing the use in both optical and electrochemical sensors. The HRP–TMB system follows a two-step catalytic cycle reported in **Figure 2.3**. Upon reaction with H_2O_2, HRP is oxidized to Compound I, a reactive intermediate featuring an oxo-ferryl center and a

porphyrin radical. Compound I subsequently oxidize one molecule of TMB to a radical cation (TMB^{+}•), reducing the enzyme to Compound II. A second one-electron transfer from a TMB molecule completes the cycle, regenerating the native enzyme and producing a diimine oxidation product (TMB-ox). This oxidized species is electroactive and can be monitored electrochemically. Electrochemical detection is typically carried out by measuring the current involved in TMB-ox reduction, occurring at approximately –0.2 V vs Ag/AgCl, under mildly acidic conditions. This potential allows selective and sensitive detection of the oxidized product, while minimizing interference from endogenous electroactive compounds normally present in biological fluids. The current intensity is directly proportional to the amount of oxidized TMB formed, on its turn proportional to enzymatic activity. The presence of GLY in solution inhibits the enzymatic activity of HRP, so that at fixing all conditions, the amount of TMB-ox formed is lower. Based on this mechanism, the detection of GLY exploits an indirect detection mechanism where the target analyte acts as an inhibitor of HRP and the current decreasing observed in the presence of the analyte is directly proportional to its concentration. Redox mediators like TMB enhance the electron transfer process and improve the analytical performance of the biosensor, particularly in terms of sensitivity and response stability.

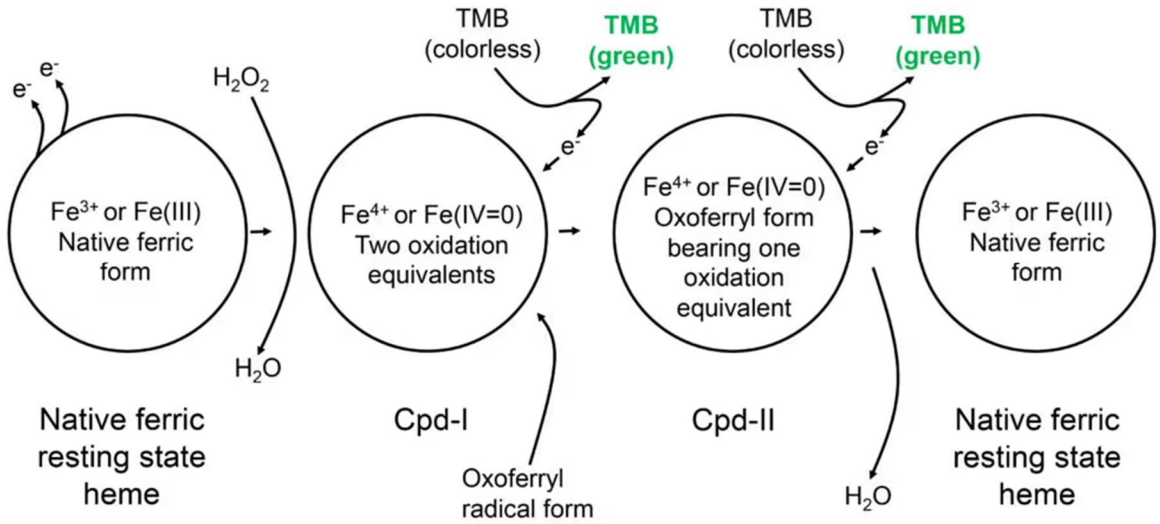

Figure 2.3. *Mechanism of TMB oxidation catalysed by HRP in the presence of H_2O_2. (Image adapted from Antibodies Inc., 2020).*

2.2 Results and Discussion

2.2.1 Preliminary analysis in synthetic urine matrix

The paper-based electrochemical sensor platform described herein represents a new solution for the analysis of biological samples, like urine. This device integrates multiple analytical functions into a single platform by exploiting the intrinsic properties of paper to act as both structural and a functional support. The capability of GLY to irreversibly inhibit the activity of HRP enzyme by binding its active site was previously exploited by Caratelli et. al [18] for the development of a paper-based device for the detection of this same analyte in aerosol samples. This detection strategy allows the indirect electroanalytical quantification of GLY based on the inhibition of HRP enzyme activity, using TMB as the substrate. Chronoamperometry was selected for the final detection of TMB by a screen-printed electrode (**SPEs**) to achieve high sensitivity and selectivity in complex matrices. The authors of the work found that the analytical performance of the sensor can be enhanced by modifying surface of the working electrode with Carbon Black (**CB**), which possesses electrocatalytic properties suitable to enable the electrochemical reduction of TMB at -0.2 V vs pseudo-Ag/AgCl. The analytical signal is directly proportional with the concentration of analyte is the inhibition percentage (I%). It can be calculated using the following equation:

Eq. (1) $$I\% = \frac{I_0 - I_f}{I_0} * 100$$

where I_0 and I_f are the currents recorded for TMB reduction produced by the reaction with HRP in absence and in presence of species capable of inhibiting the enzymatic activity, respectively. Considering the chronoamperometric responses observed for TMB reduction at -0.2 V (see **Figure 2.4**), the current values considered for **Eq. 1** are those recorded after 90 s.

To verify the applicability of this detection strategy in biological matrices, we investigated the presence of potential interfering species present in human urine, i.e. species that, similarly to GLY, can decrease the enzymatic activity of HRP. In particular, the performance of the enzymatic assay was evaluated in synthetic urine solutions at different compositions (**Table 2.1**), i.e. in presence of various components of urine samples, such as uric acid, urea, and creatinine, all tested in their typical physiological concentrations. By comparing the current values obtained for the different solutions

(**Figure 2.4a**), it was observed that urea and creatinine did not cause any notable variation in the sensor response due to TMB reduction, whereas uric acid showed a I%=60. A similar outcome was observed when the enzymatic assay was applied in the SU-2 and SU-3 media, both containing the same amount of uric acid.

Table 2.1 *– Composition of synthetic urine (**SU**) solutions tested.*

Component	***Concentration (mg mL^{-1})***	***SU-1 (g/50 mL)***	***SU-2 (g/50 mL)***	***SU-3 (g/50 mL)***
KCl	9.00	0.4505	0.4509	0.4513
NH_4Cl	3.00	0.1500	0.1534	0.1493
Na_2SO_4	3.00	0.1503	0.1500	0.1504
KH_2PO_4	2.50	0.1276	0.1307	0.1243
K_2HPO_4	2.50	0.1242	0.1246	0.1261
Creatinine	2.00	0.1008	0.1000	0.1000
Uric Acid	0.35	-	0.0175	0.0176
Urea	25.00	-	-	1.2505

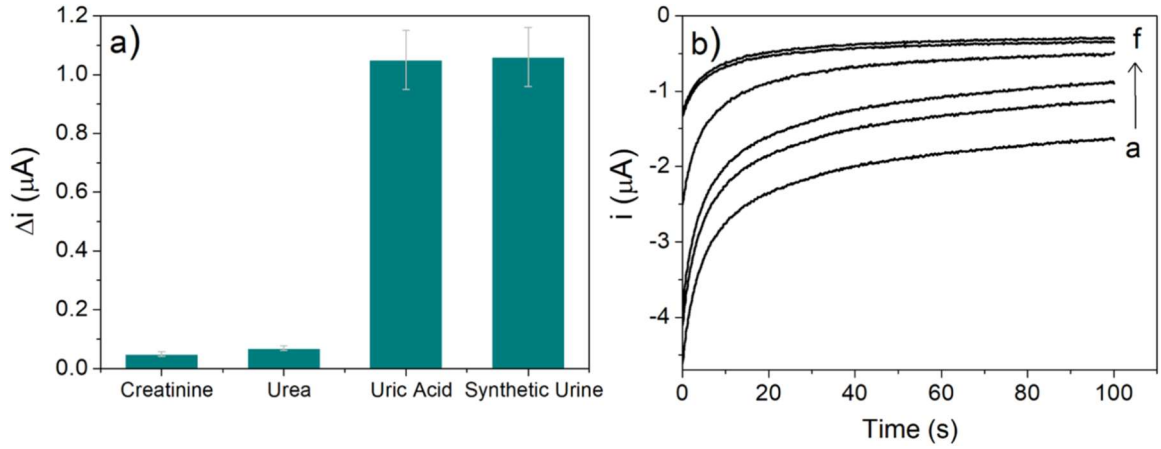

Figure 2.4 a) *The decrease in current response observed from chronoamperometric responses of the HRP-based assay after adding the TMB substrate to a 60 µL solution containing creatinine (17.7 mM), urea (412.5 mM), uric acid (2.1 mM), or SU-3 sample.* ***b)*** *Chronoamperometric responses of the HRP-based assay for a 60 µL drop containing TMB substrate and uric acid at various concentrations: 0, 0.50, 0.75, 1.5, 2.5, and 4.0 mM. Measurements were conducted in triplicate at SPE-CB, with E = -0.2 V vs Ag/AgCl pseudo-reference electrode.*

These results indicate that the activity of HRP is inhibited by the presence of this species normally present in human urine samples. Indeed, a similar reduction in HRP enzymatic activity was also observed in real urine samples. These observations are consistent with previous studies, which demonstrated that uric acid could act as an enzymatic substrate for HRP [19,20]. To better understand the impact of this species on the HRP-based assay, synthetic samples of urine containing well defined concentrations of uric acid within the physiological range were mixed with HRP and incubated for 5 minutes. TMB was added to this solution and chronoamperometric responses were collected by polarizing the electrode at -0.2 V after an additional 2-minute reaction time to quantify the amount of TMB produced by the enzyme. A significant decrease in current (about 85–100%) was observed in solutions containing a concentration of uric acid above 1 mM (***Figure 2.4b***). Considering that the physiological concentration of uric acid in human urine ranges from 1.2 to 4.4 mM [21], this poses a serious limitation for the HRP-based assay to detect GLY in urine.

2.2.2 Assessing the Interference of Uric Acid

To address the problem of uric acid interference in HRP-based assays, we explored the properties of the paper to remove or at least reduce the concentration of this interferent in the samples. This was achieved by exploiting precipitation phenomena that occur in both acidic and alkaline conditions. Indeed, uric acid is a weak diprotic acid with pKa_1 = 10.3 and pKa_2 = 5.6 (***Figure 2.5)***, showing precipitation equilibria that are strongly dependant on the pH, on the Na^+ concentration, and on the ionic strength of the solution.

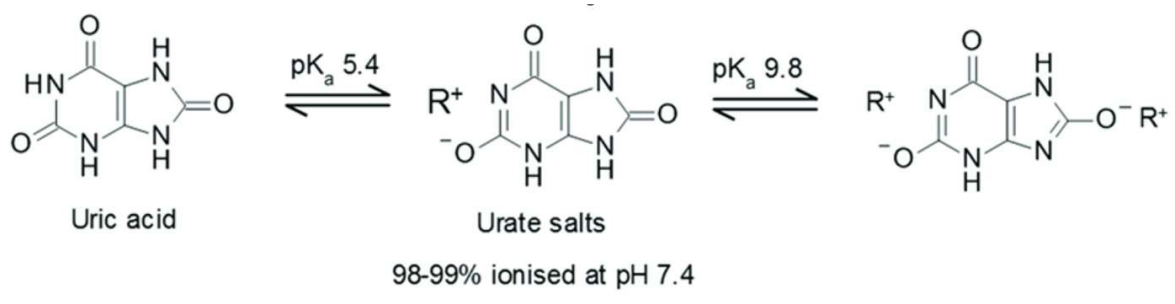

Figure 2.5) *pH-dependent equilibria of uric acid.*

The solubility curves of uric acid and its corresponding monosodium urate form exhibit a distinct pattern as a function of pH [22]. At pH levels near 8, an elevated Na^+ concentration can enhance the supersaturation of uric acid relative to the monosodium

urate form, leading to its precipitation. On the other hand, at pH values of 5 or lower, the uric acid concentration is limited by its low solubility, causing precipitation from supersaturated urate solutions [23,24]. Based on this understanding, we developed a pre-treatment procedure exploiting a pH-driven precipitation to lower the concentration of uric acid in urine samples. Both synthetic and real urine samples were adjusted to either pH 5.0 or 8.0 to promote uric acid precipitation, followed by filtration by normal siring filters. Note that for the alkaline treatment at pH 8.0, a 0.5 M NaCl solution was also added to the samples, as described in detail in **Section 2.5.3.** The effect of pH adjustment and filtration on the uric acid removal from the sample was investigated by evaluating the oxidation peak intensity (I_{pa}) due to uric acid oxidation before and after the pre-treatment step, using differential pulse voltammetry (DPV) as detection technique (see Figure 2.6).

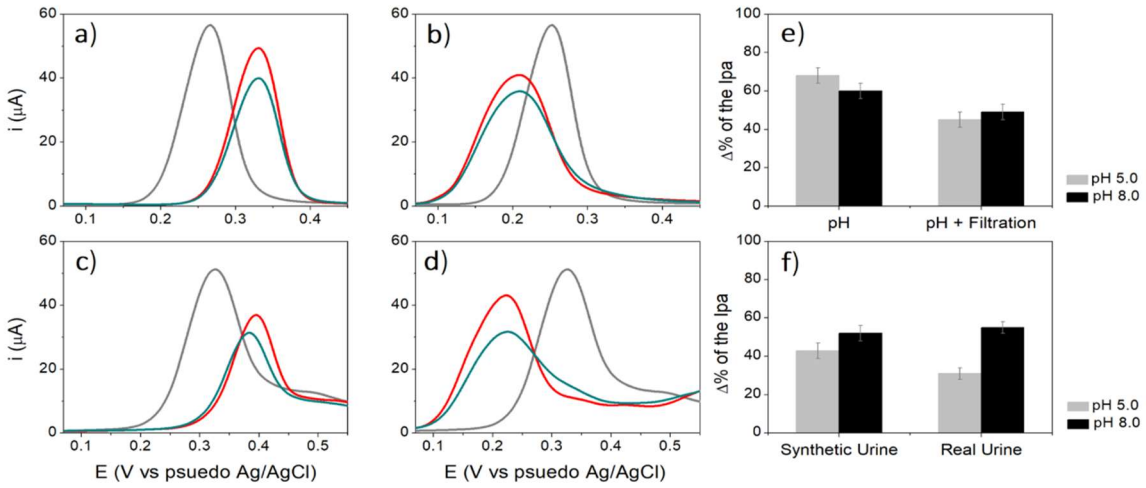

Figure 2.6) (a,b,c,d) *Comparison of the DPV voltammograms obtained for urine samples before (grey curves), after pH treatment (red curves), and after both pH treatment and filtration (green curves); results were recorded in synthetic urine with pH pre-treatment at 5.0 (**a**) and 8.0 (**b**), and in real urine with pH pre-treatment at 5.0 (**c**) and 8.0 (**d**). (**e**) Comparison of I% obtained at the two pH values after pH treatment and pH treatment + filtration. (**f**) Evaluation of the overall effectiveness of the pre-treatment (pH + filtration) in synthetic and real urine at pH 5.0 (light grey) or 8.0 (black).*

In synthetic urine, a clear reduction of I_{pa} was observed after both pre-treatment procedures, with a stronger effect when both pH adjustment and filtration were applied independently to the pH, indicating that these conditions induce precipitation equilibria involving this species.

Notably, pre-treatment at pH 5.0 or pH 8.0 resulted in a strong variation of the peak potential, consistent with the pH dependence of this electrochemical process. Similar variations of the peak intensities were also observed in real urine samples, demonstrating that the combination of pH adjustment and filtration is effective in reducing background interference, thereby enhancing the selectivity and sensitivity of the electrochemical measurements. If on the one hand it was observed that both acidic and alkaline conditions reduced the presence of uric acid in solution, the pre-treatment at pH 5.0 was proved to be more effective for the treatment of real urine samples, with I%=45–50%. A similar test performed with alkaline pretreatment leaded a weaker effect, with a I%=30–40%, as shown in Figure 2.6. Therefore, the acidic treatment followed by filtration was considered the optimal pre-treatment protocol for this study. Despite not complete, the successful reduction of uric acid levels in both synthetic and real urine samples minimizes interference in the HRP inhibition, improving the accuracy of GLY detection, as detailed in the following section.

2.2.3 Design and Development of the Sensor Platform

After defining the role of uric acid in HRP-based assays and outlining a protocol for the sample pre-treatment through pH variation and filtration to reduce interference due to the presence of uric acid, we decided to adapt this analytical strategy to the use of paper-based origami platform. This platform was specifically designed to combine the sample pre-treatment for the removal of uric acid and the detection step into a single, disposable, user-friendly, sustainable, and affordable paper strip, utilizing paper microfluidics. To achieve this, the platform was pre-loaded with all necessary reagents in different area of the strip, namely a Britton Robinson Buffer (**BRB**) for pH adjustment, and HRP and TMB for the enzymatic assay, to lead a rapid and automatic preparation of the sample. The initial phase of designing this platform focused on incorporating the treatment described in **section *2.2.2*** into the cellulose matrix. In this case, the pH-filtration process was carried out by pre-loading a solution at pH 5.0 in the treatment area (***Figure 2.7***, treatment area), utilizing the paper's natural adsorption and filtering properties to perform the filtration under acidic conditions. Specifically, 20 µL of 0.5 M BRB solution at pH 5.0 was drop-casted in the treatment area and allowed to dry. Subsequently, 60 µL of a real urine sample was applied to the sampling area. Activated by capillarity forces, it passed through the treatment zone to interact with the pre-loaded BRB. As the BRB salts dissolved for interaction with the sample, the acidic

environment was restored in the cellulose matrix, facilitating both the pH treatment and the filtration process due to the inherent properties of the filter paper. As a result, the current peak due to uric acid oxidation showed a reduction of about 50%, demonstrating the effectiveness of the pH-filtration treatment performed in the liquid phase. No significant differences in precipitation efficiency were noted when varying volumes of 0.5 M BRB were used.

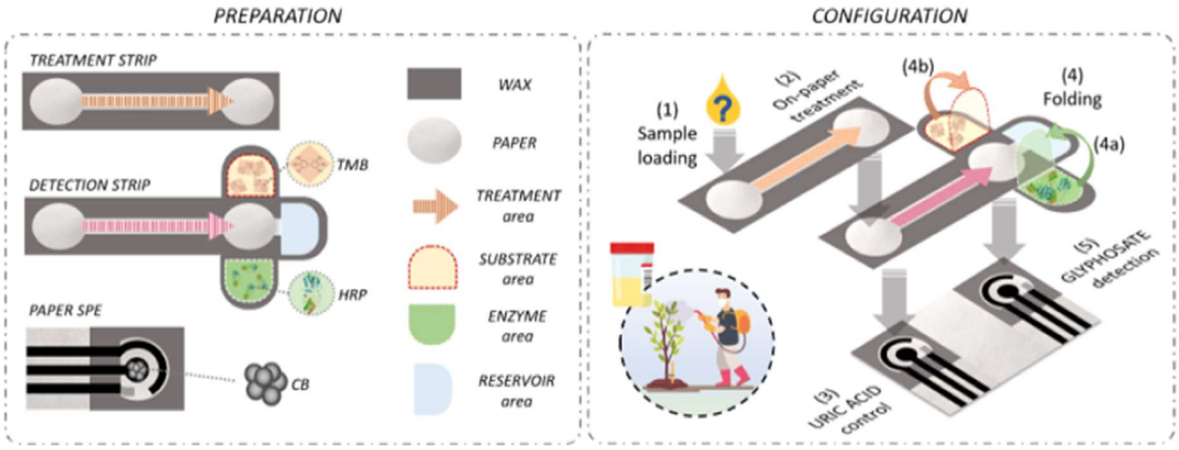

Figure 2.7) *Illustration of the paper-based electrochemical biosensing final platform for GLY detection in urine samples. Left side: description and preparation of the paper strips. Right side: origami-like configuration of the paper platform, composed of three paper layers overlapped, namely the treatment strip, the detection strip, and the layer with the screen-printed sensors.*

If the uric acid concentration remains too high after the initial on-paper treatment, an additional treatment strip can be incorporated into the platform before proceeding with the detection strip. This allows for the on-paper treatment to be repeated once or twice, further lowering the uric acid levels. We found that when the uric acid response is reduced to a current below 20 µA, GLY quantification can be performed without significant interference from uric acid, so that the DPV response for uric acid oxidation only acts as a test of the effectiveness of the interference removal.

The final platform was created with a paper layer consisting of two office paper screen-printed sensors, with the working electrodes modified using CB (SPE-CB). The Treatment and Detection strips, made of Whatman filter paper, can be assembled as illustrated in **Figure 2.7**. The biosensing platform is formed by layering filter paper strips on top of the SPE-CBs. When the sample is applied at the start of the treatment filter paper strip, it moves along the strip due to horizontal microfluidics, undergoing

treatment previously described directly within the cellulose matrix to minimize the interference due to uric acid. After treatment, the sample flows vertically to the first SPE-CB, where the residual uric acid level is measured using DPV analysis to ensure it falls below the 20-µA threshold. The sample then continues along the detection strip until it reaches the analysis area where it meets the HRP-TMB system only upon folding the pads that were separately loaded with these species. The folding sequence begins with the HRP pad to allow the enzyme to interact with the sample and potentially react with GLY.

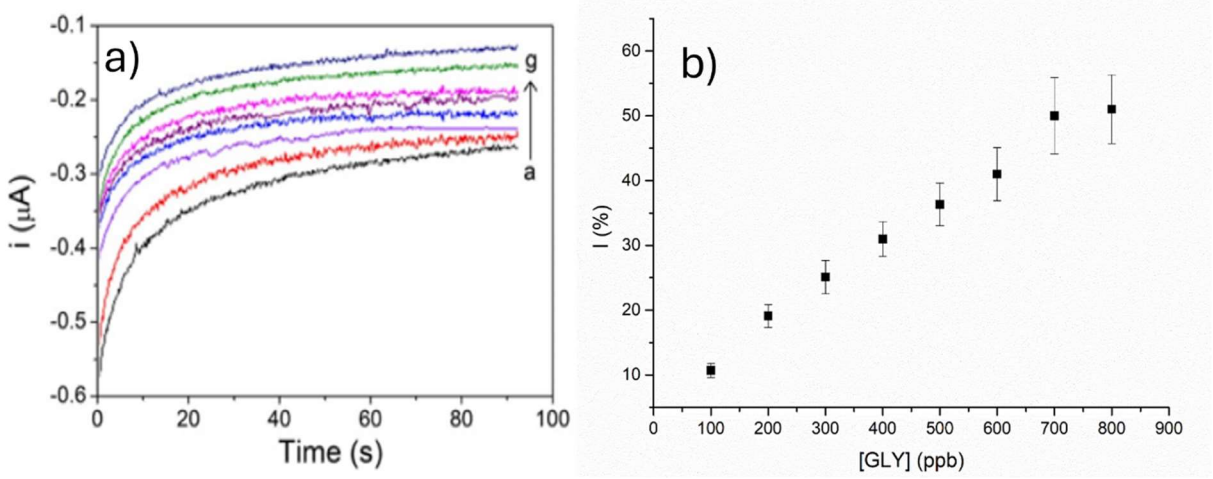

***Figure 2.8 a**) Chronoamperometric responses obtained for TMB reduction from HRP assay in real urine samples also containing GLY concentrations between 100 and 700 µg L^{-1} (0.59 µM to 4.14 µM) (from a to g); E = -0.2 V and t = 100 s; **b)** trend of the current intensity variation (I%) recorded by chronoamperometric responses for different additions of GLY in spiked real urine samples, with error bars derived from triplicate measurements.*

When the chronoamperogram at -0.2 V is recorded, it is possible to have direct detection of the actual activity of the enzyme, resulting more or less inhibited by the presence of GLY. The enzymatic process is monitored using the second SPE-CB, which is moistened by vertical flow, enabling the indirect detection of GLY through an enzyme inhibition assay. The total analysis time, from sample addition to final readout, is approximately 10 minutes, accounting for 5 minutes of HRP-sample contact, 2 minutes of incubation with TMB, and 1.7 minutes for the amperometric scan. The accuracy of the analytical procedure was evaluated using several real human urine samples spiked with known amounts of GLY up to 700 µg L^{-1} (4.14 µM). **Figure 2.8a** displays the chronoamperometric responses for HRP-based detection and the

calibration curve derived from the inhibition percentage (I%), calculated using Eq. (1). In this analysis, the I_0 value represents the chronoamperometric current obtained from real urine samples without any GLY contamination. As the concentration of the contaminant in solution increased, the chronoamperometric currents progressively decreased due to HRP inhibition (see ***Figure 2.7b***). A linear relationship was observed between I% and GLY concentration in the range of 100 to 700 µg L^{-1} (0.59 – 4.14 µM), corresponding to inhibition percentages between 10% and 50%. The limit of detection (LOD) in real urine was calculated to be I% = 10%, resulting in a value of 75 µg L^{-1}, while GLY concentrations ≥ 700 µg L^{-1} caused signal saturation, as shown in ***Figure 2.8b***. These results suggest that the origami platform effectively monitors GLY in human urine samples, overcoming interference from uric acid without the need for time-intensive sample pre-treatment. The findings are summarized in **Table 2.1**, and the screening yielded promising results, with the real and experimentally determined glyphosate concentrations showing good agreement.

Table 2.1 *Uric acid and GLY concentrations measured in real urine samples (A, B, C, D). The GLY concentrations determined using our analytical method were compared with the known amounts added to the urine samples prior to analysis, showing satisfactory percentage recoveries*.

Sample	Glyphosate spike (µg L^{-1})	Glyphosate calculated (µg L^{-1})	Recovery (%)
A	75 ± 0.1	74.3 ± 0.8	98.7
B	250 ± 1	247 ±2	98.8
C	500 ± 1	490 ± 3	99.8
D	750 ±1	745 ± 4	99.3

2.2.4 White Analytical Sustainability Assessment

The sustainability of the sensing platform was evaluated using the criteria of White Analytical Chemistry, introduced by Nowak et al.[11], which builds on previous sustainability assessment methods [25]. This innovative assessment tool highlights the most used key aspects to evaluate the sustainability of an analytical method. To apply this evaluation, 12 principles must be considered, including analytical performance

(4 "red" principles), practical and economic factors (4 "blue" principles), and environmental and safety considerations (4 "green" principles, in line with Green Analytical Chemistry principles [10]). The red, blue, and green principles together determine a "whiteness" score, like the RGB colour model, where fully saturated red, blue, and green combine to form white (see ***Table 2.3*** and ***2.4***, **section 2.5.7**). The White Analytical Chemistry approach uses a simple algorithm that assigns a score from 0 (not sustainable) to 100 (fully sustainable) for each principle, ultimately quantifying the overall sustainability (the "whiteness"). Additionally, the algorithm, available as an Excel file, allows for comparison of various analytical methods based on their sustainability scores. To critically assess the aspects of our method, a reference method for glyphosate detection was included in this evaluation. The selected reference method utilizes high-pressure anion exchange chromatography coupled with mass spectrometry (HPAEC-MS/MS) for detecting glyphosate in various samples from a cattle farm [26], including urine samples. This method was chosen not only for its relevance to our comparison but also because it provides sufficient information for the score assignment of each sustainability principle.

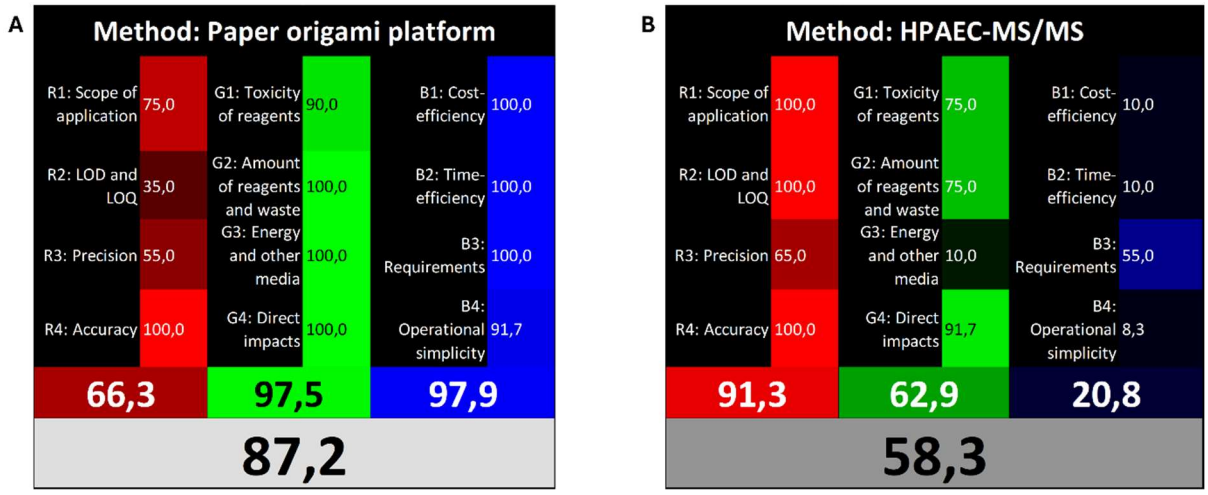

Figure 2.9) *Scores resulted from the application of the Whyte Analytical Chemistry assessment [11] for the method based on our paper origami platform (A) and a reference method for glyphosate detection, namely HPAEC-MS/MS (B).*

The assessment results are presented in **Figure 2.9** and **2.10**, showing total scores (whiteness) of 87.2 for the paper origami platform and 58.3 for HPAEC-MS/MS. It is clear that the whiteness (***Figure 2.10***) score for our method is significantly higher than that of the reference method, highlighting that our approach better fulfils sustainability criteria.Specifically, the analysis of the red principles yielded medium-to-high scores of

66.3 for the paper origami platform and 91.3 for HPAEC-MS/MS. Both methods received the maximum score for their ability to handle potential interferences, such as uric acid in urine samples for the paper origami platform, and for HPAEC-MS/MS, which can analyse urine samples without interference. However, our method shows lower performance in terms of linear range, precision, and LOD compared to HPAEC-MS/MS, indicating that the paper origami platform is a more suitable choice for sustainable early screening applications.

The evaluation of the green and blue principles further supports the greater sustainability of our method. The green aspects are particularly advantageous for the paper origami platform, with scores of 97.5 versus 62.9 for HPAEC-MS/MS, especially in terms of energy consumption. The platform requires only a portable potentiostat and a laptop, resulting in much lower energy consumption compared to chromatography and spectrometry-based systems. Additionally, the minimal volume of reagents (< 50 µL) and sample (60 µL) required for the analytical method, along with low waste production (e.g., paper strips can be incinerated, reducing waste and biological risk), significantly enhance the sustainability of our approach compared to HPAEC-MS/MS.

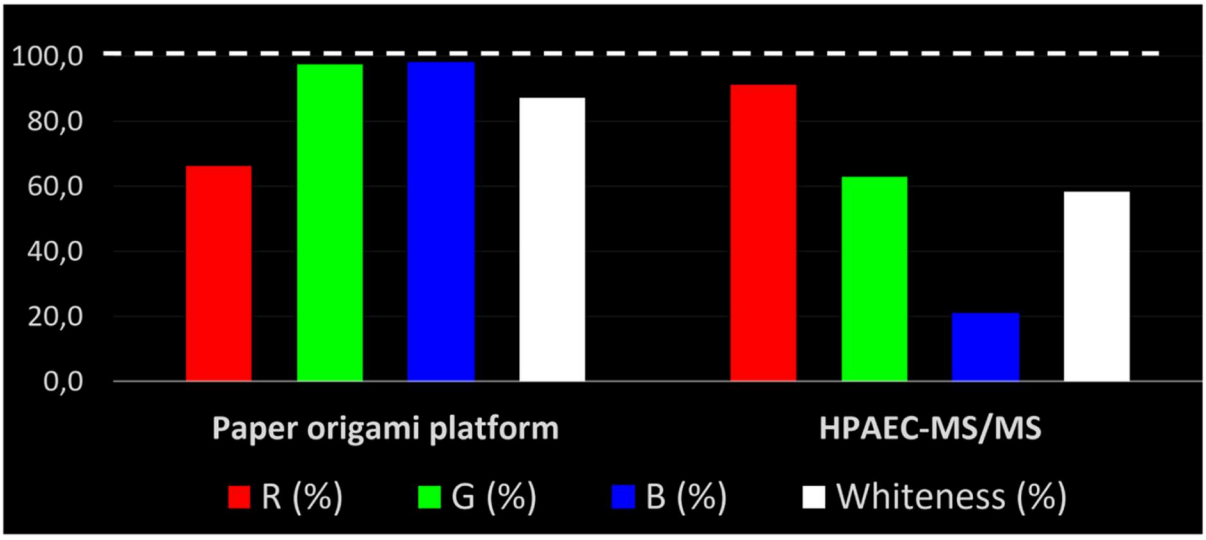

Figure 2.10) *The final scores for the red, green, and blue principles are illustrated with the resulting whiteness for the paper origami platform and the HPAEC-MS/MS method.*

The analysis of the blue principles yielded scores of 97.9 for the paper origami platform and 20.8 for HPAEC-MS/MS. Factors such as cost-efficiency, time efficiency, general requirements (including advanced instruments, skills, and facilities), and operational simplicity favour the paper origami platform. It offers very low costs (< 5 euros), a fast

analysis time (around 10 minutes), no need for skilled personnel or advanced equipment, and is easy to use with minimal sample consumption (only 60 µL needed, applied directly to the paper platform). It is a portable device suitable for at-line, in situ analysis.

In conclusion, this assessment demonstrates that the combination of paper-based properties and the analytical strategy employed has led to a sensing device that performs competitively across multiple sustainability factors, making it ideal for screening glyphosate in human urine.

2.3. Conclusions

In this chapter, I have presented the development and implementation of an HRP-based enzymatic inhibition strategy for GLY detection in human urine, a complex biological matrix. This approach is particularly relevant for identifying pesticide residues in the human body following significant exposure to contaminated environments, such as occupational settings. A key aspect of this methodology was addressing the interference caused by uric acid, which is prevalent in urine samples and can affect the accuracy of HRP-based detection.

To mitigate this issue, I first developed a pH-driven treatment that reduces the impact of uric acid on the enzymatic process. Through adjusting the pH to either acidic (pH 5.0) or alkaline (pH 8.0) conditions and incorporating a filtration step, it was possible to significantly decrease the uric acid content in the samples. Building on this treatment approach, I then integrated it into a paper origami platform. This device, utilizing the unique properties of filter paper, combines a treatment paper strip with a lateral microfluidic flow and a vertical path for electrochemical analysis using CB-modified office paper-based SPEs. The treatment and detection strips were strategically layered on top of the sensors, enabling the seamless application of the pH treatment, the measurement of residual uric acid, and the HRP-based enzyme inhibition assay for glyphosate detection.

The result is a versatile, single-use device capable of performing multiple analytical steps: 1) pH-based treatment to reduce uric acid levels, 2) assessment of treatment efficacy by measuring the remaining uric acid, and 3) execution of the HRP inhibition

assay for GLY detection. This paper origami platform, with its straightforward design, low-cost production, minimal waste, and user-friendly operation, represents a significant advancement in analytical technology. The device aligns well with sustainability goals, as it uses green materials and reagents, minimizes reagent and sample volumes, and produces minimal waste, all while maintaining the necessary analytical sensitivity.

Through the application of White Analytical Chemistry principles, the sustainability of our platform was evaluated, demonstrating that it outperforms traditional chromatography or spectrometry-based methods for glyphosate detection in terms of cost, time, and environmental impact. The promising results highlight the potential of this paper-based platform as an affordable, efficient, and practical tool for in situ screening of glyphosate exposure, particularly in environments where resources are limited. These findings emphasize the importance of sustainable innovation in analytical chemistry and underscore the need for further efforts to develop environmentally friendly and cost-effective solutions in this field

2.5 Materials and Methods

2.5.1 Reagents and equipment

The following materials were purchased from Sigma Aldrich: HRP, TMB, glyphosate (N-phosphonomethyl glycine, 99.2% w/w), uric acid, ammonium chloride, sodium chloride, disodium sulfate, urea, creatinine, and Nafion™ 117 solution. MilliQ water (18 MΩ·cm resistivity) was used to prepare all solutions. Britton-Robinson buffer (BRB) at 0.2 M concentration was prepared using H_3PO_4, H_3BO_3, and CH_3COOH, and its pH was adjusted to 5 by adding NaOH (0.2 M). A 0.1 M phosphate-buffered saline (PBS) solution with pH 7.0 was prepared by combining Na_2HPO_4 and NaH_2PO_4 (0.1 M) and adding 0.05 M KCl. Syringe filters (PTFE/Ø13 mm/0.22 µm/Organic) were sourced from Biocomma. The office paper-based SPE, consisting of graphite working and counter electrodes, and an Ag/AgCl pseudo-reference electrode (S4M-OP02), with a working electrode surface area of 12.6 mm^2, were provided by SENSE4MED Company (Rome, Italy). Additional commercial carbon SPEs (DR.110) were obtained from Dropsens-Metrohm, possessing a working electrode surface area of 12.6 mm^2. Paper pads and strips were wax-printed on filter paper (67 g/m^2, Cordenons, Italy) as previously

described [14]. Commercial carbon black (CB, N220), of industrial standard grade, was supplied by Cabot Corporation. Synthetic urine solutions, with a defined chemical composition to test different components' effects on enzymatic inhibition, were prepared based on methods reported in earlier studies [27]. Electrochemical measurements were performed using a portable potentiostat, Sensit Smart (PalmSens, Netherlands), connected to a laptop. Data were recorded with PSTrace5 software and analyzed using OriginPro 8.5.

2.5.2 Electrochemical enzymatic assay and preliminary tests

The inhibition of the HRP enzymatic activity was assessed through chronoamperometric measurements using an SPE that had been previously modified by drop casting 2µL of a 1 mg/mL CB dispersion. Before proceeding to the real matrix, preliminary tests were conducted using synthetic urine with a defined composition, as reported in Table 2.1. A 20 µL drop of synthetic urine was applied to the surface of the working electrode on the SPE-CB. Following this, 2 µL of a 25 U/mL HRP solution in PBS was added, and the system was incubated for 5 minutes to allow for any enzyme inhibition. After incubation, 20 µL of TMB solution, diluted 1:5 v/v with synthetic urine, was introduced, followed by a second 2-minute incubation to initiate the enzymatic reaction. The enzymatic reaction product was then detected via chronoamperometric analysis by applying a potential of -0.2 V vs. pseudo-Ag/AgCl to the working electrode for 100 seconds. The inhibition percentage (I%) was calculated using **Eq. 1**.

2.5.3 Urine Sample Pre-treatment

Real urine samples were obtained from the Microbiology Laboratory of the "Casa di Cura Giovanni XXIII of Monastier" in Treviso, Italy. The samples, each with a volume of 5 mL, were immediately stored at -20 °C after collection, then thawed at 4 °C prior to analysis and brought to room temperature (20 °C). During initial testing, the pH of each sample was measured using a pH electrode (HI1083B, Hanna Instruments™). Depending on the recorded pH value, small amounts of either 1.0 M HCl or NaOH were added to adjust the pH to 5.0 or 8.0, to facilitate uric acid precipitation. Only minimal volumes of HCl or NaOH were used to prevent significant dilution. For samples adjusted to pH 8.0, NaCl was added to a final concentration of 0.5 M to enhance uric acid precipitation. After a 5-minute incubation, all samples (at pH 5.0 and 8.0) were filtered using syringe filters (polytetrafluoroethylene, pore size 0.22 µm), which had

been activated with methanol and rinsed with MilliQ water prior to use. The pre-treated samples were stored at 4 °C until further testing. It should be noted that the same pre-treatment procedure was applied to synthetic urine samples, as detailed in **section 2.2.3.** For all spiked samples, glyphosate or uric acid was added before the pre-treatment process.

2.5.4 Electrochemical Detection of Uric Acid Level

The uric acid concentration in the samples following treatment was assessed through direct oxidation using the DPV technique, within a potential range of -0.1 to +0.6 V vs. pseudo-Ag/AgCl. A potential step of 7 mV and a pulse potential of 40 mV with a 100 ms pulse duration were applied, along with a scan rate of 0.015 V/s. For the solution tests, 40 µL of the sample was directly deposited on the SPE-CB for DPV analysis. In the case of paper strip testing, 60 µL of the sample was applied to the sampling area, where it flowed through the treatment zone and into the uric acid detection area, where DPV analysis was performed at the SPE-CB.

2.5.5 Paper-based Analytical Platform

The paper platform, designed in an origami-like structure, consists of three layers: the treatment strip, the detection strip, and the layer with screen-printed sensors (as shown in ***Figure 2.6***). The treatment strip, measuring approximately 6 cm in length, includes a microfluidic pathway (around 0.7 x 8.0 cm) formed by a wax pattern. This pathway is pre-loaded with 20 µL of BRB at pH 5.0 to create the on-paper treatment area. The wax pattern is produced using a ColorQube 8580 Xerox printer. The treatment strip is then placed over the detection strip, allowing the sample to move through the layers via vertical flow, reaching the layer below where two SPE-CB sensors are positioned. At the end of the detection strip, another microfluidic pathway (about 0.7 x 8.0 cm) is provided, with two pads enclosed by the wax barrier to separately hold the HRP enzyme (2 µL of a 25 U/mL HRP solution in PBS) and the TMB substrate (20 µL of TMB solution diluted 1:5 v/v in PBS), both of which are left to dry at room temperature before use. A reservoir area is also included for adding 0.1 M PBS buffer during the enzyme inhibition assay, ensuring the dissolution of the reagents from the cellulose matrix and facilitating their reactions. The sample flows laterally along the treatment and detection strips, as well as vertically through the paper layers.

2.5.6 Analytical Protocol

When 60 µL of the sample are applied to the beginning of the treatment strip, they moves through the lateral microfluidic pathway where the treatment takes place. In this area, the pre-loaded BRB (pH 5.0) establishes the acidic conditions that promote uric acid precipitation, as explained in **section 2.3.3**. After passing through the treatment zone, the sample flows vertically through the layers, reaching the first SPE-CB, where the residual uric acid is measured using DPV. If necessary, the treatment process can be repeated with additional strips until the signal from uric acid oxidation is sufficiently reduced (below 20 µA). Simultaneously, the sample continues to flow along the lateral microfluidic pathway of the detection strip until it reaches the area where the enzyme inhibition assay is performed. This assay is initiated by folding the pads, which are pre-loaded with the enzyme and substrate. Before the assay, 10 µL of PBS (pH 7.4) is added to the reservoir area to aid the sample's diffusion through the microfluidic pathway of the detection strip, dissolve the reagents, and adjust the solution's pH for the enzyme inhibition test. Next, the HRP-loaded pad is folded onto the strip, exposing the enzyme to the sample for 5 minutes. Afterward, the TMB-loaded pad is folded over the HRP pad, allowing a 2-minute reaction time. Finally, the chronoamperometric signal is recorded by applying a potential of -0.2 V vs. pseudo-Ag/AgCl for 100 seconds. The presence of glyphosate is detected by analysing the chronoamperometric response, and the inhibition percentage (I%) is calculated relative to I0 (the current of the enzymatic activity without inhibitors), using **Eq. 1**.

2.5.7 Sustainability Principles According to White Analytical Chemistry.

A summary of the White Analytical Chemistry [11] is here reported hereafter to facilitate the reading of the resulting scores.

Red principles:

R1 - Scope of application. It includes the range of applicability in terms of the number of simultaneously determined analytes, range of linearity, compatibility with various types of samples and resistance to the presence of potential interferences.

R2 - LOD and LOQ. Low LODs and LOQs are recommended, according to the effective concentrations that is needed to detect in the real target samples.

R3 - Precision. High precision is recommended, in terms of repeatability and reproducibility.

R4 - Accuracy. High accuracy is recommended, in terms of minimal relative error and recovery % close to 100%.

Green principles:

G1 - Toxicity of reagents. The lowest possible toxicity of reagents is recommended, and biodegradable, renewable, or nature-based reagents and materials must be preferred.

G2 - Number and amount of reagents and waste. The lowest possible consumption of reagents and production of waste is recommended.

G3 - Energy and other media. The lowest possible consumption of electricity and other utilities is recommended.

G4 - Direct impacts. Impact on humans (hazardous exposure), animals (or use of animals), and genetic effects must be avoided.

Blue principles:

B1 - Cost-efficiency. The total cost of analysis (including instruments, materials, tools, and personnel) must be as low as possible.

B2 - Time-efficiency. The total time of analysis (including overall methodology, sample treatment, and all the analytical steps involved) must be as low as possible.

B3 - Requirements. The practical requirements (including the amount of sample used, the need for advanced equipment, advanced personnel qualifications, and laboratory infrastructure) must be as less as possible.

B4 - Operational simplicity. The highest possible level of miniaturization, integration, automation (on-line methods, AI technologies), and portability (on-site measurements) are recommended.

Table 2.3 *Specific criteria assignment of scores here applied to some red principles of the sustainability assessment according to the White Analytical Chemistry [1]. For glyphosate (GLY), the scores of the LOD were assigned considering that a 100-value can be associated with the HPAEC-MS/MS method (LOD of 8.3 ppb); the score then decreases by one decade for each LOD value that increases by 10.*

Score	LOD (GLY, ppb)	Repeatability according to the Relative Standard Deviation %	Accuracy (recovery %)
100-91	< 10	< 1	100-91
90-81	10-20	1-2.5	90-81
80-71	20-30	2.5-5	80-71
70-61	30-40	5-7.5	70-61
60-51	40-50	7.5-10	60-51
50-41	50-60	10-15	50-41
40-31	60-70	15-20	40-31
30-21	70-80	20-25	30-21
20-11	80-90	25-30	20-11
10-0.1	90-100	30-50	10-0
< 0.1	110	--	--

Table 2.4 *Specific criteria assignment of scores here applied to some green principles of sustainability assessment according to the White Analytical Chemistry [11].*

Score	Toxicity of reagents (impact and biodegradation)	Reagent consumption (mL)	Waste production	Direct impact (personnel safety)
100	Natural-based reagents/material or totally biodegradable	Minimal volume/number of reagents needed (< 1 mL)	Non-toxic waste produced equal or lower to the amount of reagents used	No hazardous activity
75	Aqueous non-toxic reagents and minimal impact on the environment and living beings; no pictograms associated	Reduced volume/number of reagents needed (1-50 mL)	Low-toxic minimal waste produced	Low hazardous activities
50	Possible adverse effects on the environment and living beings; few pictograms associated	Moderate volume/number of reagents needed (51-100 mL)	Medium amount of waste produce with eventual toxicity	Medium hazardous activities
25	Severe adverse effects on the environment and living beings; multiple pictograms associated	Large volume/number of reagents needed (> 100 mL)	Medium amount of waste produce with eventual toxicity and safety disposal required	Hazardous activities
0	Long-term adverse effects on the environment and living beings; multiple pictograms associated	Large volume/number of reagents needed (> 100 mL, multiple reagents)	High amount of waste produce with eventual toxicity and safety disposal required	Hazardous activities with permanent impact

Table 2.4. *Scores assigned for the paper origami platform for GLY detection and a reference method for GLY detection in human urine, according to the sustainability assessment of White Analytical Chemistry [1]. The criteria used for each principle described in the WAC is reported.*

White Analytical Chemistry Principles		Paper origami platform	Score	HPAEC-MS/MS method	Score	Criteria for score assignment
R1. Scope of application (the mean value is considered for R1 score)	Range of linearity	100-700 µg/L	50	1-20 µg/L	100	50-score is assigned to the paper origami platform since it presents a large linear range that is suitable for early screening, revealing glyphosate in urine samples after severe exposure, e.g. due to occupational exposure; 100-score is assigned to HPAEC-MS/MS since it presents a linear range that is suitable for trace level of glyphosate in urine, at any time after the exposure (samples with higher concentrations of glyphosate can be diluted before being analysed)
	Resistance to the presence of potential interferences	Uric acid interference can be overcome by on-paper treatment integrated in the device; synthetic urine medium, urea, and creatinine do not significantly interfere	100	Calibration curves is made using the matrix medium to take account of any difference in the response due to the medium	100	100-score is assigned to the paper origami platform since it is customized to overcome the possible interferences observed in urine samples; 100-score is assigned to HPAEC-MS/MS since it allowed for analysing urine samples without any interfering matrix effects
R2. LOD	LOD (ppb)	75 µg/L	35	8.3 ng/g	100	Scores assigned according to Table S1
R3. Precision	RSD% (repeatability)	≤ 10	55	7	65	Scores assigned according to Table S1
R4. Accuracy	Recovery (%)	~ 99%	100	98	100	100-score is assigned to both methods since there are no significant differences

G1. Toxicity of reagents		The device is based on paper that is a biodegradable material; aqueous non-toxic reagents and minimal impact on the environment and living beings; no pictograms associated	90	Aqueous non-toxic reagents and minimal impact on the environment and living beings; no pictograms associated	75	Scores assigned according to Table S2. The score for the paper origami platform takes into account that the paper that is a biodegradable material
G2. Amount of reagents and waste (the mean value is considered for G2 score)	Reagent consumption	Total volume for the paper platform preparation < 50 µL; total volume for the analysis = 70 µL	100	Total volume of ultra-pure water for extraction and HPAEC-MS/MS analysis = 50 mL per sample	75	Scores assigned according to Table S2 (the mean value is considered for G2 scores)
	Waste production	Related to the reagent consumption + the paper strip (which can be incinerated, with minimal solid waste production)	100	Waste production is related to decontamination and extraction procedure = 20 mL of ultra-pure water per sample + 1 Polypropylene Centrifuge Tubes	75	
G3. Consumption of energy		Very low (portable potentiostat + laptop)	100	High consumption of energy and multiple instrumentation or tools involved (e.g., sample storage, refrigeration, fume hood systems, supplies, others)	10	100-score is here assigned to the very low consumption of the paper origami platform, while a minimal score (10) is assigned to spectrometry instrumentation, which is considered among the highest consumption of energy in a common laboratory
G4. Direct impacts	Safety of users	No hazardous activity	100	Low hazardous activity	75	Scores assigned according to Table S2
	Use of animals or GMO (0 if no, 1 if yes)	No	0	No	0	

B1. Cost efficiency	Total cost estimated	< 5 euros (including 3 paper printed sensors, wax patterned filter paper, reagents); no skilled personnel needed	100	High-cost instrumentation; medium costs related to reagent consuming and long-time analysis; trained personnel needed	10	100-score is here assigned to the very low cost of the paper origami platform, while a minimal score (10) is assigned to spectrometry instrumentation, which is associated to the highest costs in a common laboratory, with the need for technical preparation
B2. Time efficiency	Speed of analysis	About 10 min each analysis	100	The time of analysis is determined by the need for sample preparation, calibration curve, standard tests, standard procedures for the instrumentation starting; for one analysis about 40 minutes are needed	10	100-score is here assigned to the very fast time of analysis with the paper origami platform, while a minimal score (10) is assigned to spectrometry instrumentation, which is associated to the longest time of analysis in a common laboratory
B3. Requirements	Sample consumption	Only 60 µL of sample needed for the analysis, directly dropped on the paper platform	100	100 µL of sample needed for the analysis	100	Scores assigned using the criterium for "reagent consumption" in Table S2
	Other needs: advanced instruments, skills, facilities	No need for advanced instruments or skills	100	Advanced instruments and skills are required	10	100-score is here assigned to the very few requirements of the paper origami platform, while a minimal score (10) is assigned to spectrometry instrumentation, which presents a variety of requirements
B4. Operational simplicity	Portability	In situ applicability	100	No	0	100-score is here assigned to portable sensing system, while 0-score is assigned to non-portable instrumentations
	Automation	At-line: applicable in field, need for dropping the sample and to start the analysis after the treatment step	75	Off-line: need for sampling and sample transport in a formal lab setting	25	100 for in-line analysis, 75 for on-line analysis, 50 for at-line analysis, 25 for off-line analysis
	Miniaturization	Handheld	100	Bench	0	100-score is here assigned to miniaturized sensing system, while 0-score is assigned to bench instrumentations

References

[1] G.M. Dill, R.D. Sammons, P.C.C. Feng, F. Kohn, K. Kretzmer, A. Mehrsheikh, M. Bleeke, J.L. Honegger, D. Farmer, D. Wright, E.A. Haupfear, GLYPHOSATE: DISCOVERY, DEVELOPMENT, APPLICATIONS, AND PROPERTIES, 2010.

[2] R. Mesnage, M.N. Antoniou, Roundup ready! Glyphosate and the current controversy over the world's leading herbicide, in: Encyclopedia of the Anthropocene, Elsevier, 2017: pp. 149–153. https://doi.org/10.1016/B978-0-12-809665-9.09981-X.

[3] Cara Munez, Weed Killer Glyphosate Found in Most Americans' Urine., Robin Foster HealthDay, U.S. News, (2022). https://www.healthday.com/health-news/public-health/glyphosate-herbicide-2657652916.html (accessed February 7, 2025).

[4] D. Grau, N. Grau, Q. Gascuel, C. Paroissin, C. Stratonovitch, D. Lairon, D.A. Devault, J. Di Cristofaro, Quantifiable urine glyphosate levels detected in 99% of the French population, with higher values in men, in younger people, and in farmers, Environmental Science and Pollution Research 29 (2022) 32882–32893. https://doi.org/10.1007/s11356-021-18110-0.

[5] C.M. Benbrook, Trends in glyphosate herbicide use in the United States and globally, Environ Sci Eur 28 (2016) 1–15. https://doi.org/10.1186/s12302-016-0070-0.

[6] E. Noviana, C.P. McCord, K.M. Clark, I. Jang, C.S. Henry, Electrochemical paper-based devices: Sensing approaches and progress toward practical applications, Lab Chip 20 (2020) 9–34. https://doi.org/10.1039/c9lc00903e.

[7] N. Colozza, V. Caratelli, D. Moscone, F. Arduini, Paper-based devices as new smart analytical tools for sustainable detection of environmental pollutants, Case Studies in Chemical and Environmental Engineering 4 (2021). https://doi.org/10.1016/j.cscee.2021.100167.

[8] V. Caratelli, E. Di Meo, N. Colozza, L. Fabiani, L. Fiore, D. Moscone, F. Arduini, Nanomaterials and paper-based electrochemical devices: merging strategies for fostering sustainable detection of biomarkers, J. Mater. Chem. B 10 (2022) 9021–9039. https://doi.org/10.1039/D2TB00387B.

[9] F. Arduini, S. Cinti, V. Caratelli, L. Amendola, G. Palleschi, D. Moscone, Origami multiple paper-based electrochemical biosensors for pesticide detection, Biosens Bioelectron 126 (2019) 346–354. https://doi.org/10.1016/j.bios.2018.10.014.

[10] A. Gałuszka, Z. Migaszewski, J. Namieśnik, The 12 principles of green analytical chemistry and the SIGNIFICANCE mnemonic of green analytical practices, TrAC - Trends in Analytical Chemistry 50 (2013) 78–84. https://doi.org/10.1016/j.trac.2013.04.010.

[11] P.M. Nowak, R. Wietecha-Posłuszny, J. Pawliszyn, White Analytical Chemistry: An approach to reconcile the principles of Green Analytical Chemistry and functionality, TrAC - Trends in Analytical Chemistry 138 (2021). https://doi.org/10.1016/j.trac.2021.116223.

[12] F. Arduini, Electrochemical paper-based devices: When the simple replacement of the support to print ecodesigned electrodes radically improves the features of the electrochemical devices, Curr Opin Electrochem 35 (2022). https://doi.org/10.1016/j.coelec.2022.101090.

[13] C. Dincer, R. Bruch, E. Costa-Rama, M.T. Fernández-Abedul, A. Merkoçi, A. Manz, G.A. Urban, F. Güder, Disposable Sensors in Diagnostics, Food, and Environmental Monitoring, Advanced Materials 31 (2019). https://doi.org/10.1002/adma.201806739.

[14] W. Dungchai, O. Chailapakul, C.S. Henry, Electrochemical detection for paper-based microfluidics, Anal Chem 81 (2009) 5821–5826. https://doi.org/10.1021/ac9007573.

[15] M. Gutiérrez-capitán, A. Baldi, C. Fernández-sánchez, Electrochemical paper-based biosensor devices for rapid detection of biomarkers, Sensors (Switzerland) 20 (2020). https://doi.org/10.3390/s20040967.

[16] C. Te Kung, C.Y. Hou, Y.N. Wang, L.M. Fu, Microfluidic paper-based analytical devices for environmental analysis of soil, air, ecology and river water, Sens Actuators B Chem 301 (2019). https://doi.org/10.1016/j.snb.2019.126855.

[17] N. Colozza, V. Caratelli, D. Moscone, F. Arduini, Origami paper-based electrochemical (Bio)sensors: State of the art and perspective, Biosensors (Basel) 11 (2021). https://doi.org/10.3390/BIOS11090328.

[18] V. Caratelli, G. Fegatelli, D. Moscone, F. Arduini, A paper-based electrochemical device for the detection of pesticides in aerosol phase inspired by nature: A flower-like origami biosensor for precision agriculture, Biosens Bioelectron 205 (2022). https://doi.org/10.1016/j.bios.2022.114119.

[19] A. Padiglia, R. Medda, S. Longu, J.Z. Pedersen, G. Floris, Uric acid is a main electron donor to peroxidases in human blood plasma, Med Sci Monit 8 (2002) BR454—9. http://europepmc.org/abstract/MED/12444370.

[20] E.S. Canellakis, A.L. Tuttlej, P.P. Coheis, A COMPARATIVE STUDY OF THE END-PRODUCTS OF URIC ACID OXIDATION BY PEROXIDASES*, n.d.

[21] L.A. Pachla, D.L. REYNOLDS Warner-Lamberti, P. Tkissinger, PharmacokineticslDrug Metabolism 2800 Plymouth Rd, n.d. https://academic.oup.com/jaoac/article/68/1/1/5704468.

[22] H. Iwata, S. Nishio, M. Yokoyama, A. Matsumoto, M. Takeuchi, Solubility of uric acid and supersaturation of monosodium urate: Why is uric acid so highly soluble in urine?, Journal of Urology 142 (1989) 1095–1098. https://doi.org/10.1016/S0022-5347(17)39003-1.

[23] W.R. Wilcox, A. Khalaf, A. Weinberger, I. Kippen, J.R. Klinenberg, Solubility of uric acid and monosodium urate, Med Biol Eng 10 (1972) 522–531. https://doi.org/10.1007/BF02474201.

[24] M.G. Simic, S. V Jovanovic, Antioxidation mechanisms of uric acid, J Am Chem Soc 111 (1989) 5778–5782. https://doi.org/10.1021/ja00197a042.

[25] P.M. Nowak, P. Kościelniak, What color is your method? adaptation of the rgb additive color model to analytical method evaluation, Anal Chem 91 (2019) 10343–10352. https://doi.org/10.1021/acs.analchem.9b01872.

[26] M.S.R.P.C.B. Matteo Feltracco Elena Barbaro, A. Gambaro, Detection of glyphosate residues in feed, saliva, urine and faeces from a cattle farm: a pilot study, Food Additives & Contaminants: Part A 39 (2022) 1248–1254. https://doi.org/10.1080/19440049.2022.2066194.

Chapter 3: Salting-Out Meets Electrochemistry: A Paper-Based Solution for Urine Sample Pre-Treatment

3.1 Introduction

The ability to accurately detect and quantify biomolecules in biological fluids is crucial for disease diagnosis, therapeutic monitoring, and overall health status assessment. Biological fluids such as blood, plasma, and urine are a valuable source of information for disease diagnosis, therapeutic monitoring, and health status assessment. Among these fluids, urine presents significant advantages due to its non-invasive collection, stability, and comprehensive metabolomic profile.

As previously mentioned in Chapter 1 (**Section 1.3**), biological fluids pose great challenges for electrochemical sensing due to the complex matrix effect and for the presence of many interfering species. Endogenous compounds such as proteins, salts, and organic molecules can lead to non-specific adsorption on the electrode surface, resulting in electrode passivation [1,2], which causes decreasing of the signal intensity and compromises sensor sensitivity and reproducibility. Proteins in biological matrices are also electroactive, impairing the accuracy of electrochemical detection.

Several strategies have been explored to mitigate the effect imparted by the presence of proteins in biological samples, including surface coatings with antifouling materials such as self-assembled monolayers (**SAMs**), hydrophilic polymers, and biomimetic coatings [3,4]. These approaches can effectively reduce protein surface interaction, but often introduce additional complexity in sensor fabrication, limit the electroactive surface area, and may not address protein interference at elevated concentration, making it necessary additional pre-analytical steps. To address these limitations, conventional protein removal techniques such as centrifugation, ultrafiltration, and precipitation with reagents like ammonium sulfate or trichloroacetic acid have been widely employed [5]. These methods, while effective, require specialized laboratory equipment, long processing times, and relatively large sample volumes, making them unsuitable for point-of-care (**POC**) applications. Centrifugation and ultrafiltration, for instance, rely on high-speed separation techniques that are not easily scalable for portable devices, whereas chemical precipitation methods, though simpler, often

require additional reagents and multiple handling steps, increasing the risk of sample contamination and variability.

The salting out process is a strategy often proposed for protein removal during the analytical pre-processing of urine samples [6]. Protein precipitation by salting-out effect, is induced by the increasing of the ionic strength of the solution. Indeed, addition of high concentration of electrolytes to the solution leads to disruption of the hydrogen bonds and, thus aggregation and precipitation of proteins, as examined in further detail in Section 3.2. This method, when combined with paper-based microfluidic devices, offers effective protein removal [7,8] with a very simple and rapid automatic process, not requiring manual filtration or centrifugation of the sample**.** Paper-based device provides further advantages in this context: the porous structure of the paper facilitates capillary action, enabling efficient liquid transport and filtration without external pumps, while the fibrous network acts as a natural filter. Furthermore, paper-based devices are cost-effective, biodegradable, and easily customizable, making them ideal for developing portable and disposable diagnostic platforms [9,10]. Wang et al. previously demonstrated that $(NH_4)_2SO_4$ is the salt that, in combination with paper, is the most effective in removing proteins for urine samples [11]. However, the efficiency of this method is still unknown, making it difficult to compare it with other pre-analytical strategies. Herein, we aim to bridge this knowledge gap by systematically quantifying protein removal using both colorimetric and electrochemical measurements. Our findings indicate that an efficiency of 71% can be achieved without requiring additional pre-treatment steps, representing a significant improvement over previous study. This quantitative data allows for direct comparison with traditional methods, such as filtration and ultracentrifugation, demonstrating that salting-out combined with paper-based microfluidics provides comparable efficiency while offering additional benefits in terms of cost, portability, and ease of integration into sensing platforms. Additionally, it requires minimal sample volume and no energy consumption, making it ideal for point-of-care applications [12].

The integration of this pre-analytical strategy with electrochemical detection enables the direct analysis of biomolecules such as tryptophan, chosen as benchmark analyte to demonstrate that the electrochemical analysis in untreated urine samples is feasible.

Although tryptophan is not classified as a contaminant of emerging concern, it was included in this work as a model analyte since the electrochemical oxidation process falls in the same potential range in which interference from endogenous compounds, especially proteins, typically occurs. In complex biological fluids, such as urine, the oxidation signals of proteins and metabolites often produce broad, unresolved voltammetric features that hinder the accurate detection of target compounds. Tryptophan, by contrast, provides a clearly identifiable oxidation peak, making it a suitable probe to evaluate the effectiveness of sample clean-up and protein-removal strategies. Its inclusion in this study thus supports the development and validation of pre-analytical workflows aimed at improving signal clarity and selectivity in biosensing platforms for biological monitoring.

Beside this proof-of-concept reason, the determination of free tryptophan in urine is quite important, since it offers valuable insights into a patient's health, as this essential amino acid plays key roles in physiological processes such as serotonin and melatonin synthesis. Elevated levels of tryptophan in urine samples are linked to metabolic disorders and systemic diseases. For instance, overactivation of the tryptophan pathway occurs in carcinoid syndrome due to excessive serotonin secretion by neuroendocrine tumors [13]. Similarly, elevated tryptophan levels are observed in liver diseases like cirrhosis, resulting from protein metabolism dysfunction [14]. Detecting free tryptophan in urine using electrochemical sensors is challenging due to overlapping oxidation potentials with co-existing proteins; however, our approach effectively mitigates this interference, enabling reliable measurements with carbon screen-printed electrodes (CSPEs). By integrating the salting-out effect with paper-based microfluidic platforms, we demonstrate a streamlined, cost-effective, and portable solution for urine sample preparation and electrochemical sensing. This approach significantly reduces the complexity and resource demands of traditional preanalytical steps, paving the way for more accessible and efficient POC diagnostic technologies.

3.1.1 The Salting out effect and the Hofmeister Series

In plain terms, the salting effect refers to the change in solubility of a non-electrolyte in an aqueous solution. As the concentration of an added electrolyte increases, the solubility of a non-electrolyte can either increase or decrease, leading to phenomena

known as salting-in and salting-out, respectively. In this context, electrolytes refer to salts with high solubility, while non-electrolytes are salts with low solubility [6]. The salting-out effect results from the competition between water molecules available to solvate the salt ions and those needed to keep the solute in solution. Historically, the salting-out effect was systematically studied by Franz Hofmeister, who, in 1888, classified ions based on their ability to precipitate proteins, leading to the formulation of the Hofmeister series. This series ranks cations and anions according to their effectiveness in promoting solubility (salting-in) or precipitation (salting-out) of macromolecules in solutions. Ions are typically classified as kosmotropic or chaotropic. Kosmotropic ions, such as the cations Li^+, Na^+, Mg^{2+}, Ca^{2+} and the anions SO_4^{2-}, F^-, Cl^-, tend to stabilize intramolecular interactions in proteins and promote their precipitation by reducing their solubility in solution. This effect is due to their strong hydration, which sequesters water molecules away from the solute, leading to its aggregation and eventual precipitation.

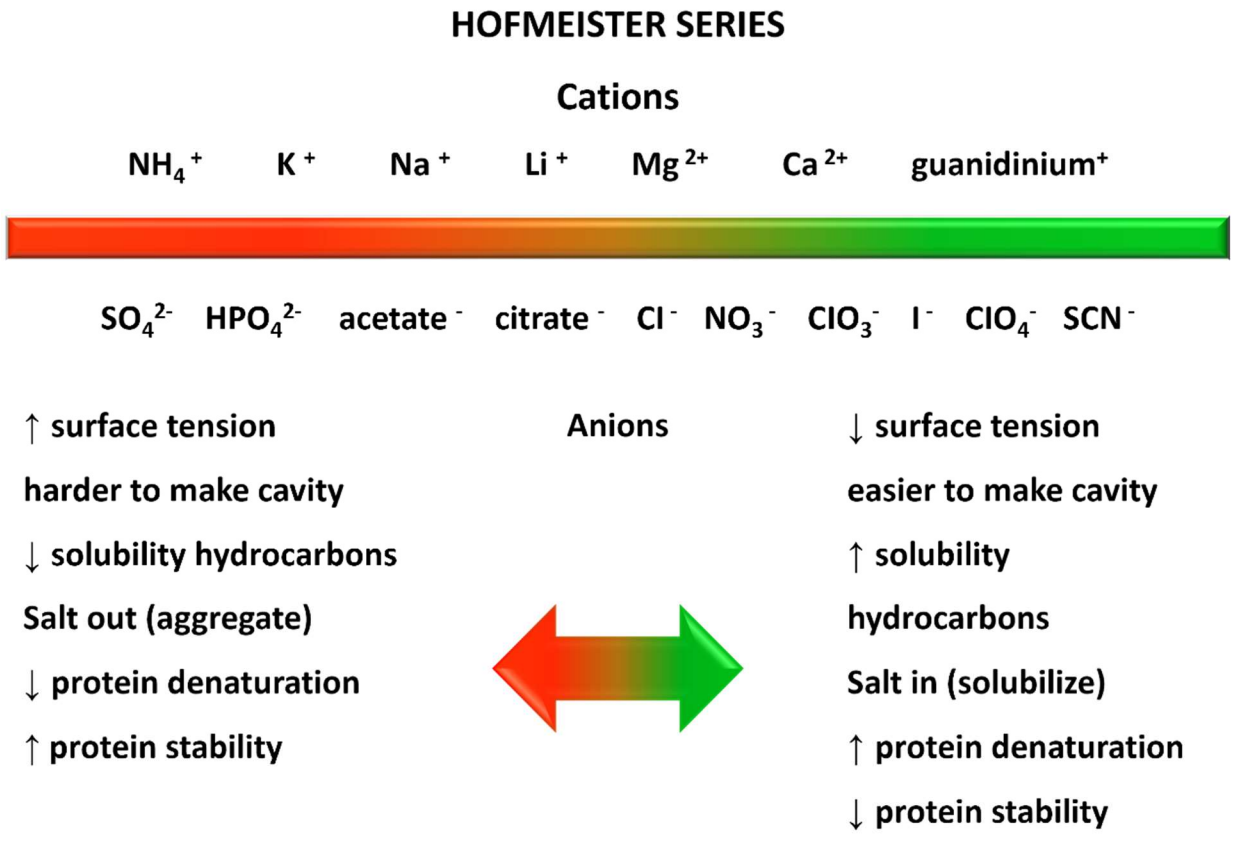

Figure 3.1) *Schematic representation of the Hofmeister series*.

In contrast, chaotropic ions, such as the cations K^+, Rb^+, Cs^+, NH_4^+ and the anions I^-, ClO_4^-, SCN^-, have a lower affinity for water and interact more strongly with protein surfaces, destabilizing protein structures and increasing their solubility (salting-in). The traditional interpretation of the Hofmeister series (***Figure 3.1***) attributed these effects to the ability of ions to influence water structure. However, more recent studies suggest that the key factor is the direct interaction between ions and protein surfaces. Specifically, weakly hydrated anions such as SCN^- and ClO_4^- tend to preferentially interact with apolar regions or peptide groups of proteins, leading to structural destabilization and increased solubility. Conversely, strongly hydrated anions like SO_4^{2-} and F^- are excluded from protein surfaces, favoring salting-out. For cations, more strongly hydrated species, such as Mg^{2+} and Ca^{2+}, are more effective in promoting protein precipitation, whereas less hydrated cations, like K^+ and Cs^+, favor salting-in. This modern understanding of the Hofmeister effect is crucial for numerous biochemical and analytical applications, including protein purification, macromolecule crystallization, and the optimization of stability conditions for biological systems in solution.

3.1.3 Paper devices for sample treatment and analysis

Wax printing on paper represents a cost-effective technique for producing paper-based sensors, leveraging the ability of wax to create hydrophobic barriers that precisely define microfluidic channels. This technology allows for controlled fluid flow and uniform sample distribution within the device, optimizing the chemical or biochemical reactions required for analysis. The rapid processing time and compatibility with a wide range of sensing materials, including enzymes, nanoparticles, and indicator dyes, make this technique particularly suitable for developing disposable diagnostic tools. Furthermore, paper-based sensors offer significant environmental benefits, being biodegradable and reducing the use of plastic in traditional diagnostic devices. Paper has also been widely employed both as a reagent storage device and as a filtration tool, thanks to its absorbent properties and its ability to facilitate chemical reactions in a controlled environment.

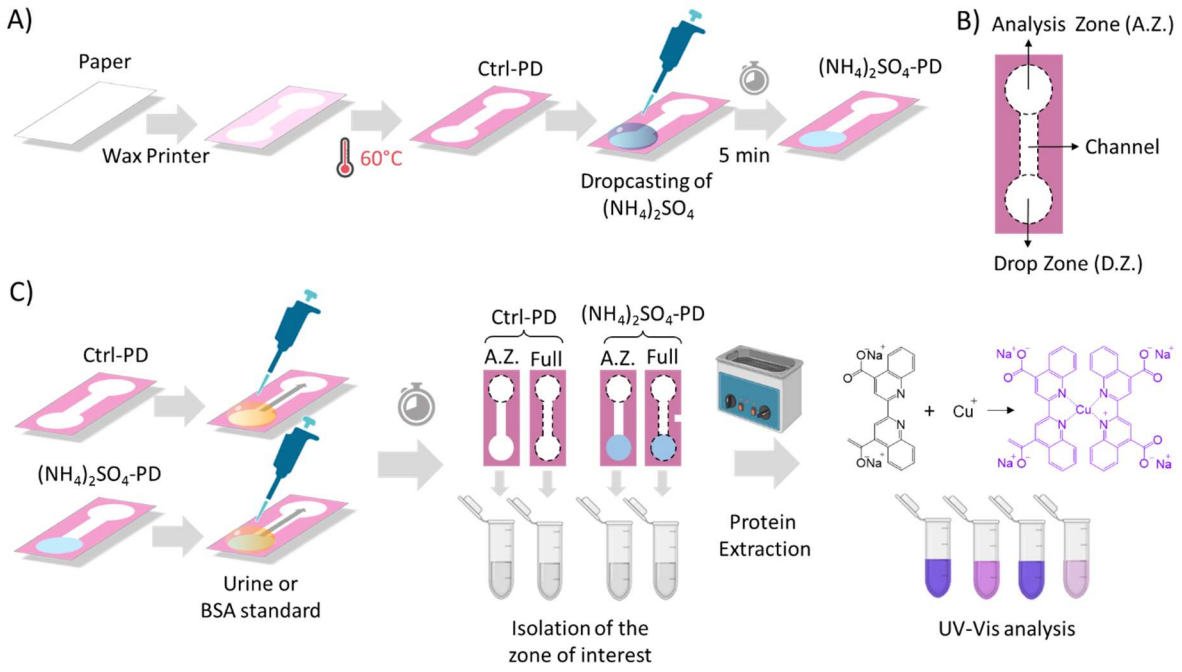

Figure 3.2) *Schematic representation of the preparation and use of paper-based devices (PDs) used in this work. a) Creation of PDs via wax printing, thermal treatment, cutting, and reagent deposition. b) Virtual separation of the different PDs areas. c) sample application, protein extraction and analysis using sonication and BCA assay with UV-Vis spectrophotometry.*

In particular, it can be combined with the use of ammonium sulfate ($(NH_4)_2SO_4$) for protein precipitation by salting-out effect to obtain a highly efficient and versatile approach for the realization of portable devices for the rapid analysis of biological fluids. The preparation of paper-based devices (**PDs**) for sample analysis must follow a series of precise steps, graphically represented in **Figure 3.2a** for the specific case adopted in this work. The process begins with a sheet of paper treated using wax printing technology to create hydrophilic and hydrophobic regions. The printed sheet is then heated at 60 °C to allow the wax to fully penetrate the paper structure, stabilizing the hydrophobic areas and defining the hydrophilic channel within which solution diffuses by capillarity. After thermal treatment, the sheets are cut to obtain individual PDs. At this stage, reagents are deposited: the control PD (**Ctrl-PD**) receives no additional treatment, whereas the ammonium sulfate-treated PD ($(NH_4)_2SO_4$-PD) is prepared by depositing of ammonium sulfate and allowing it to dry as detailed in **section 3.4.2.** For a better understanding of the analytical procedure, each PD was virtually divided into three areas shown in **Figure 3.2b**: Analysis Zone (A.Z.), Channel,

and Drop Zone (D.Z.). Once the PD is ready, the sample is applied (***Figure 3.c***) by dropping a defined volume (20 µL) onto the designated area and, due to capillarity, it can flow from the drop to the analysis zone. The presence of ammonium sulfate in the channel induces protein precipitation, affecting subsequent analytical performance. Although a similar approach has been already proposed in the literature [11], it lacks in studying the process in more detail, particularly concerning the precipitation grade. Aim at studying in more details these aspects, after the sample reached the A.Z and the PDs resulted fully dried, they were processed to extract the residual proteins reaching each zone: the device was cut to isolate either the full PAD or just the A.Z, the selected portion was then placed in an Eppendorf tube and subjected to sonication to extract retained proteins. Finally, the extracted sample was analyzed using the Bicinchoninic Acid (**BCA**) assay to quantify the residual amount of proteins and achieve a real quantification of the precipitation process occurred on the different regions of the PDs. In addition, to demonstrate the real advantages in inducing protein precipitation on the PDs, the device was applied for the detection of tryptophan.

3.2 Results and Discussion

3.2.1 Quantification of the protein remotion efficiency

Quantifying the protein removal efficiency is fundamental to compare emerging approaches with the benchmark ones. To assess the efficacy of salting out precipitation process applied on the paper-based devices, we verified: I) the contribution provided just by the paper filtration by operating on a Ctrl-PD and II) the contribution of the salting-out induced by the presence of $(NH_4)_2SO_4$ in the paper filtration, by using a $(NH_4)_2SO_4$-PD. In this series of experiments, we used a 2 mg mL^{-1} Bovine Serum Albumin (**BSA**) solution as a standard and we deposited 5µL of 90% saturated $(NH_4)_2SO_4$ solution onto the PD. We chose this concentration to ensure that the protein could be quantified by BCA assay after the paper-based pre-treatment. A 20 µL drop of BSA solution was deposited on the drop zone of both $(NH_4)_2SO_4$-PD and Ctrl-PD and let flow through the channel until reaching the analysis zone. The concentration of proteins that reached the analysis zone was estimated by isolating this area from the PD, extracting the proteins by sonication, and performing the BCA colorimetric test. All the experiments were conducted in triplicate. Since the extraction of proteins from the

paper may not be completed, we estimated the total amount of proteins by performing the same analysis on the full PD, to estimate the fraction that reached the A.Z in both PADs.

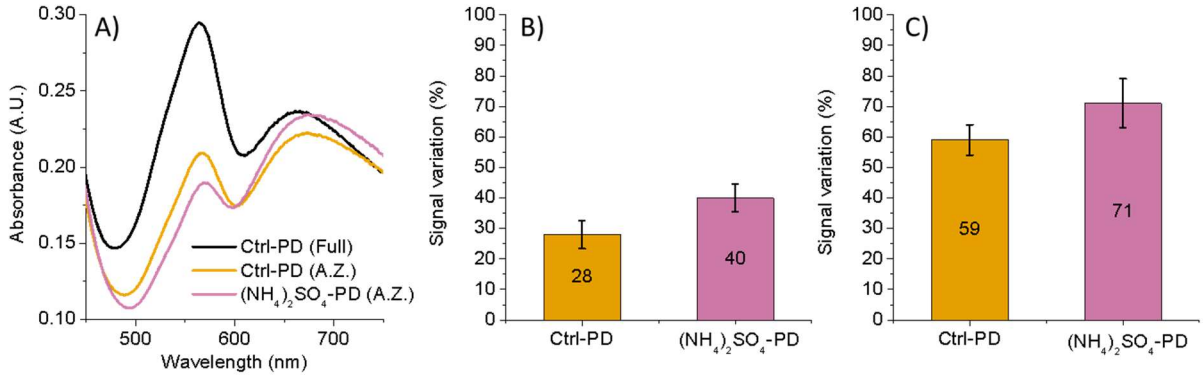

Figure 3.3) a) *UV-Vis spectra of BSA solutions extracted from full Ctrl-PD, Ctrl-PD (A.Z), and a $(NH_4)_2SO_4$-PD (A.Z) and treated with BCA. The quantification of proteins can be defined based on the absorbance at 562 nm.* ***b)*** *Comparison of protein removal efficiency between Ctrl-PD and $(NH_4)_2SO_4$-PD tested with a 2 mg mL^{-1} BSA solution.* ***c)*** *Comparison of protein removal efficiency performed on a real urine sample.*

Figure 3.3a reports the UV-Vis spectra of the BCA colorimetric test performed on the full Ctrl-PD and limited on the analysis zones of Ctrl-PD and $(NH_4)_2SO_4$-PD. The adsorption at 562 nm, whose intensity is directly proportional to the protein concentration, is lower on passing from the full to the PAD limited to the A.Z. This observation indicates that paper as such can induce partial removal of proteins by capillary filtration. The absorption at 562 nm further decrease in a PAD also containing $(NH_4)_2SO_4$, demonstrating the effectiveness of the salting out process occurring in the PAD. The protein removal efficiency (η%) was calculated using the following formula:

$$\eta\% = \frac{S_{tot} - S_{AZ}}{S_{tot}} * 100$$

Where S_{AZ} is the signal derived from the BCA colorimetric test for the proteins extracted by the analysis zone and S_{tot} is the signal derived from the full paper device. The **Ctrl-PD** presented an η% equal to 28%, while in the presence of $(NH_4)_2SO_4$ in the PAD the precipitation efficiency further increased to 40% (***Figure 3.3b***).

We repeated the same experiments using real urine samples collected from healthy volunteers, demonstrating that in this case the protein removal was even more efficient, with η% equal to 59% for **Ctrl-PD** and 71% for **$(NH_4)_2SO_4$-PD** (***Figure 3.3c***). This data confirms once again that the paper has a fundamental role in filtering the proteins which can be improved by inducing the protein precipitation by the salting-out effect.

The increased filtration efficiency of the paper strip in removing proteins from real urine compared to a standard water solution of BSA can be attributed to several factors: **a)** the physiological concentration of proteins in urine is typically below 2 mg mL^{-1}, which may enhance adsorption efficiency on paper compared to more concentrated protein standard solutions. Additionally, the presence of electrolytes, salts, and metabolites can influence electrostatic interactions between cellulose and proteins, modulating their adhesion to the support surface. **b)** Real urine contains proteins different from BSA (e.g., human albumin or smaller proteins), which could have a distinct structure, surface charge, or hydrophobicity. These properties may influence the efficiency of adsorption onto the paper. **c)** The viscosity or other physical properties of real urine might influence the liquid flow through the paper, promoting filtration efficiency. For example, bovine albumin in the standard solution might behave differently from human albumin or other urinary proteins [15,16]. A control experiment was performed, comparing the signal obtained from complete Ctrl-PD and $(NH_4)_2SO_4$-PD to check that the presence of ammonium sulphate did not interfere with the protein extraction process. By confirming that the extraction efficiency was not significantly different regardless the presence of ammonium sulphate, we could verify that the observed increase in protein removal efficiency was genuinely due to the salting-out effect rather than any artifact introduced by the BCA assay (***Figure 3.4a***).

After confirming the positive effect of $(NH_4)_2SO_4$ on the protein removal efficiency, we investigated the influence of the volume deposited on paper strips. To such a purpose, we tested three volumes of $(NH_4)_2SO_4$ solution, namely 5 to 10 and 15 µL. ***Figure 4b*** shows that there is no significant difference among the η% for the different volumes tested. This outcome may be attributed to the saturation of protein binding capacity on the paper matrix, as described in studies of paper-based microfluidic systems for protein assays [8,17]**.**

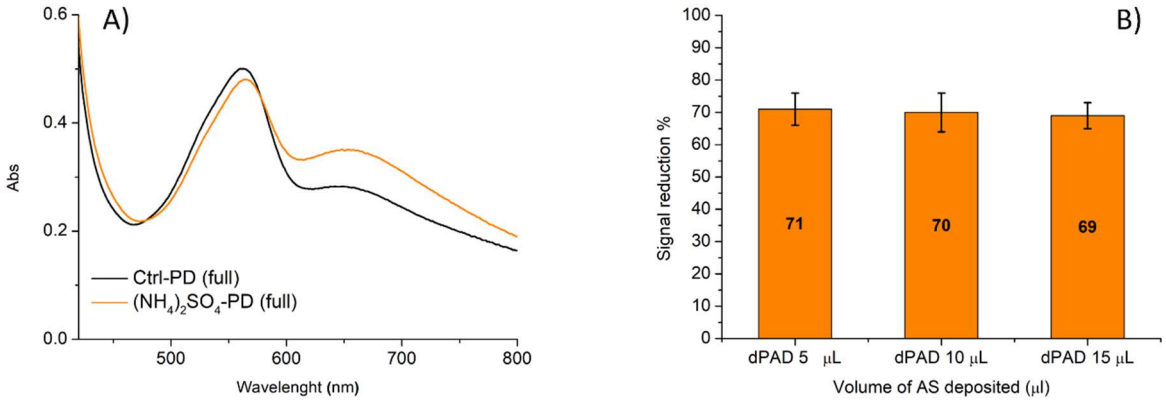

Figure 3.4. a) *Comparison of the UV-Vis spectra recorded from proteins extracted from a complete Ctrl-PD and a $(NH_4)_2SO_4$-PD.* ***b)*** *Effect of the volume of $(NH_4)_2SO_4$ solution deposited on the PAD on protein removal efficiency (η%).*

Additionally, the protein precipitation efficiency might reach a plateau due to the solubility limits of ammonium sulfate once reached with the sample or to the limited diffusion of proteins into a PAD containing a too large amount of salt. Previous studies demonstrated that, beyond a threshold, further addition of precipitating salts does not substantially enhance protein removal [5].

3.2.2 Electrochemical detection of tryptophan in real urine samples

After verifying the efficiency of the paper platform in removing proteins through UV-Vis spectrophotometric analysis, we assessed its applicability for electrochemical sensor measurements. As a model analyte, we selected tryptophan, an amino acid that exhibits a well-defined oxidation peak at approximately +0.7 V vs Ag/AgCl. This potential range overlaps with the broad electrochemical signals often attributed to the presence of proteins and other endogenous species in biological matrices, which tend to generate poorly resolved voltammetric features. Because of this, tryptophan serves not only as a biologically relevant molecule but also as a strategic analytical probe for assessing the effectiveness of pre-treatment strategies in reducing protein-related interference. Although tryptophan is not classified as an emerging contaminant, its oxidation process underlines the key analytical challenges posed by complex biological fluids—particularly when no selective recognition sensing elements are employed, making it a suitable target to demonstrate the feasibility of pre-analytical methodologies, which are within the scope of this thesis.

To perform electrochemical analysis, we employed CSPEs electrochemically activated in sulfuric acid. This oxidation process plays a crucial role in enhancing the electrode's performance by introducing oxygen-containing functional groups, such as carboxyl, carbonyl, and hydroxyl groups, onto the carbon surface. These functional groups significantly improve the electrode's hydrophilicity and enhance electron transfer kinetics, thereby promoting a more efficient redox process for the analyte of interest. Additionally, the introduction of oxygen-based functionalities changes the surface charge of the working electrode, facilitating the adsorption of biomolecules [18]. **Figure 3.5a** shows the responses recorded by cyclic voltammetry (CV) in a real urine sample, acidified to approximately pH 3 using 0.1 M HCl, using both pristine and oxidized CSPEs, demonstrating the effectiveness of the oxidized moieties present of the surface in imparting electrocatalytic performance to the electrode surface. It is worth to mention that this exploratory analysis were performed at pH 3 to characterize the redox behaviour of tryptophan under conditions in which it exhibits enhanced peak intensity and resolution due to improved proton-coupled electron transfer kinetics [20].

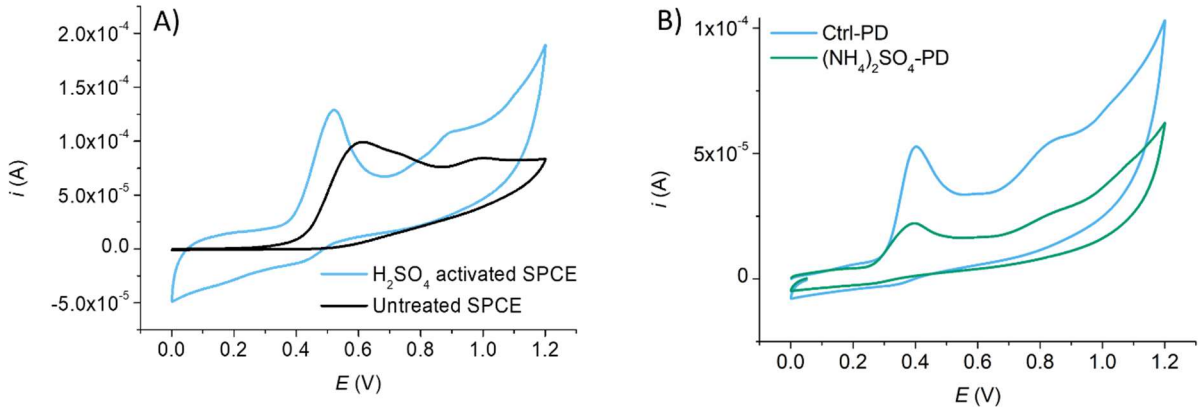

***Figure 3.5: a**) CVs responses of a urine sample, acidified to pH = 3, recorded with pristine and electrochemically oxidized CSPEs. **b**) Effect of $(NH_4)_2SO_4$-PD pretreatment on the electrochemical response of tryptophan.*

As expected, we could observe that the oxidation peak ascribable to tryptophan is approximately centered at +0.9 V vs Ag/AgCl, whereas a second oxidation process, recorded at approximately +0.45 V, can be ascribable to uric acid, in agreement with previous literature reports [19]. Resolution between these oxidation processes is only possible at oxidized CSPEs, thanks to the electrocatalytic properties previously described. Unfortunately, despite the higher resolution observed in this case, the

oxidation of the protein fraction of the sample falls in the same potential region in which tryptophan toxidation occurs.

The marked decrease in the overall electrochemical signal observed after $(NH_4)_2SO_4$ treatment on the paper device (***Figure 3.5b***) reflects a general suppression of matrix-related background currents deriving from the presence of proteins in the sample. While the tryptophan peak also appears diminished in intensity, this effect is not necessarily due to analyte loss, but rather to the significant reduction of electroactive interfering species that otherwise contribute to current enhancement in untreated samples. In this context, the cleaner matrix resulting from protein precipitation leads to lower total current, but improved selectivity and baseline definition.

These findings highlight the benefits of the pre-treatment strategy and electrode modification for electrochemical sensing applications. The electrode surface not only imparts electrocatalytic properties in the oxidation of tryptophan but also enhances the overall sensitivity and selectivity of the response, making it more suitable for the analysis of complex biological matrices, such as urine samples.

The concentration of tryptophan in urine samples was estimated using the standard addition method to compensate for matrix effects and ensure accurate quantification in real samples. Tryptophan levels in urine samples can vary significantly depending on physiological and pathological conditions. The estimated concentration of free tryptophan for healthy adult ranges between 2.5 and 39 μg mL^{-1}, based on an average daily excretion of 5–39 mg and a typical urine output of 1–2 liters per day. While these estimates offer a reasonable approximation, actual concentrations may vary due to individual differences in metabolism, diet, renal function, and fluid intake, and significantly higher levels are observed in patients with metabolic disorders, neuropsychiatric diseases, hepatic dysfunctions, and certain cancers [21]. Based on these findings, a concentration range of 0.01 to 0.1 mg mL^{-1} was selected to encompass clinically relevant values associated with various disease states, ensuring the applicability of this method for tryptophan quantification as a biomarker.

To construct a calibration curve, urine samples were spiked with increasing concentrations of tryptophan within this range. Each spiked solution (20 μL) was applied onto a paper-based PAD pre-treated with 5 μL of ammonium sulfate, following the protocol developed in the previous section. The solutions were allowed to diffuse to the AZ, where solvent was let to dry. Subsequently, 5 μL of phosphate-buffered saline solution (PBS) were added to facilitate sample rehydration and ensure proper

contact between the paper and the surface of the activated CSPE. Differential pulse voltammetry (DPV) measurements were carried out at pH 6.4, which more closely matches the native pH of urine. It is worth to notice that also at this different pH value, the peak due to uric acid and tryptophan oxidation appear narrow and well-resolved from each other (***Figure 3.6a***), confirming that the analysis can be carried out at this pH. The oxidation peak observed around +0.7 V was assigned to tryptophan, as confirmed by the linear increase of current peak at increasing tryptophan concentration. These findings align with prior electrochemical studies, which emphasize the strong pH dependence of tryptophan oxidation [22].

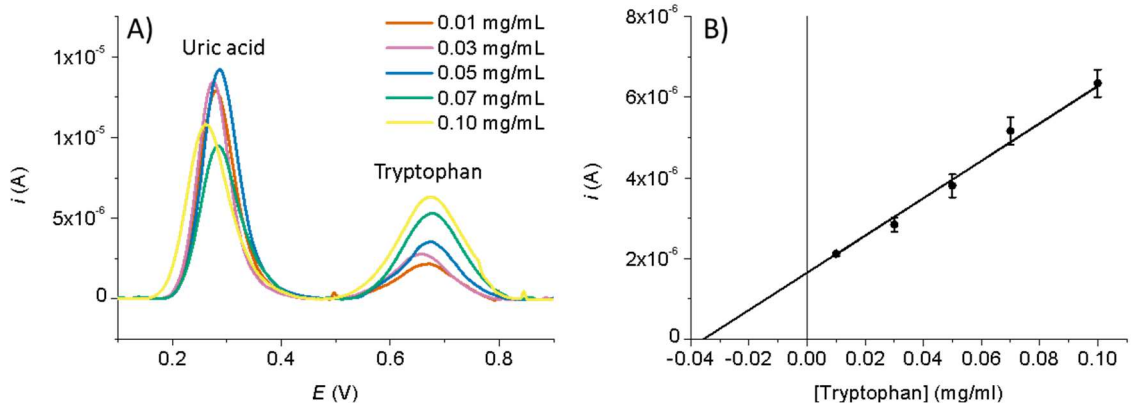

Fig 3.6) a*) DPV responses recorded with oxidized CSPE in real urine samples spiked with increasing amount of tryptophan (concentration range: 0.01–0.1 mg mL^{-1}).* ***b)*** *Calibration plot reporting correlation between the peak current intensity ($I_{p,a}$) at +0.68V vs concentration of the added tryptophan; R^2 = 0.989.*

The calibration plot obtained from DPV measurements (***Figure 3.6b***) displayed a linear response (R^2 = 0.989) of the current peak registered at +0.7 V *vs.* the concentration of tryptophan added, confirming the effectiveness of this electrochemical method for quantification of this amino acid in urine samples. The estimated value of tryptophan concentration in the sample analyzed, obtained through application of the standard addition method, was 35.2 ± 2.1 µg mL^{-1}, resulting from the following calibration equation:

$$I_{p,a}\ (A) = (1.63 \pm 0.05) \times 10^{-6} + (4.64 \pm 0.24) \times 10^{-5}\ [Trp]\ (mg\ mL^{-1}).$$

The analysis performed led us to conclude that the integration of the salting-out approach on a paper-based device ensured minimal protein-related interference, while

the electrode setup, consisting of activated carbon-based surfaces, provided good resolution of the two signals. Moreover, the standard addition method ensured a reliable quantification of tryptophan at both physiological and pathological concentrations. Unfortunately, confirmatory analysis to verify the accuracy of the voltammetric detection was not possible within the timeline of the PhD thesis, so that only speculative conclusions related to the sensing strategy can be given. This notwithstanding, the very narrow DPV responses observed, which cannot be obtained in presence of high content of electroactive proteins in solution, the excellent linearity across the tested concentration range (0.01–0.1 mg/mL) and the value of tryptophan concentration defined that is within the range supposed, contribute to define the reliability of the analytical strategy proposed to minimize matrix effects. Overall, these results confirm that the proposed sensing strategy is highly effective for removing the matrix effect imparted by the protein fraction of urine samples, offering a reliable and accessible tool for the voltammetric analysis of various target analytes in biological matrices. It is worth to notice that the pre-treatment strategy here proposed, based on salting-out protein precipitation combined with paper filtration, can be also combined with sensor platforms containing more selective recognition elements, e.g. molecularly imprinted polymers (MIPs) or bioreceptors, that could further improve the performance of the voltammetric detection. Still in this case, the removal of the protein fraction from the sample can reduce the background currents often affecting the performance of the sensor.

3.3 Sustainability assessment

Aiming at “quantifying” the efficiency of our pre-treatment method, we did a direct comparison with standard approaches such as centrifugation and ultrafiltration. **Table 5.1** summarizes the key parameters considered in this evaluation, including cost per sample, processing time, sample volume required, necessary equipment, operating principle, portability, automation potential, protein removal efficiency (η%), and susceptibility to interference. The cost per sample was estimated based on consumables and equipment requirements. For centrifugation (**3–7€ per sample**), the cost includes chemical reagents for protein precipitation, centrifuge tubes, pipette tips, and the amortized cost of the centrifuge. Ultrafiltration (**5–15€ per sample**) accounts

for disposable filtration membranes, potential pre-treatment solutions, and the filtration system's operational cost. In contrast, the paper-based device (**0.10–0.50€ per sample**) relies only on treated paper, droppers or pipettes, and minimal reagent use, eliminating the need for bulky equipment and electricity.

Table 5.1 – Key performance indicators for different possible strategies for protein removal from urine samples

	Centrifugation	**Ultrafiltration**	**Paper-Based Device**
$\eta\%$	**~70-90%**	**~90-95% ***	**71%**
Cost per sample (€)	3-7	5-15	0.10-0.50
Time per sample (min**)**	30-60	15-30	5-10
Minimum required volume (µL**)**	500 - 1000	100-500	~20
Required equipment	Bench centrifuge, pipettes, chemical reagents	Filtration system, pump and membrane	PD and dropper
Operating principle	Centrifugal force + chemical precipitation	Size-selective filtration through a membrane	Paper filtration + salting-out
Portability	Non-portable	Non-portable	Portable
Automatization	Low	Moderate	High (fully integrated pre-treatment on PAD)
Susceptibility to interference	Moderate	Low	Low

*for proteins >10 kDa

Centrifugation, widely used for protein removal, achieves high efficiency (70–90%) but requires expensive equipment, significant sample volumes (500–1000 µL), and long processing times (30–60 min), making it unsuitable for point-of-care applications. Additionally, it relies on electrical power, which limits its use in resource-limited settings. Ultrafiltration improves efficiency (90–95%) and reduces the required volume (100–500 µL) but remains costly (5–15€ per sample) and dependent on specialized filtration systems that also require electricity. In contrast, the proposed paper-based device, integrating filtration and salting-out, offers a cost-effective (0.10–0.50€ per sample) and rapid (5–10 min) alternative with minimal sample requirements (~20 µL). Unlike centrifugation and ultrafiltration, it operates as a passive fluidic system, requiring no external power source. Its portability and full integration with electrochemical platforms

allow for seamless on-site implementation, making it particularly advantageous for decentralized diagnostics.

Although the protein removal efficiency (71%) is slightly lower than ultrafiltration, the method effectively reduces interference while eliminating the need for bulky instrumentation and energy consumption. This comparison highlights the strengths of our approach in affordability, speed, and ease of use, demonstrating its potential as a viable alternative to conventional pre-treatment methods in electrochemical sensing applications.

3.4 Conclusions

This study presents a paper-based strategy for urine sample pre-treatment tailored to electrochemical sensing applications. The method combines protein precipitation induced by the presence of ammonium sulfate with the natural filtration properties of cellulose-based devices, offering a low-cost and portable alternative to traditional laboratory-based sample preparation techniques. A protein removal efficiency of approximately 71% was achieved, significantly reducing matrix-related interferences without the need for centrifugation, ultrafiltration, or other bulky equipment, making the approach highly suitable for point-of-care and resource-limited settings. The sample pre-treatment proposed was applied to the quantification of tryptophan in urine samples by standard addition method, finding a very nice correlation between the oxidation peak at +0.7 V and the concentration of analyte added in solution. This correlation was possible thanks to the very narrow oxidation peaks due to to uric acid and tryptophane oxidation and to the very good resolution between these processes. It si worth to notice that tryptophan was chosen as a model analyte to study the effectiveness of the procedure proposed for its well-defined electrochemical behavior in a potential window commonly affected by protein-related interference. This allowed for a systematic evaluation of the effectiveness of the pre-treatment in reducing the background noise. The successful application of this approach suggests that the integration of such pre-treatment steps could significantly enhance the performance of electrochemical sensors, also when more selective recognition elements might be used for the sensor response. Expanding the platform to accommodate a wider range of clinically and environmentally relevant biomarkers would further validate its potential as a robust, low-cost solution for decentralized biomonitoring.

3.5 Material and Methods

3.5.1 Reagents and equipment

Phosphate buffer saline (PBS) at a concentration of 0.1 M and at a pH of 7.0 was prepared starting by a 0.1 M solution of disodium mono hydrogen phosphate (Na_2HPO_4) and of monosodium dihydrogen phosphate (NaH_2PO_4) in a 1:1 molar ratio and adjusting the pH. 0.05 M of KCl was add to fix the potential of the pseudo-reference electrode. All previous mentioned reagents were purchased from Sigma Aldrich.
Bovine Serum Albumine and ammonium sulphate were purchased from Sigma Aldrich. Pierce™ BCA Protein Assay Kits was purchased by Thermo Fisher scientific. Commercial carbon screen-printed electrode (CSPE) DR-110 were purchased from Dropsens-Metrohm (geometric working electrode surface area equal to 0.125 cm^2). Paper PADs and the paper strip were wax printed on Whatman filter paper (67 g m^{-2}, Cordenons, Italy) using a Xerox Colorcube 8810 wax printer. UV-Vis measurements were carried out using a Cary UV-Vis Spectrometer, Agilent.

3.5.2 PAD preparation

The wax patterns were designed using Adobe Illustrator and then printed onto Whatman filter paper sheet using the wax printer Xerox Colorcube 8810. After printing, the sheet was placed in an oven at 60 °C to allow the permeation of the wax into the cellulose pores. The process was complete when the print pattern became visible on the back of the sheet. The obtained paper device consists of a hydrophobic area (magenta) and a hydrophilic area (white). The device can be divided into three zones: a drop zone (4mm diameter), an analysis zone (4mm diameter), and a channel (15mm long and 3mm wide) as shown in **Figure 3.2.** Two types of paper devices (**PD**) were prepared: in the first one a solution of $(NH_4)_2SO_4$ (5.2M, 90% of saturation) was loaded on the drop zone (**$(NH_4)_2SO_4$ -PD**); the second one was untreated (**Ctrl-PD**). Three different volumes were tested to prepare the **$(NH_4)_2SO_4$ -PD:** 5,10 and 15µL. **$(NH_4)_2SO_4$ -PDs** were used once the precipitating agent was fully dried.

3.5.3 Protein extraction procedure and UV-Vis analysis

A 20 µL drop of the sample, both urine or standard BSA solution, is applied to the designated drop zone and allowed to flow through the paper device until reaching the

analysis zone. After complete evaporation, the hydrophilic part of the analysis zone was isolated. The proteins that reached the analysis zone were then extracted by immerging the analysis zone in 100 µL of Milli-Q water and sonicating for 30 minutes. After sonication, 50 µL of the extraction solution was used to perform the BCA assay for protein quantification via UV-Vis spectrophotometry. The BCA working reagent is prepared by mixing BCA reagent A (bicinchoninic acid solution) with BCA reagent B (copper sulfate solution) in a 50:1 ratio. Subsequently, 50 µL of each standard or unknown sample is combined with 200 µL of the prepared reagent in a 500 µL Eppendorf tube and incubated at 37 °C for 30 minutes for 30 minutes to allow for color development. After incubating the mixture for 30 mins at 37 °C, the sample is ready for the UV-Vis analysis.

3.5.4 Electrode electrochemical oxidation

Before the measurement, the SPE DR-C110 electrode was activated by performing electrochemical oxidation through cyclic voltammetry (**CV**; from 1.0 to +1.7 V vs Ag/AgCl at a scan rate of 0.1 V/s) in a 60 µL drop of 0.5M sulfuric acid [23]. Afterward, the electrode was cleaned by applying 5 CV cycles in a 60µL drop of PBS (from 0 to 1.2 V vs Ag/AgCl, at a scan rate of 0.1 V/s).

3.5.5 Electrochemical detection of Tryptophan

A 20 µL urine sample was carefully deposited onto the drop zone of the paper-based device, allowing it to diffuse towards the analysis zone through capillary action. Once the sample had been completely dried, a 5 µL drop of PBS solution was added to the analysis zone to ensure optimal contact between the paper and the electrode surface while also buffering the pH during the electrochemical analysis. The detection of tryptophan in urine samples was performed using the standard addition method, targeting a concentration range between 0.01 and 0.1 mg mL^{-1}. Electrochemical measurements were conducted using both CV, with a potential window from 0 to 1.2V vs Ag/AgCl and a scan rate of 0.05 V/s, and DPV, with a potential window from 0 to 1.2V vs Ag/AgCl, a step potential of 4 mV, a modulation amplitude of 0.05 V, a modulation time of 0.05 s, and an interval time of 0.5 s.

References

[1] J.Y. Lichtenberg, Y. Ling, S. Kim, Non-specific adsorption reduction methods in biosensing, Sensors (Switzerland) 19 (2019). https://doi.org/10.3390/s19112488.

[2] B.L. Hanssen, S. Siraj, D.K.Y. Wong, Recent strategies to minimise fouling in electrochemical detection systems, Rev Anal Chem 35 (2016) 1–28. https://doi.org/10.1515/revac-2015-0008.

[3] G. Misia, C. Evangelisti, J.P. Merino, E. Pitzalis, A.M. Abelairas, J. Mosquera, A. Criado, M. Prato, A. Silvestri, Design and optimization of an electrochemical sensor based on carbon nanotubes for the reliable voltammetric detection of serotonin in complex biological fluids, Carbon N Y 229 (2024). https://doi.org/10.1016/j.carbon.2024.119550.

[4] X. Xiao, X. Yan, E. Magner, J. Ulstrup, Polymer coating for improved redox-polymer-mediated enzyme electrodes: A mini-review, Electrochem Commun 124 (2021). https://doi.org/10.1016/j.elecom.2021.106931.

[5] R.R. Burgess, Chapter 20 Protein Precipitation Techniques, in: Methods Enzymol, Academic Press Inc., 2009: pp. 331–342. https://doi.org/10.1016/S0076-6879(09)63020-2.

[6] P.K. Grover, R.L. Ryall, Critical appraisal of salting-out and its implications for chemical and biological sciences, Chem Rev 105 (2005) 1–10. https://doi.org/10.1021/cr030454p.

[7] A.K. Yetisen, M.S. Akram, C.R. Lowe, Paper-based microfluidic point-of-care diagnostic devices, Lab Chip 13 (2013) 2210–2251. https://doi.org/10.1039/c3lc50169h.

[8] A.W. Martinez, S.T. Phillips, M.J. Butte, G.M. Whitesides, Patterned paper as a platform for inexpensive, low-volume, portable bioassays, Angewandte Chemie - International Edition 46 (2007) 1318–1320. https://doi.org/10.1002/anie.200603817.

[9] S. Malik, J. Singh, K. Saini, V. Chaudhary, A. Umar, A.A. Ibrahim, S. Akbar, S. Baskoutas, Paper-based sensors: affordable, versatile, and emerging analyte detection platforms, Analytical Methods 16 (2024) 2777–2809. https://doi.org/10.1039/d3ay02258g.

[10] A. Silvestri, S. Vázquez-Díaz, G. Misia, F. Poletti, R. López-Domene, V. Pavlov, C. Zanardi, A.L. Cortajarena, M. Prato, An Electroactive and Self-Assembling Bio-Ink, based on Protein-Stabilized Nanoclusters and Graphene, for the Manufacture of Fully Inkjet-Printed Paper-Based Analytical Devices, Small 19 (2023). https://doi.org/10.1002/smll.202300163.

[11] W. Wang, S. Ding, Z. Wang, Q. Lv, Q. Zhang, Electrochemical paper-based microfluidic device for on-line isolation of proteins and direct detection of lead in urine, Biosens Bioelectron 187 (2021) 113310. https://doi.org/https://doi.org/10.1016/j.bios.2021.113310.

[12] H. Neto, I. Arantes, A. Ferreira, G. Nascimento, G. Meloni, W. De Araujo, T. Paixão, W. Coltro, Recent advances on paper-based microfluidic devices for bioanalysis, TrAC Trends in Analytical Chemistry 158 (2022) 116893. https://doi.org/10.1016/j.trac.2022.116893.

[13] H. Nasimi, J.S. Madsen, A.H. Zedan, A.V. Schmedes, A. Malmendal, P.J.S. Osther, F.A.Z. a. Alatraktchi, Tyrosine and tryptophan in urine as biomarkers for prostate cancer: A validation study, J Pharm Biomed Anal 250 (2024). https://doi.org/10.1016/j.jpba.2024.116398.

[14] R. Xu, V. Vatsalya, L. He, X. Ma, W. Feng, C.J. McClain, X. Zhang, Altered urinary tryptophan metabolites in alcohol-associated liver disease, Alcohol: Clinical and Experimental Research 47 (2023) 1665–1676. https://doi.org/10.1111/acer.15148.

[15] P.K. Smith, R.I. Krohn, G.T. Hermanson, A.K. Mallia, F.H. Gartner, M.D. Frovenzano, E.K. Fujimoto, N.M. Goeke, B.J. Olson, D.C. Klenk, Measurement of Protein Using Bicinchoninic Acid', 1985.

[16] K.C. Duong-Ly, S.B. Gabelli, Salting out of proteins using ammonium sulfate precipitation, in: Methods Enzymol, Academic Press Inc., 2014: pp. 85–94. https://doi.org/10.1016/B978-0-12-

[17] A.K. Yetisen, M.S. Akram, C.R. Lowe, Paper-based microfluidic point-of-care diagnostic devices, Lab Chip 13 (2013) 2210–2251. https://doi.org/10.1039/c3lc50169h.

[18] G. Maccaferri, F. Terzi, Z. Xia, F. Vulcano, A. Liscio, V. Palermo, C. Zanardi, Highly sensitive amperometric sensor for morphine detection based on electrochemically exfoliated graphene oxide. Application in screening tests of urine samples, Sens Actuators B Chem 281 (2019) 739–745. https://doi.org/10.1016/j.snb.2018.10.163.

[19] T. Fukuda, H. Muguruma, H. Iwasa, T. Tanaka, A. Hiratsuka, T. Shimizu, K. Tsuji, T. Kishimoto, Electrochemical determination of uric acid in urine and serum with uricase/carbon nanotube /carboxymethylcellulose electrode, Anal Biochem 590 (2020) 113533. https://doi.org/https://doi.org/10.1016/j.ab.2019.113533.

[20] C. Yıldız, D. Eskiköy Bayraktepe, Z. Yazan, Electrochemical low-level detection of l-tryptophan in human urine samples: use of pencil graphite leads as electrodes for a fast and cost-effective voltammetric method, Monatshefte Für Chemie - Chemical Monthly 151 (2020) 871–879. https://doi.org/10.1007/s00706-020-02620-7.

[21] Alan H.B. Wu, Tietz Clinical Guide to Laboratory Tests, 4th ed., 2006.

[22] C. Yıldız, D. Eskiköy Bayraktepe, Z. Yazan, Electrochemical low-level detection of l-tryptophan in human urine samples: use of pencil graphite leads as electrodes for a fast and cost-effective voltammetric method, Monatsh Chem 151 (2020) 871–879. https://doi.org/10.1007/s00706-020-02620-7.

[23] C. Zanardi, E. Ferrari, L. Pigani, F. Arduini, R. Seeber, Development of an electrochemical sensor for NADH determination based on a caffeic acid redox mediator supported on carbon black, Chemosensors 3 (2015) 118–128. https://doi.org/10.3390/chemosensors3020118.

Chapter 4: Development of an Ion Chromatography-Mass Spectrometry Method for the Analysis of Haloacetic Acids in Urine and Preliminary Investigation of an Electrochemical Sensor Approach

4.1 Introduction

Haloacetic acids (**HAAs**) are a class of disinfection by-products (**DBPs**) primarily formed during the chlorination of water, deriving from the chemical reaction among defined disinfectants (such as chlorine, chloramine, and chlorine dioxide) and the organic matter. Their occurrence in water is influenced by various transport and transformation processes, such as leaching into groundwater, runoff into surface waters, and atmospheric deposition. HAAs can also undergo degradation through hydrolysis, photolysis, and microbial metabolism, which impact their persistence and distribution [1]. Their presence in the water compartment poses potential health risks due to their suspected carcinogenicity and environmental persistence, that forced the authorities to introduce effective analytical procedures for their detection in water.

Currently, five HAAs are regulated by the U.S. Environmental Protection Agency (**EPA**), namely trichloroacetic acid (**TCAA**), dichloroacetic acid (**DCAA**), monochloroacetic acid (**MCAA**), monobromoacetic acid (**MBAA**), and dibromoacetic acid (**DBAA**). The actual maximum concentration limit imposed by European Union is 60 μg L^{-1} in drinking water, considered as combination of the five species previously listed. However, still unregulated HAAs, including iodinated species, are increasingly recognized for their higher toxicity compared to chlorinated and brominated counterparts [3], so that new analytical approaches are nowadays under study to overcome this limit of the actual regulation.

Traditional analytical approaches for the detection of these contaminants normally rely of chromatographic methods coupled with mass spectrometry detection. These methods provide very high sensitivity and selectivity, allowing them to achieve very low limits of detection. However, as already mentioned in the previous chapters, they often require extensive sample preparation, which limits their applicability for routine monitoring. As an alternative approach, electrochemical sensors offer a promising alternative due to their portability, cost-effectiveness, and rapid response times.

The widespread presence of HAAs in drinking water and in the environment has highlighted the urgent need for in-depth studies to develop analytical strategies for their detection in biological fluids to evaluate their toxicological impacts and to identify their action mechanisms within the body. Although regulatory agencies continue to evaluate and to update safety standards, the complete understanding of the risks associated with HAAs exposure remains a challenge. Notwithstanding the extensive study of HAAs in environmental matrices, such as drinking water and swimming pool water, their presence in biological systems remains poorly explored. HAAs can enter the human body through ingestion, inhalation, or dermal absorption of contaminated water or air. Once absorbed, they may be metabolized and excreted in biological fluids, like urine and saliva, making these matrices benchmarks of the exposure levels. Moreover, a recent study suggests that HAAs could also arise from endogenous metabolic processes, adding complexity to their detection and quantification [2].

In this study, we propose a new chromatographic method, based on ion chromatography coupled with mass spectrometry, for the quantification of HAAs in biological fluids, namely saliva and urine. In addition, the first attempts for the development of an electrochemical strategy for their rapid detection are also reported.

4.2 Development of an Ion Chromatography-Mass Spectrometry Method for Haloacetic Acid Detection

The chromatographic method for the quantification of HAAs in biological matrices, namely saliva and urine, was developed by adapting a previous approach for the quantification of these analyte in PM2.5 atmospheric aerosols [4]. The application of the ion chromatography-electrospray ionization tandem mass spectrometry (**IC-ESI-MS/MS**) method to biological fluids required addressing the interferences deriving from the quite complex chemical composition of these matrices, such as the presence of proteins and many organic compounds. Unlike aerosol analysis, where sample integrity can be preserved through controlled extraction methods due to the relatively stable composition, the analysis of biological fluids presents greater challenges. The high variability in their composition and the presence of complex matrix effects, such as proteins, lipids, and salts, can interfere with detection. As a result, different and more advanced sample preparation and cleanup strategies are

required to minimize these interferences and ensure reliable analytical results. Ion chromatography (**IC**) is a powerful technique for the separation of ionic compounds, offering high selectivity, reproducibility, and efficiency in aqueous matrices. Its ability to differentiate analytes based on their charge and interaction with the stationary phase makes it particularly suitable for the analysis of halogenated acids. IC alone provides robust quantification with excellent resolution and minimal sample preparation. This technique provides high sensitivity and specificity, with the added advantage of analysing polar compounds without the need for derivatization, normally required by gas chromatography (**GC**) analysis. Previous studies have demonstrated that IC can be successfully applied for the analysis of HAAs in various matrices, while detection sensitivity can be further enhanced by coupling IC with mass spectrometry. For instance, Krasner et al. [5] demonstrated the possible use of IC to the detection of HAAs in drinking water, showing its effectiveness in isolating single halogenated acids even when present at low concentrations. However, the application of IC to complex biological matrices like urine and saliva presents several challenges, primarily due to the presence of interfering substances and the low concentrations of target compounds in these fluids.

Despite the presence of chromatographic methods for the analysis of HAAs, to date limited efforts have been made to optimize analytical methodologies specifically directed to the detection of these analytes in urine and saliva samples, where the interference from endogenous substances can pose significant analytical challenges. This study aims to address these gaps by developing and validating an IC-ESI-MS/MS method for the detection and quantification of HAAs in human urine and saliva. By optimizing sample preparation protocols and chromatographic conditions, this work seeks to achieve the required sensitivity, accuracy, and reproducibility for HAA detection. The results will provide valuable insights into human exposure to HAAs, with potential applications in environmental health, toxicology, and biomonitoring studies.

4.2.1 Preliminary test on Chromatography coupled with Orbitrap detector

The initial tests were conducted using high pressure liquid chromatography (**HPLC**) coupled with an ESI-LTQ Orbitrap XL. In the development of analytical methods for HAA detection, the choice of mass spectrometric detectors plays a crucial role in determining sensitivity, resolution, and overall performance of the analytical method. While triple quadrupole mass spectrometers (**QQQ**) have traditionally been employed

for targeted analysis due to their high selectivity and fast acquisition rates, orbitrap-based high-resolution mass spectrometry (**HRMS**) provides higher mass accuracy and resolution, allowing for more precise identification and differentiation of closely related species. This is particularly beneficial in complex biological matrices, where background noise and isobaric interferences can compromise quantification. Furthermore, orbitrap technology enables full-scan analysis with retrospective data processing, allowing for the detection of unexpected chemical species without prior method reconfiguration. This contrasts with QQQ instruments, which rely on predefined multiple reaction monitoring (**MRM**) transitions, limiting their flexibility for untargeted screening. Additionally, the superior mass resolution of orbitrap instruments improves peak definition and reduces the risk of misidentification, enhancing confidence in analytical results. Given these advantages, integrating orbitrap HRMS into the workflow for HAAs detection presents a powerful approach for both targeted quantification and exploratory analysis of novel disinfection by-products. Chromatographic separation was performed using a Kinetex XB-C18 column. The gradient profile, based on methanol and ultrapure water, is reported in **Table B1**, **Appendix B.** Source parameters and flow rates were optimized by analyzing a 50 ng mL^{-1} standard mix under different conditions (***Table B2, Appendix B***), with selected values highlighted. Both solvents did not contain any additional additives or modifiers.

Sample extraction followed the SPE protocol of Redondo-Hasselerharm et al. (2022) [6]. After thawing and centrifugation, 3.5 mL of supernatant was diluted and acidified before loading onto a conditioned Oasis HLB SPE cartridge. Elution was carried out with methanol:water (20:80), and the extracts were dried and reconstituted. However, no detectable peaks were observed. The high solubility and volatility of HAAs were suspected to cause analyte breakthrough and degradation during SPE and evaporation. To investigate these issues, 1 mL of a 100 ng mL^{-1} HAA standard was loaded onto four different SPE cartridges and eluted with methanol. The cartridges were selected to compare materials with varying properties, capable of retaining compounds with diverse chemical characteristics such as haloacetic acids. The cartridges tested were Oasis HLB, Strata-X, Sep-Pak C18, and Oasis WAX, representing different retention mechanisms for polar and ionizable molecules. This selection allowed for evaluation of which cartridge material would be most effective in extracting these analytes from complex biological matrices like urine. Exploring these

different interaction modes was essential to optimize the analytical extraction procedure. Each analyte was quantified using its corresponding internal standard (ISTD), indicated as [HAA]-ISTD (e.g., TCAA-ISTD for TCAA). The internal standards were carbon-13 (^{13}C)-labeled compounds, chosen for their identical chemical structure and similar chromatographic behavior, allowing correction for losses during extraction, evaporation, and instrumental analysis. HLB and Strata-X provided the best recovery, while WAX and Sep-Pak C18 were ineffective. HLB was chosen for its superior retention of TCAA, the lowest-responding ISTD (***Table B3, Appendix B***).

Further tests using HLB cartridges explored analyte stability during evaporation. Evaporation to dryness resulted in complete signal loss, while partial concentration led to significant reduction in peak areas. These results strongly suggest that the volatility and chemical instability of HAAs under drying conditions—particularly in the absence of stabilizing agents or derivatization—represent a major bottleneck in sample preparation for LC-HRMS analysis. The inability to preconcentrate the sample without significant analyte loss ultimately undermines the sensitivity and robustness of the method, especially when working with low-concentration biological samples.

Real urine samples fortified with 10 ng mL^{-1} HAAs-ISTD were processed using the optimized HLB protocol. Despite further adjustments—such as reducing elution volume and avoiding evaporation—no analytes were detected. These repeated failures highlighted the limitations of Orbitrap-based detection for HAAs in biological matrices, due to volatility, matrix effects, and low analyte concentrations.

Given these limitations, the Orbitrap-based method was ultimately discarded in favor of the use of QQQ detector. As already outlined, ion chromatography coupled to tandem mass spectrometry (IC-ESI-MS/MS) is, at least in principle, a more selective and robust approach that should also allow achieving much lower limits of detection (LODs) for small and highly polar compounds like HAAs.

4.3 Validation and Optimization of HPAEC-MS/MS for Biological Matrices

Given the challenges encountered with Orbitrap-based analysis, the method was revised by coupling high-performance anion-exchange chromatography to high-resolution electrospray ionization tandem mass spectrometry (**HPAEC-MS/MS**). Although a method for the determination of HAAs with this instrumental setup was

already available, it had not been previously validated for biological matrices. One of the primary concerns for the application of this technique to urine samples was the high salt concentration, which could potentially overload or even damage the ion suppressor in the anion-exchange chromatographic system. To mitigate this issue, a series of dilution tests were carried out aiming at defining the most proper sample preparation strategy. Urine samples were diluted at factors of 1:5000, 1:2000, 1:200, and 1:50 using ultrapure water, and a 990 µL aliquot of each diluted matrix was fortified with 10µL of a 1µg mL^{-1} HAAs-ISTD mix, corresponding to an absolute mass of 10 ng per ISTD and resulting in a final concentration of 10ng mL^{-1}. The presence of residual ions in each dilution was assessed using a conductometer, while HAAs quantification was performed via mass spectrometry. As expected, signal suppression increased with decreasing dilution factors, with chloride (Cl^-) representing the most abundant interfering ion. To further investigate and address this issue, additional dilutions were prepared and subjected to elution through a conditioned IC-Ag column to facilitate chloride removal. Notably, the chloride ions were effectively eliminated, and the elution process did not lead to any detectable loss of chlorinated analytes. The 1:25 IC-Ag dilution was selected as the optimal compromise between minimizing chloride ion interference and maintaining adequate signal intensity for the internal standards.

***Table 4.1**: Semiquantitative analysis for different factors adopted. for urine samples, with and without the use of an IC-Ag column.*

Dilution factor used	Cl^- area	MCAA-ISTD area	MBAA-ISTD area	DCAA-ISTD area	TCAA-ISTD area
1:5000	2.4	21322.9	38193.7	160622.1	6437.5
1:2000	5.1	19631.5	34316.5	160190.5	6150.7
1:200	41.6	11033.1	16166.8	154186.3	5054.9
1:50	208.8	5188.7	4277.0	112065.3	2219.3
1:200 IC-Ag	0.3	16392.2	28718.5	174109.9	6222.8
1:50 IC-Ag	3.5	10126.9	17288.0	138126.5	3037.9
1:25 IC-Ag	**7.6**	**8513.4**	**14897.7**	**166139.8**	**1340.8**

This dilution level provided consistently high peak areas for all target analytes, indicating sufficient sensitivity, while avoiding excessive dilution that could reduce detection capability. Additionally, the reduced chloride concentration at this dilution helps to improve analytical reliability and accuracy in complex biological matrices. The

results are highlighted in ***Table 4.1.*** The selected HPAEC-MS/MS method offers several advantages in terms of environmental impact and operational simplicity: *i)* unlike methods requiring derivatization, halogenated solvents, or extensive sample manipulation, IC enables direct analysis of HAAs without prior chemical modification, thereby reducing the use of hazardous reagents and minimizing waste generation; *ii)* the use of aqueous mobile phases and the absence of toxic organic solvents such as acetonitrile or methanol further enhance its environmental compatibility; *iii)* the reduced sample volume request and the relatively short analysis times contribute to lower energy and resource consumption. Although the instrumentation itself is not inherently low-cost, the method aligns well with several principles of green analytical chemistry, namely safer solvents, waste minimization, and direct analysis of target compounds, making it a suitable choice for sensitive and eco-conscious pollutant monitoring in biological matrices.

4.3.1 Real Sample Analysis

The analytical method for HAAs was applied to urine and saliva samples collected from two swimmers and one smoker, providing preliminary insights into the presence of these compounds in biological fluids. For the swimmers, samples were collected both before entering the swimming pool environment and immediately after exposure, allowing assessment of potential uptake due to pool water exposure. For the smoker, samples were collected at least 12 hours after the last cigarette, a timeframe chosen based on literature indicating that the elimination half-life of many tobacco-related metabolites ranges between 4 and 12 hours, thus reducing the likelihood of detecting HAAs directly attributable to recent smoking. While the limited number of samples prevents definitive conclusions, these data allow initial hypotheses on analyte distribution and accumulation to be formulated and compared with existing scientific knowledge.

4.3.2 Analysis of urine samples

The concentration of HAAs defined in urine samples collected and analysed according with the method developed is reported in **Table 4.2**. As observed, DCAA was present in all the samples analysed, with concentrations ranging from 0.9 to 5.9 μg L^{-1}. The detection of DCAA in both swimmers and the smoker suggest multiple exposure pathways. For swimmers, DCAA formation can occur due to the reaction of chlorine-

based disinfectants with organic matter in pool water [7], although this species is present even before the immersion in the swimming pool, i.e. exposure to chlorinated water. Smokers, on the other hand, may be exposed to DCAA through the inhalation of tobacco smoke, which contains various halogenated compounds [3]. For swimmers, the concentration of all HAA tested increases after exposure, i.e. a swimming session of a couple of hours, suggesting that swimming in chlorinated pools lead to the formation and absorption of these species, possibly through dermal contact or incidental ingestion of pool water.

***Table 4.2**: Concentration of HAAs and bromate in urine samples collected from swimmers before and after pool exposure, as well as from a smoker. The values are expressed in μg L^{-1}.*

Urine sample	MCAA (μg L^{-1})	DCAA (μg L^{-1})	BCAA (μg L^{-1})
Smoker	2.2	3.6	0.2
Swim. 1 Pre	N/D	4.6	N/D
Swim. 1 After	1.1	5.9	0.2
Swim. 2 Pre	N/D	0.9	0.1
Swim. 2 After	1.2	1.8	0.2

4.3.3 Analysis of saliva samples

The concentration of HAAs defined in saliva samples collected and analysed according with the method developed is reported in **Table 4.3**. The analysis revealed the presence of monoiodoacetic acid (**MIAA**) and diiodoacetic acid (**DIAA**), particularly in swimmers after exposure. The formation of iodinated HAAs in swimming pools has been documented, especially when iodide is present in the source water [4]. The detection of these compounds in saliva post-swimming indicates potential exposure through inhalation of aerosolized water or ingestion. TCAA was found in the saliva of both swimmers and the smoker, with higher concentrations observed post-swimming. TCAA is a common disinfection by-product in chlorinated water [2] and can also be present in tobacco smoke [3]. The elevated levels post-swimming suggest that pool exposure contributes significantly to TCAA presence in saliva.

Swimmers are primarily exposed to HAAs through ingestion, inhalation, and dermal absorption of chlorinated pool water. Studies have shown that HAAs can appear in

urine within 20-30 minutes post-exposure and are typically eliminated within 3 hours. In our study, urine samples from swimmers contained measurable levels of **MBAA**, **DBAA**, and Tribromo acetic acid (**TBAA**). The presence of these brominated HAAs aligns with findings that bromine-containing disinfectants contribute to the formation of such byproducts in pool water [8].

***Table 4.3**: Concentration of HAAs and bromate in saliva samples collected from swimmers before and after pool exposure, as well as from a smoker. The values are expressed in µg L^{-1}.*

Saliva sample	MCAA (µg L^{-1})	BrO_3^- (µg L^{-1})	MIAA (µg L^{-1})	DIAA (µg L^{-1})	TCAA (µg L^{-1})
Smoker	N/D	1,0	7,8	1,4	0,8
Swimmer 1 Pre	N/D	0,8	7,4	N/D	N/D
Swimmer 1 After	2,7	1,0	22,2	10,0	N/D
Swimmer 2 Pre	0,1	0,7	9,1	1,2	N/D
Swimmer 2 After	1,9	0,9	9,2	6,9	N/D

Smokers are exposed to HAAs primarily through inhalation of tobacco, which contains various halogenated organic compounds. The combustion of tobacco produces chlorinated and brominated by-products, including DCAA and TCAA, which can be absorbed through the respiratory tract and excreted in urine and saliva [9]. Previous studies have indicated that smokers exhibit higher levels of HAAs in biological fluids compared to non-smokers due to their continuous exposure [10]. The presence of bromate ion (BrO_3^-) was consistently detected at low but measurable concentrations in all saliva samples, including both pre- and post-exposure samples from swimmers and the smoker. The relatively stable levels of bromate before and after swimming suggest that its occurrence may not be strongly influenced by short-term exposure to swimming pool water in this limited sample set. This could indicate either a background exposure from other sources or a low bioaccumulation tendency in saliva over the timeframe considered.

4.3.4 Matrix-Specific Distribution

The differential detection of HAAs in urine and saliva may be influenced by several factors, including the physico-chemical properties of the analytes, routes of exposure, and individual metabolic processes. For instance, compounds with higher water

solubility may be more readily excreted in urine, while those with affinity for mucosal tissues might be detected in saliva. Additionally, the timing of sample collection relative to exposure plays a crucial role, as HAAs exhibit varying half-lives and metabolic pathways [11]. In conclusion, while the small sample size limits broad generalizations, the observed data align with existing literature on HAAs exposure pathways in swimmers and smokers. Further studies with larger cohorts are necessary to elucidate the dynamics of HAAs distribution across biological matrices and to understand the implications for human health.

4.4 Preliminary investigation of a sensing strategy for HAA detection

In the second part of this study, I explored the possibility of detecting HAAs with an amperometric sensor. The detection is based on the direct electrochemical reduction of these analytes on silver-based surfaces, since this metal possesses electrocatalytic properties in the reduction of halogenated organic compounds [12]. To enhance the performance of the electrochemical detection, particularly concerning the sensitivity and resolution or the voltammetric responses, different surface etching procedures were tested. Indeed, according to a literature report, silver halides (AgX) act as a redox-active mediator for the electrochemical detection of HAAs [13]. They can be obtained by polarizing Ag surfaces at positive potentials in presence of chloride ions in solutions. The porous structure obtained through this electrochemical etching process significantly increases the electroactive area, enhancing the adsorption of the analyte on the surface and improving the response sensitivity. Similar etching process can be also obtained by performing voltammetric cycles in TCAA solution, using this molecules both as a source of Cl^- and as a template for the realization of cavities possessing the dimension of the target analyte (**Figure 4.1**).

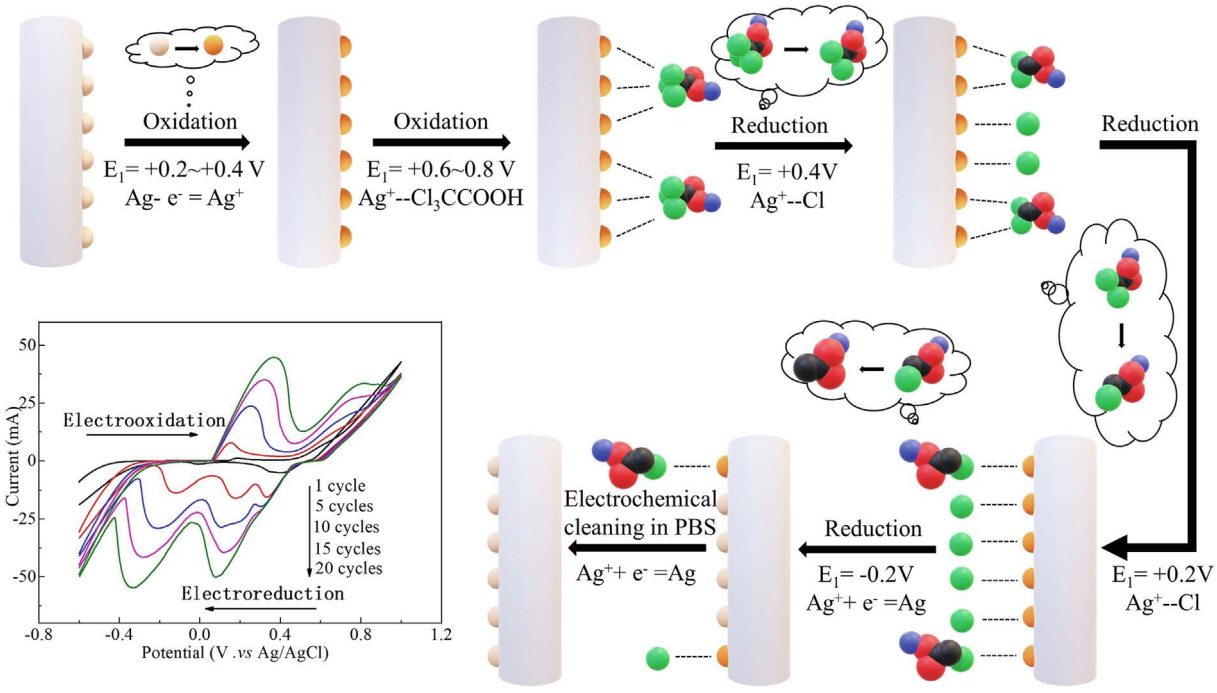

***Figure 4.1**) Schematic representation of the etching procedure, highlighting the different steps in the oxidation and reduction processes that take place during the procedure. Image adapted from Chu Y. et al. [14].*

Indeed, the electrochemical reduction of this analytes, occurring at negative potential values, produces chloride ions that then react with silver ions produced in the following scan toward positive potential. The etching process takes advantage of the adsorption of TCAA, acting at a template. This same study also demonstrates that the resulting silver-based electrode enables the stepwise electrochemical reduction of HAAs, allowing for their quantification based on distinct reduction peaks. Starting from this pioneering work of Chu Y et al. [14] , different etching protocols were tested during my research activities to optimize the detection capability of silver wire electrodes. This preliminary electrochemical investigation is aimed at highlighting the advantages in the use of silver-based surfaces for the detection of HAAs, which is at the basis of the realization of an efficient sensor system.

4.4.1 Electrochemical Reduction of Trichloroacetic Acid

According to what described by the literature [15], the electrochemical reduction of TCAA follows a stepwise mechanism involving the sequential cleavage of the three carbon-chlorine (C-Cl) bonds, so that during voltammetry experiments toward negative potentials, three distinct reduction peaks can be observed [16]. Literature indicates that these electrochemical reductions primarily occur at mercury and at carbon-based electrodes due to their catalytic properties in promoting dehalogenation reactions on the one hand and in the overvoltages implied in the electrochemical reduction of protons normally present in water media, on the other. Surface interactions between TCAA and the electrode material strongly impact the electrochemical process, affecting peak resolution [17], so that the three peaks are not distinctly observed at these surfaces due to overlapping reduction processes or kinetic limitations associated with electron transfer rates [18]. Factors such as the composition of the supporting electrolyte, the pH of the solution, and the chemical nature of working electrode can influence the electrochemical response of TCAA, potentially leading to merged or broadened reduction signals. Understanding the electrochemical reduction of TCAA at different surfaces is essential to improve the detection and the quantification in environmental and biological samples.

4.4.2 Etching procedures of Ag surfaces

The analysis performed constitutes a preliminary investigation of the applicability of silver-based surfaces for the detection of HAAs. To this end, four silver wires were prepared as follows:

i) **Bare Ag surface**: a silver wire subjected only to mechanical cleaning.

ii) **Ag wire etched in HNO_3**: the silver wire was subjected to oxidation and reduction cycles in 0.1 mol·L^{-1} HNO_3 During this process, silver is oxidized to silver ions in nitric acid, which are subsequently redeposited as metallic silver (Ag^0) during the negative potential scan, resulting in a roughened surface structure. To prevent excessive stripping of the silver surface, the potential window for the cyclic voltammetry (CV) was limited to the range from 0 to +0.30 V vs. Ag/AgCl.

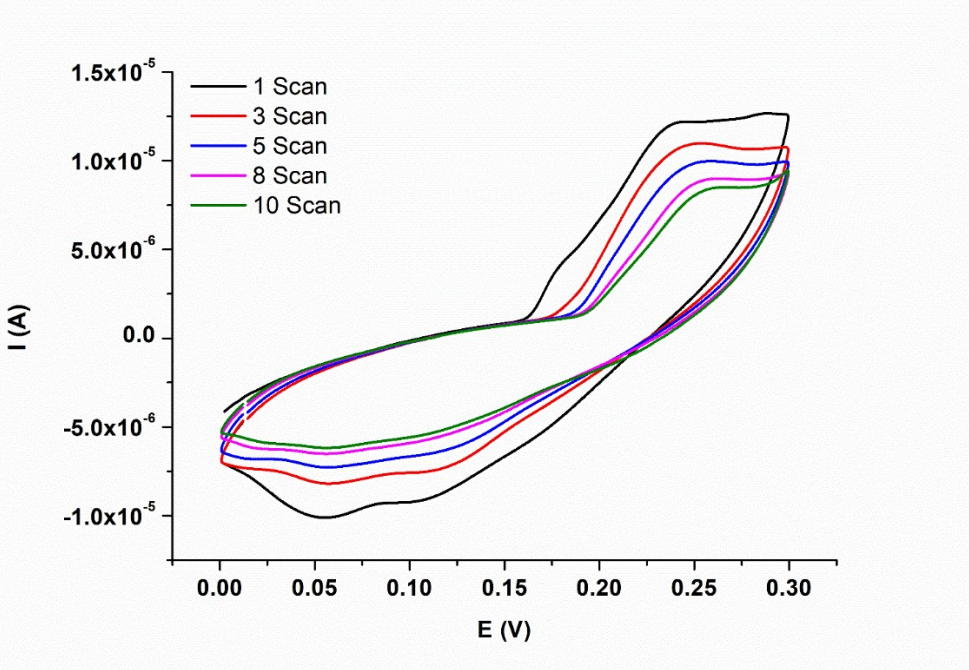

Figure 4.2) *CV responses obtained during the etching process of a Ag wire performed in 0.1 mol·L^{-1} HNO_3 at a scan rate of 50 mV s^{-1} for 10 cycles, within a potential window between E_1= 0V and E_2= 0,3V vs Ag/AgCl. The CV profile exhibits oxidation and reduction peaks related to silver surface.*

iii) **Ag wire etched in HCl**: the silver wire was subjected to subsequent oxidation and reduction steps in 0.5 mol·L^{-1} HCl ***(Figure 4.3)***, involving the formation of silver chloride that is subsequently reduced back to metallic silver upon potential reversal. The number of voltammetric cycles to perform in this case was estimated based on the intensity of this reduction peak observed, ensuring a controlled and reproducible surface modification comparable with the TCAA etching (see procedure *iv*). The shape of the voltammograms confirms that the electrochemical response is primarily governed by the formation of AgCl, with no additional reduction processes. At the end of the voltammetric deposition, the surface was conditioned by polarizing the electrode at -0.6 V for 300 in a phosphate buffer solution.

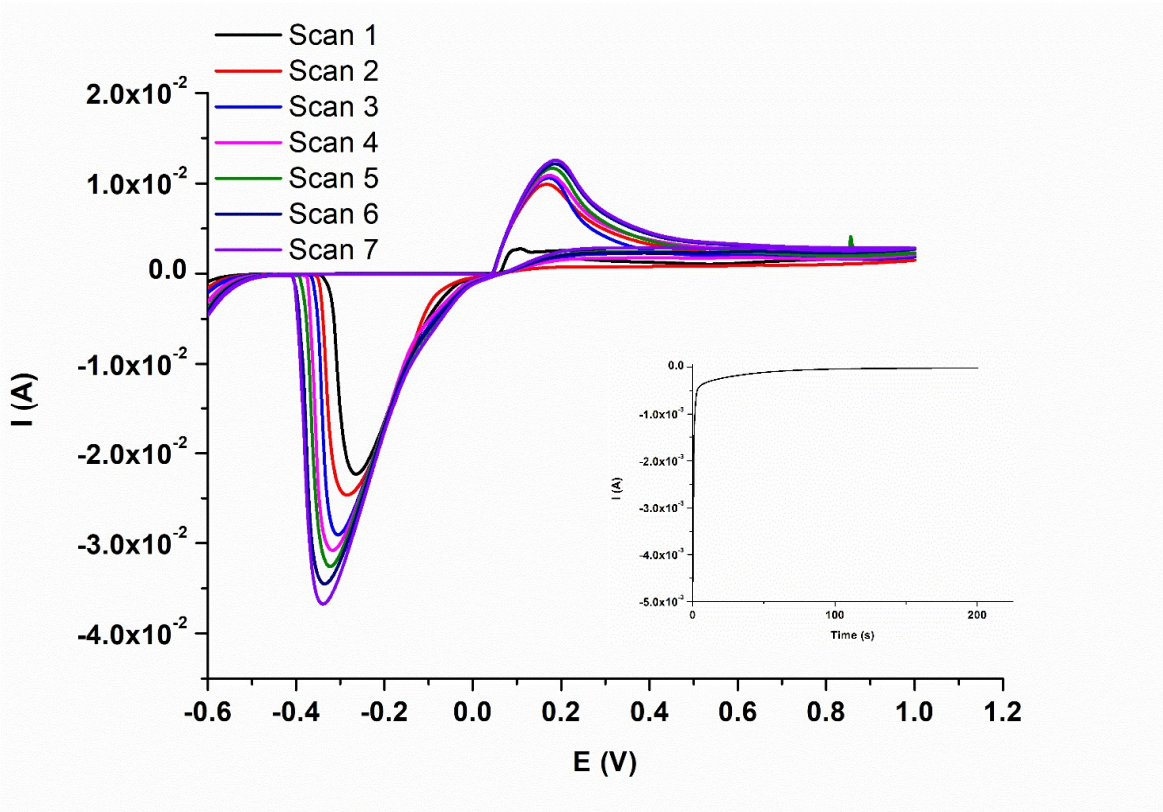

Figure 4.3) *CV responses obtained during the etching process of an Ag wire in a* 0.5 mol·L^{-1} *HCl at a scan rate of 50 mV s^{-1} for 7 cycles, within a potential window between E_1= -0.6V and E_2= +1.0V vs Ag/AgCl. The inset shows the following chronoamperometric cleaning performed by polarizing the electrode at -0.6 V vs Ag/AgCl for 200 s in PBS (pH 6.8) to remove residual chloride species.*

iv) Ag wire **etched in TCAA**: the silver wire was subjected to subsequent oxidation and reduction steps in 0.5 mol·L^{-1} TCAA, followed by the same electrochemical "cleaning" step polarizing the electrode at -0.6 V for 300 in a phosphate buffer solution. The literature [12] indicates that during the voltammetric scan toward negative potentials, TCAA is reduced with formation of free chlorine ions close to the electrode surface. During the following scan toward positive potentials they react with silver metal ions, leading to the formation of silver chloride. At difference with the etching in HCl solution, the presence of TCAA introduces additional interactions that influence the electrode structure as schematized in **Figure 4.1**. As observed from **Figure 4.4**, this interaction results in a voltammetric response that is well different from that collected in HCl solution (see ***Figure 4.3***): three distinct reduction peaks are observed at approximately +0.4 V, +0.15 V, and -0.35 V vs. Ag/AgCl. These peaks cannot be merely attributable to the reduction of AgCl, since it typically exhibits only a single process. Over the 20 scans performed for the etching procedure, the first two reduction peaks tend to merge into a single one, likely due to changes in surface morphology.

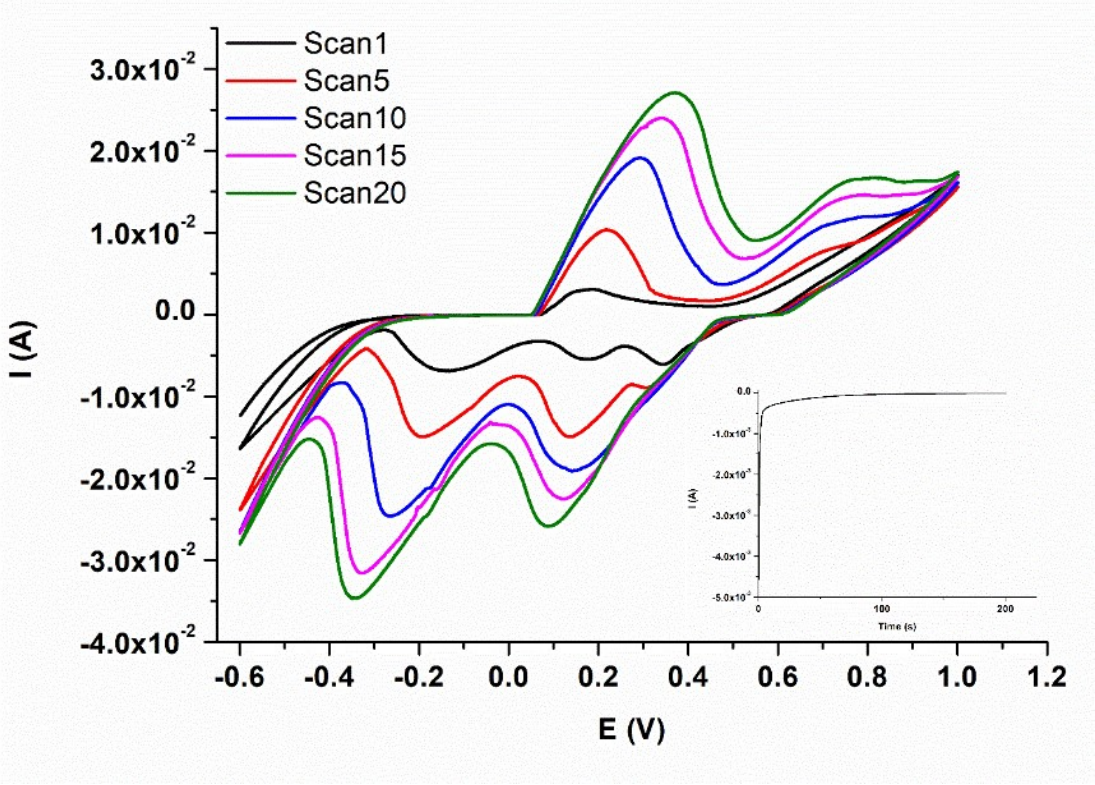

Figure 4.4) *CV responses obtained during the etching of an Ag wire electrode in a* 0.5 mol·L^{-1} *TCAA at a scan rate of 50 mV s^{-1} for 20 cycles, within a potential window between E_1= -0,6V and E_2= +1.0V vs Ag/AgCl. The inset reports the following chronoamperometric cleaning step performed by polarizing the electrode at -0.6 V vs Ag/AgCl for 200 s in PBS (pH 6.8).*

4.4.3 Trichloroacetic acid detection at different Ag surfaces

The electrochemical process of TCAA reduction was evaluated at the different silver electrodes to provide insight into the performance of the various surfaces in resolving the electrochemical reduction peaks. It is worth underlining that all the electrochemical measures described were carried out in triplicate and in nitrogen-saturated environment after degassing the electrochemical cell solution with N_2 gas for approximately 10 minutes. The TCAA concentration tested for the detection ranged from 0.11 mmol L^{-1} to 0.91 mmol L^{-1}.

i) **Bare** silver electrode exhibits a single broad peak, indicating that the expected three electrochemical process cannot be resolved by using this surface (***Figure 4.5a***). In the absence of an etching process, the silver remains in its native state, with a relatively smooth morphology and, thus the sensitivity and of the electrochemical process does not seems particularly interesting (***Figure 4.5b***). This behavior reflects the intrinsic properties of untreated silver, where the lack of intentional modifications limits any enhancement in response resolution. The analysis of this response provides a crucial reference starting point for evaluating how different surface treatments impact the electrochemical characteristics of the sensor.

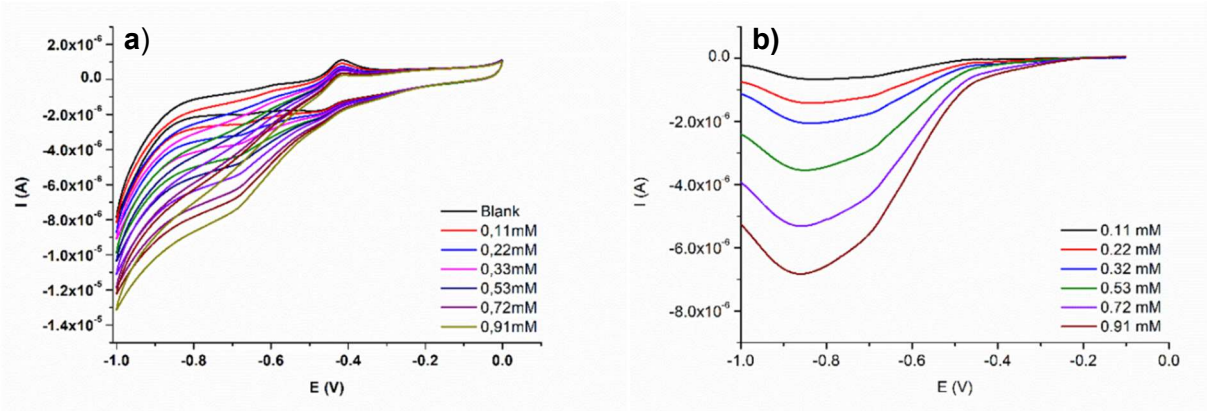

Figure 4.5) (a) *CV responses recorded at pristine Ag wire electrode in 0.02 mol L^{-1} PBS (pH 6.8) in absence and in presence of different concentration of TCAA, 20 mV·s^{-1} potential scan rate; (**b**) reports only the forward response subtracted for the blank signal.*

ii) CV responses recorded for the **HNO_3-etched** electrode exhibit a single broad reduction peak spanning the entire potential range where TCAA reduction was expected (***Figure 4.6a***). This behaviour closely resembles that observed for the bare silver electrode, suggesting that etching in nitric acid does not lead to significant

enhancement of the resolution. This is quite expected since nitrate has poor complexing capability for silver ions. After background subtraction of the response collected in the absence of analyte (***Figure 4.6b***), it becomes evident that the recorded voltammogram results from a combination of poorly resolved reduction processes.

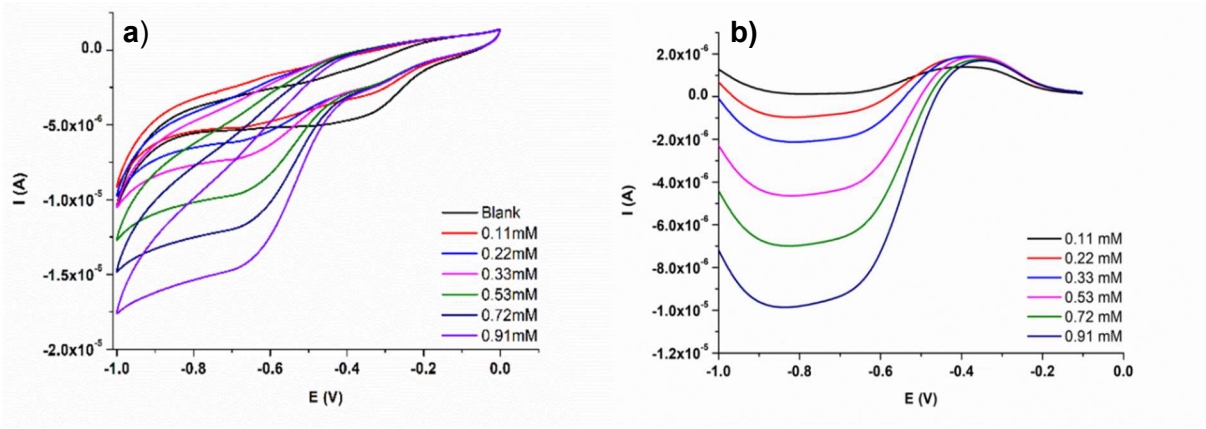

Figure 4.6) (a) *CV responses recorded at HNO_3-etched Ag electrode in 0.02 mol L^{-1} PBS (pH 6.8) in absence and in presence of different concentration of TCAA, 20 mV·s^{-1} potential scan rate; (**b**) reports only the forward response subtracted for the blank signal.*

iii) The **HCl-etched** electrode exhibits CV responses (***Figure 4.7***) characterized by a significant improvement in resolution compared to the bare and the HNO_3-etched electrodes. Three distinct reduction peaks can be identified, indicating that the etching process in HCl enhances the electrode's ability to resolve the stepwise electrochemical reduction of TCAA.

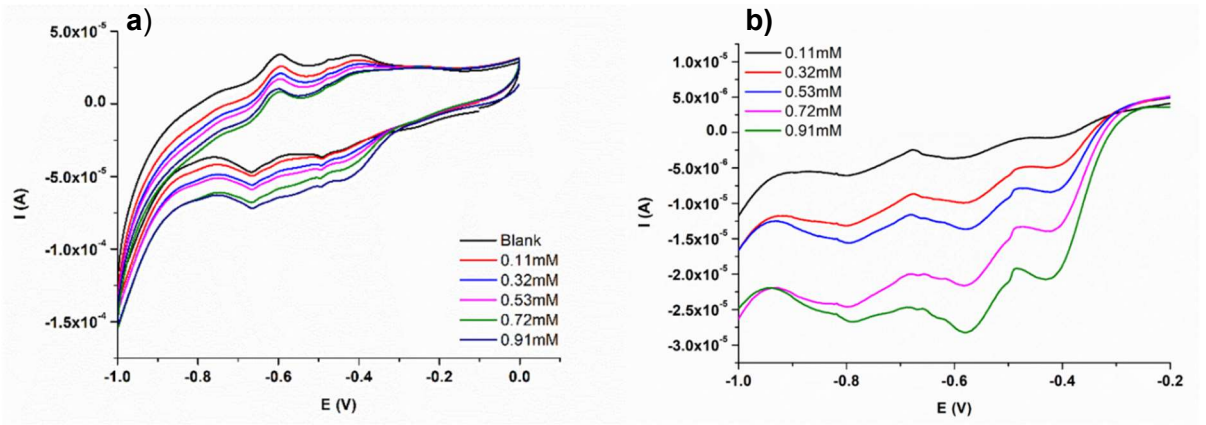

Figure 4.7) *(**a**) CV responses recorded at HCl-etched Ag electrodes in 0.02 mol L^{-1}PBS (pH 6.8) in absence and in presence of different concentration of TCAA, , 20 mV·s^{-1} potential scan rate; (**b**) reports the forward traces after blank-subtraction.*

While the peak resolution is not optimal, this result provides an initial indication that surface modification through chloride-based etching can facilitate a more defined detection of chlorinated species. However, further refinement of the etching procedure is necessary to maximize peak resolution and ensure reliable differentiation of the halogenated species in complex sample matrices.

iv) The **TCAA-etched** electrode exhibits three well-defined reduction peaks at approximately -0.35 V, -0.55 V, and -0.9 V vs. Ag/AgCl (***Figure 4.8a***), in agreement with literature reports [13]. These peaks become more evident after background subtraction and considering the forward scan only (***Figure 4.8b***). The TCAA-etched electrode demonstrates improved separation of the first two reduction steps, suggesting that the etching process introduces structural modifications that enhance peak resolution. However, while the first two peaks remain well-defined, the third one at -0.9 V appears broadened.

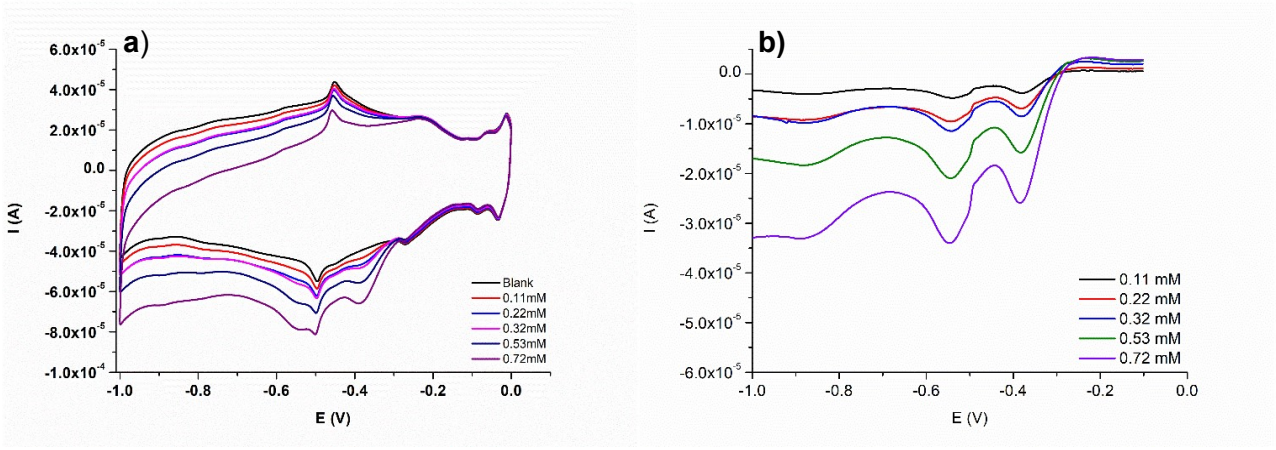

Figure 4.8) *(**a**) CV responses collected at TCAA-etched Ag electrode in 0.02 mol L^{-1} PBS (pH 6.8) in absence and in presence of different concentrations of TCAA, 20 $mV \cdot s^{-1}$potential scan rate. In (**b**) the forward traces of the same responses are reported after blank-subtraction.*

The improved resolution observed with the TCAA-etched electrode highlights the role of molecular imprinting in shaping the surface properties and influencing the electrochemical behavior of the silver substrate. The presence of TCAA during the etching process likely facilitates the formation of a structured AgCl layer, which may contribute to better-defined interactions with the analyte. This controlled surface modification appears to enhance selectivity and signal definition, making the TCAA-etched electrode a promising candidate for the detection of chlorinated species.

Nonetheless, the broadening of the third peak suggests that further optimization of the etching parameters could be beneficial in refining the electrode's performance, particularly in applications requiring precise differentiation of structurally similar analytes.

Figure 4.9a compares the responses obtained after blank subtraction for the different electrodes tested at a fixed TCAA concentration (0.53 mM). It clearly shows that the TCAA-etched electrode (magenta curve) exhibits the highest resolution of three reduction peaks and the highest sensitivity in the sensor response indicating the active role played by the deposition of AgCl in combination with the templating activity played by TCAA. Conversely, the HCl-etched electrode (blue curve) shows a lower sensitivity and resolution. The HNO_3-etched electrode (red curve) and the bare electrode (red curve) display a less sensitive response, with less defined peak structures.

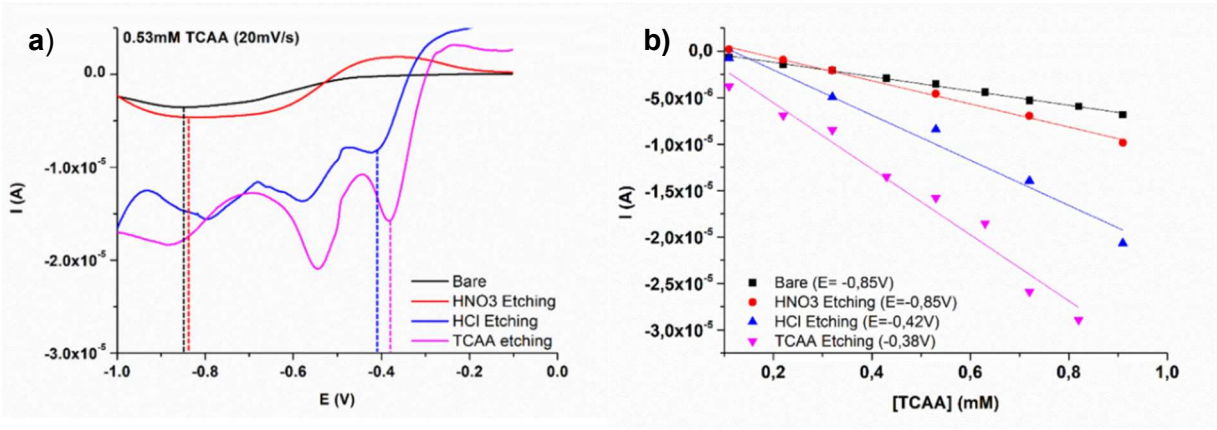

Figure 4.9) *(**a**) Forward CV responses recorded in 0.53 mM TCAA solution at different Ag electrodes and subtracted for the relevant blank signal: bare silver (black), HNO_3-etched (red), HCl-etched (blue), and TCAA-etched (magenta). Dashed lines indicate the potentials at which the calibration curves were plotted. (**b**) Calibration curves obtained for TCAA detection using these same electrodes, plotted at the selected reduction potentials.*

The dashed lines in **Figure 4.9a** highlight the potentials at which the calibration curves can be plotted for the different electrodes. In particular, -0.85 V vs Ag/AgCl was chosen for both bare and HNO_3-etched electrodes, as a representative value for the broad reduction response observed. On the contrary, the potential selected for the HCl- and TCAA-etched electrodes corresponds to the peak associated with the reduction of the first carbon-chlorine bond in TCAA. This choice ensures that the calibration is performed at the most representative electrochemical response for TCAA reduction,

even when possibly in present with further chloro derivatives. Quite interestingly, it is evident that the formation of an AgCl deposit induces an electrocatalytic reduction of TCAA, so that the process is shifted at less negative potential and the signal results, as a consequence, significantly higher. This effect is even more evident when TCAA-etched electrode is used. **Figure 4.9b** reports the relevant calibration plot obtained by considering the current value recorded at these potentials after blank subtraction. **Table 4.7** reports the values calculated for slope, standard errors of the calibration, and correlation coefficients (R^2) from the linear fits of the calibration curves shown in **Figure 4.9b**.

Table 4.7 *Values calculated for slope, standard errors of the calibration, and correlation coefficients (R^2) from the linear fits of the calibration curves.*

Etching Procedure	*Slope ($\mu A*mM^{-1}$)*	*Standard Error (μA)*	*R^2*
Bare	***-7.69***	***0.171***	***0.99***
HNO_3	***-12.5***	***0.367***	***0.99***
HCl	***-24.3***	***2.22***	***0.97***
TCAA	***-35.5***	***2.57***	***0.96***

The TCAA-etched electrode displays the highest sensitivity, indicating its superior electrocatalytic activity for TCAA reduction, as evidenced by the shift in peak position observed in **Figure 4.9a**. Compared to the HCl-etched electrode, the reduction peaks for the TCAA-etched electrode appear at slightly more positive potentials, suggesting a more favourable electron transfer process. This shift highlights the enhanced reactivity of the modified surface, likely due to improved interaction with TCAA molecules, further supporting the electrode's superior performance in selective detection.

Figure 4.10 investigates the effect of scan rate on the electrochemical response of the TCAA-etched electrode, using a TCAA concentration of 1mmolL^{-1} to ensure a clearly distinguishable electrochemical signal. The results confirm literature findings, demonstrating that a scan rate of 20 mV/s optimizes peak resolution, whereas higher or lower values tend to reduce both resolution and signal intensity.

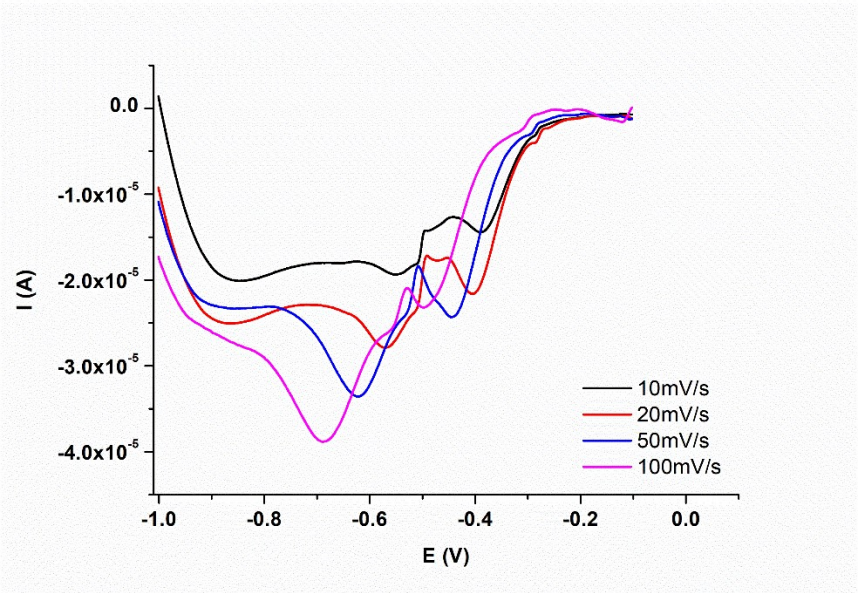

Figure 4.10) *Effect of scan rate on the response of the TCAA-etched electrode with 0.53 mmol* L^{-1} *TCAA.*

4.4.4 Detection of DCAA Using TCAA- and HCl-Etched Silver Electrodes

Since the electrode coatings containing chloride derivatives showed the best peak resolution among the tested electrodes, the detection of DCAA and MCAA were attempted only at TCAA- and HCl-etched Ag electrodes.

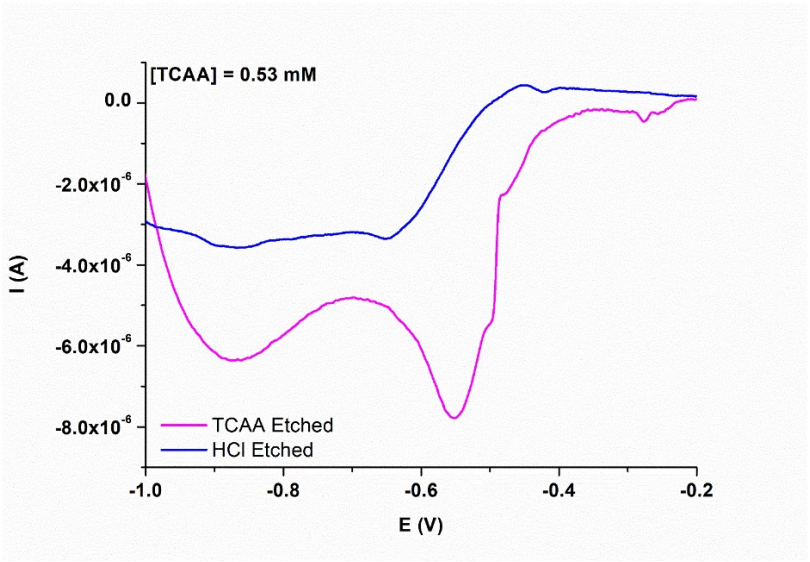

Figure 4.11) *Comparison of the voltammetric responses obtained after blank subtraction for the electrochemical reduction of 0.53mM DCAA at TCAA-etched (magenta) and at HCl-etched (blue) Ag electrodes.*

The HCl-etched electrode was used as a reference to define whether DCAA detection is also possible using a different template in the etching procedure. Electrochemical detection of DCAA was carried out using CV, as previously reported in **section 4.4.3**, revealing once more a different behaviour for the two electrode surfaces (***Figure 4.11***). Indeed, the reduction of this analyte at TCAA-etched electrode resulted in two sharp and well-defined peaks, whereas the HCl-etched electrode showed broader and less resolved signals.

Figures 4.12 and **4.13** shows the signal registered in solution of DCAA at different concentration using TCAA- and HCl-etched silver electrodes, respectively. As already well evident from **Figure 4.11**, the curves obtained after blank-subtraction indicate that the TCAA-etched electrode provides the highest sensitivity and peak resolution, with well-defined reduction peak at -0.55 V and -0.88 V vs Ag/AgCl (***Figure 4.12***). Conversely, the HCl-etched electrode produces broader peaks centered at -0.6 V and -0.85 V (***Figure 4.13***).

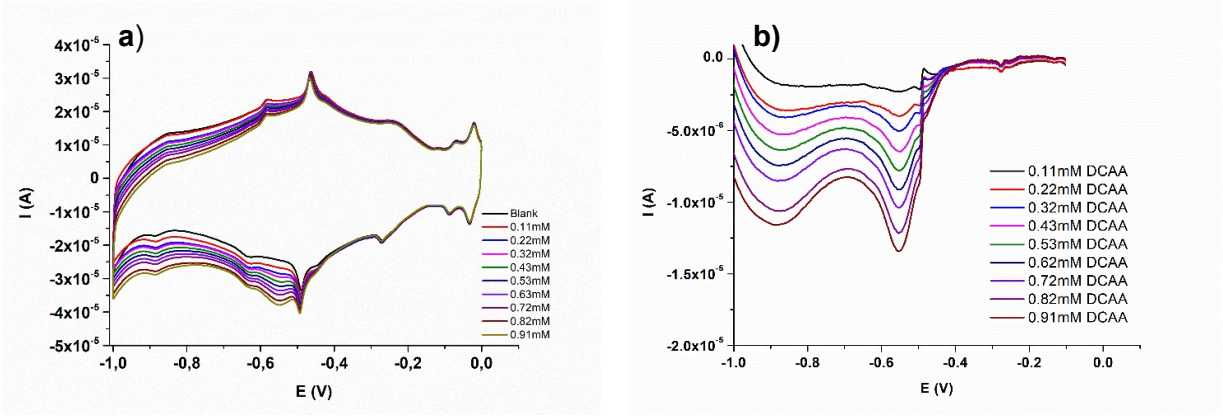

Figure 4.12) *Electrochemical responses recorded for DCAA reduction using TCAA-etched Ag electrodes. The panel presents (**a**) the CV responses recorded in 0.02 mol L^{-1} PBS (pH 6.8) in the potential ì from E_1=0.0 V to E_2= −1.2 V vs Ag/AgCl and scan rate of 20 $mV \cdot s^{-1}$; (**b**) reports only the forward responses subtracted by the blank signal.*

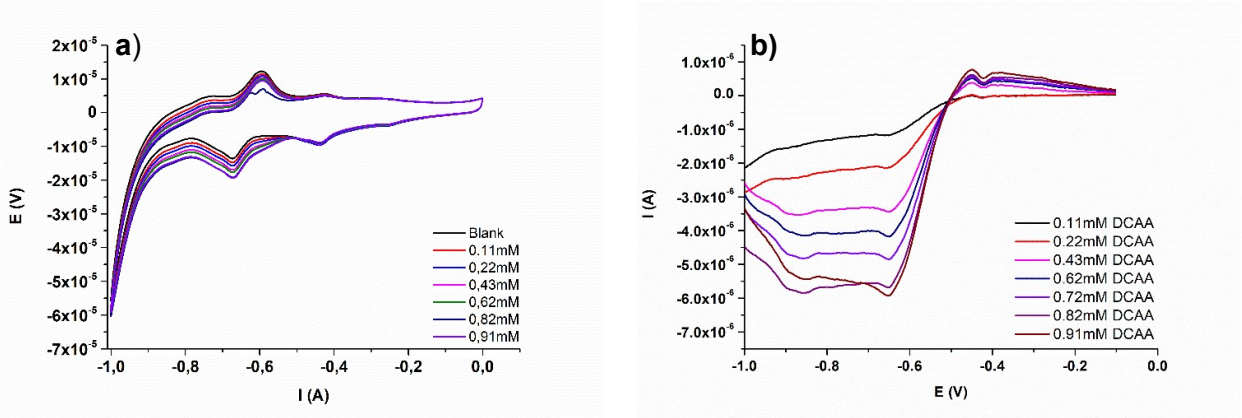

Figure 4.13) *Electrochemical responses recorded fro DCAA reduction using HCl-etched Ag electrodes. The panel presents (**a**) the CV responses recorded in 0.02 mol L^{-1} PBS (pH 6.8) in the potential window from E_1=0 V to E_2= −1.2 V vs Ag/AgCl and scan rate of 20 $mV \cdot s^{-1}$; (**b**) reports only the forward responses subtracted by the blank signal.*

The calibration data obtained from the responses shown and reported in **Table 4.8** further confirm that TCAA-etched electrode shows the highest sensitivity even for DCAA detection.

Table 4.8 *Values of slope, standard error, and R^2 obtained from the linear regression calculated from responses obtained in DCAA solutions.*

Electrode	***Peak potential (V)***	***Slope ($\mu A*mM^{-1}$)***	***Standard Error (μA)***	***R^2***
TCAA-etched	*E = -0.55*	*-13.7*	*0.212*	*0.99*
HCl-etched	*E = -0.64*	*-5.04*	*0.502*	*0.94*

The enhanced peak definition observed for DCAA reduction using the TCAA-etched electrode is quite surprising and suggests that the morphology of the surface obtained facilitates a more effective interaction with the HAA in solution, irrespectively to their exact chemical structure used. Notably, this possibility has never been previously explored [14] and would merit a deeper understanding of the etching process and of the morphology, thus, obtained.

4.4.5 Detection of MCAA using TCAA-Etched Silver electrode

The MCAA detection was carried out using only the TCAA etched electrode, as it showed the most promising performance. As shown in the voltammograms recorded in solution at different concentration (***Figure 4.14a***), no well-defined peaks are observed in this case despite subtracting the blank signal. However, plotting the current values obtained at potential value in which the reduction of MCAA is expected to occur (around -0.9 V vs Ag/AgCl), a calibration curve with reasonable linearity was obtained. This suggests that, despite the absence of a well-defined peak, the system is still capable of providing a quantitative response for MCAA detection. The observed behaviour may be attributed to the specific interaction between MCAA and the electrode surface, which differs from that of DCAA and TCAA.

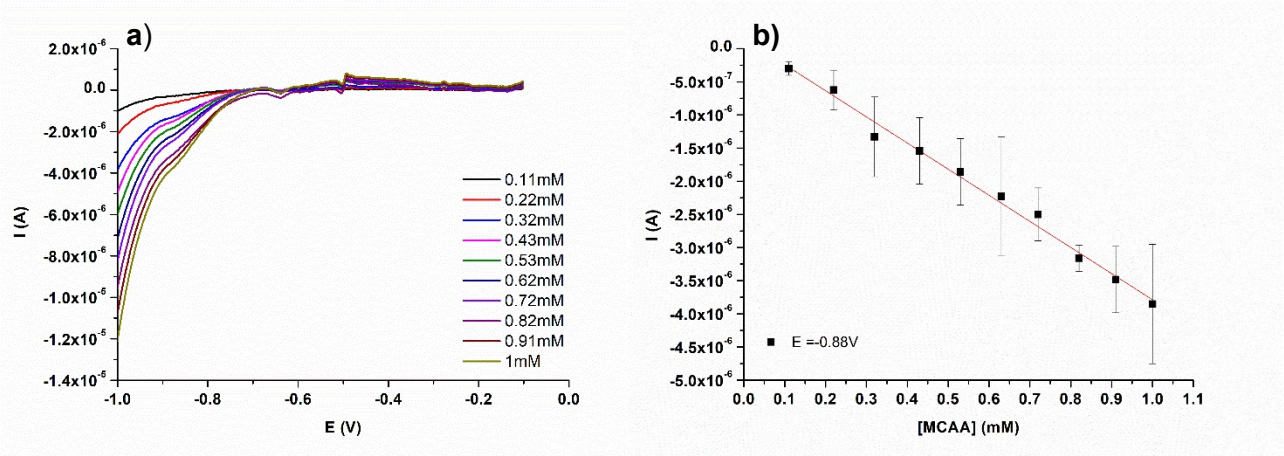

Figure 4.14*) a) Voltammetric responses recorded in MCAA solutions at different concentration (0.02 mol L^{-1} PBS - pH 6.8 after black subtraction) using TCAA etched Ag electrodes in the potential range from E_1=0 V to E_2= −1.2 V vs Ag/AgCl and scan rate of 20 mV·s^{-1}. (**b**) reports the relevant calibration plot obtained with the current values recorded at -0.9 V.*

Table 4.9 reports the calibration parameters for MCAA detection using the TCAA-etched Ag electrode. The reduction peak at -0.88 V exhibits a high R-square value, indicating good linearity; however, the lower slope compared to DCAA and TCAA suggests reduced sensitivity, likely due to the peak's poor resolution near the hydrogen evolution region, which further complicates its clear identification.

Table 4.9 *Performance indicators calculated for the calibration curve of MCAA obtained at -0.88 V for the TCAA-etched silver electrode.*

Peak potential (V)	***Slope ($\mu A*mM^{-1}$)***	***Standard Error (μA)***	***R^2***
-0.88 V	*-3.94*	*0.137*	*0.99*

Further evaluation of the electrochemical parameters involved in the surface modifications would improve sensitivity and peak resolution for MCAA determination, improving the overall performance of the detection system.

4.4.6 Limitations and Perspectives for the Practical Application of Electrodes Prepared via Etching in TCAA

Despite the advantages offered by TCAA-based etching in obtaining electrodes with a highly porous surface and increased electroactive area, the practical applicability of these electrodes remains limited due to several critical issues. The mechanical resistance of the obtained electrodes is extremely low, since the porous layer easily detaches from the surface after electrochemical measurements, making difficult the prolonged use. This aspect compromises the mechanical stability of the electrodes and limits the prolonged use, which are key factors for potential real-world implementation. To improve this aspect, we studied the effect of reducing the number of cycles for the etching procedure, so that the performance of TCAA-etched surfaces obtained from 20, 15, 10, and 5 cycles was evaluated. However, the mechanical stability resulted still poor and the progressive loss of material from the surface remained an issue suggesting that the surface morphology intrinsically weakens the silver structure, regardless of the intensity of the treatment. This notwithstanding, the peak resolution resulted still better that that observed for bare Ag surfaces.

Although the results reported here only represents a preliminary study, the performance observed appear insufficient for the application in real samples. Measurements conducted so far showed very low signal variation with respect to the background in solutions containing the analyte at the lowest concentration tested, namely at 0.11 mM, corresponding to 10, 14, and 18 mg L^{-1} for MCAA, DCAA, and TCAA, respectively. These thresholds are significantly higher than the concentrations

previously found in biological matrices, highlighting the need for different strategies to lower the detection limit. Since only CV measurements were performed, a more refined assessment of sensitivity would require the use of pulsed techniques, namely differential pulse or square wave.

In addition, further investigations must be planned to transfer this approach to portable devices, like screen-printed electrodes. In this respect, it must be underlined that preliminary investigation performed in the frame of the thesis with commercial Ag-electrodes showed heavy experimental issues probably due to redox active species present in the ink and covering the actual signal due to the analyte. In addition, the thickness of the Ag layer seemed too low, so that it is completely detached during the etching process. Further experiment directed to overcome all these issues are required to adapt the methodology for disposable electrodes, ensuring reproducibility and stability in biological matrices such as saliva.

Future studies could focus on the fabrication of silver electrodes through conductive ink printing, applying multiple layers until reaching a thickness sufficient to maintain electrical conductivity and resist the etching process without deterioration. In particular, the use of silver flake-based screen-printing inks could be explored to obtain electrodes with the desired mechanical and electrochemical properties. Other potential solutions to overcome these limitations could involve the introduction of post-etching treatments, such as controlled thermal annealing or deposition of protective layers, to preserve porosity while improving mechanical stability. Previous studies on modified electrodes for sensor applications have shown that integrating nanostructured layers, such as conductive polymer films or carbon-based nanocomposites, can enhance both sensitivity and operational durability. These considerations suggest that, although TCAA etching provides advantages in terms of increasing the active area, the current electrode configuration is not yet suitable for practical applications without significant modifications to the preparation parameters or the type of electrode used.

4.5 Conclusions

The analytical method developed for the analysis of HAAs, based on IC-ESI-MS/MS, was successfully applied for the analysis of urine and saliva samples of a smoker and two swimmers. The results obtained highlight several key findings that contribute to a deeper understanding of the effect of body exposition to chloro derivatives. In addition, this study contributed to the development of a new chromatographic method applicable to the analysis of complex biological samples without requiring extensive sample preparation. The simplicity of the dilution-based pretreatment proved advantageous in minimizing matrix effects while maintaining adequate sensitivity. This suggests that IC can be applied without complex extraction-based techniques. The method was found suitable to resolve complex mixtures of HAAs, ensuring clear differentiation between structurally similar compounds, and characterized by adequate detection limits for the analysis of these contaminants. Although some analytes exhibited slightly lower sensitivity than others, the overall method performance was considered satisfactory for practical applications. This highlights the potential of IC for routine analysis in clinical and toxicological studies. Additionally, our investigation revealed that the choice of eluent composition and column type played a crucial role in optimizing retention times and peak resolution. Fine-tuning these parameters allowed us to achieve a balance between separation efficiency and total run time, making the method both practical and time efficient. These findings provide a valuable reference for future analytical method development in this domain. Despite the promising results, some limitations must be acknowledged. First, the reliance on a dilution-based approach, while effective, may not be suitable for the detection of analytes at extremely low concentrations, where pre-concentration steps might still be necessary. Second, matrix effects, though reduced, could still pose challenges in samples with high variability in composition. Addressing these limitations through complementary analytical techniques or further refinements in sample preparation could enhance the robustness of the method.

The second part of the chapter was focused on the electrochemical detection of MCAA, DCAA, and TCAA using Ag electrodes modified through electrochemical etching. The electrochemical performances of the various electrodes were defined by recording voltammetric responses in solutions of the target analytes, demonstrating the superior performances imparted by the electrode pre-treatment in TCAA acid. This electrode allowed to record responses characterized by sharp and well-resolved peaks, leading

to best sensitivity with respect to further electrodes testes. This notwithstanding, the detection limits obtained remained relatively high (>0.11 mmol L^{-1}) if compared to the concentration values obtained in the biological fluids analysis by IC-ESI-MS/MS. In addition, the mechanical stability of the electrodes obtained resulted not optimal for subsequent analysis, despite various attempts to improve this issue. Future research activities should focus on alternative strategies to improve electrode robustness, such as incorporating protective coatings, optimizing etching parameters, or exploring alternative fabrication methods, including the use of disposable sensing platforms, like ink-jet or screen printed electrodes.

4.6 Materials and Methods

4.6.1 Development of an Ion Chromatography-Mass Spectrometry Method for Haloacetic Acid Detection

4.6.1.1 Reagents and Equipment

Monochloroacetic acid (MCAA), monobromoacetic acid (MBAA), dichloroacetic acid (DCAA), dalapon (DA), bromochloroacetic acid (BCAA), cloroiodoacetic acid (CIAA), dibromoacetic acid (DBAA), trichloroacetic acid (TCAA), bromodichloroacetic acid (BDCAA) were purshased from LGC Standard (Teddington, UK). Monochloroacetic acid-2-13C (MCAA-ISTD), monobromoacetic acid-1-13C (MBAA-ISTD), dichloroacetic acid-2-13C (DCAA-ISTD) and trichloroacetic acid-2-13C (TCAA-ISTD) were purchased from Thermo Fisher Scientific (Waltham, USA). Ultrapure water was produced using a Purelab Ultra System (Elga®, High-Wycombe, UK) (18.2 MΩ-cm, 1 ppb TOC). HPLC grade methanol (MeOH) was purchased from Merck KGaA (Darmstadt, Germany). Dionex OnGuard™ II Ag 1cc Cartridge (IC-Ag) were purchased from Thermo Fisher Scientific. Salivette® Cortisol, code blue were purchased from SARSTEDT AG & Co. KG (Sarstedt, Germany).

4.6.1.2 Sample processing, instrumental analysis and quality control

Urine and saliva samples were collected from donors affiliated with the University Ca' Foscari of Venice and subsequently stored at -80 °C. Saliva samples were obtained using Salivette® Cortisol. Each donor was instructed to place the swab in their mouth, typically in the cheek, for a duration of two minutes without chewing. If an insufficient amount of saliva was produced, the swab was left in the mouth for a longer period.

Following collection, the swab was placed inside its container, which was then sealed. Urine samples were stored in 50 ml polypropylene (PP) centrifuge tubes, while saliva samples were stored in the respective salivettes used for sampling. Validation was conducted using real urine and saliva samples from individuals who had not been exposed. Synthetic urine and saliva exhibited excessively high concentrations of salts, leading to the formation of an $AgNO_3$ precipitate following IC-Ag purification, which resulted in significant signal suppression. All plastic and glass laboratory equipment were meticulously cleaned twice using HPLC-grade MeOH prior to sampling or any laboratory use. All procedures were conducted under a fume hood to ensure safety. Biological samples were exclusively handled within a designated fume hood for biological sample treatment, which was thoroughly disinfected daily, both before and after sample processing.

4.6.1.3 Urine processing

Urine and saliva samples were placed at -20 °C the afternoon prior to the day of analysis and subsequently thawed at room temperature to mitigate excessive thermal shock. Once fully thawed, urine samples were centrifuged at 14,500 relative centrifugal force (rcf) for 5 minutes to separate protein particulates. A volume of 987.5 ml of supernatant urine was spiked with 12.5 µl of 10 µg ml^{-1} internal standard mix, resulting in a total of 125 ng, and achieving a final concentration of 125 ng ml^{-1} for each labeled internal standard (ISTD). A 120 µl aliquot of the spiked sample was then diluted to 3 ml with ultrapure water in a 4 ml glass vial, resulting in a 1:25 dilution and yielding an expected final ISTD concentration of 5 ng ml^{-1}. The IC-Ag cartridge and the PTFE filter were conditioned with 5 ml of MeOH, followed by 5 ml of ultrapure water. Samples were eluted through the conditioned Dionex OnGuard™ II Ag 1cc Cartridge for purification. The eluted urine was subsequently filtered through a conditioned 0.45 µm polytetrafluoroethylene (PTFE) filter (Biocomma, Guangdong, China) to remove any remaining particulate matter. A volume of 1 ml of the eluted sample was collected in a 1.5 ml autosampler vial and stored at -20 °C until analysis.

4.6.1.4 Saliva processing

Salivettes were centrifuged at 14,500 rcf for 3 minutes to extract liquid saliva from the swabs. This process pushed the saliva to the bottom of the salivette, facilitating easy collection. A volume of 250 µL of saliva was spiked with 20 µl of 1 µg mL^{-1} internal standard mix, resulting in a concentration of 20 ng mL^{-1} for each labeled internal

standard (ISTD). This spiked sample was then diluted with 730 µL of ultrapure water in a 1.5 ml autosampler vial, achieving a 1:4 dilution and an expected final concentration of ISTD of 5 ng mL^{-1}.

4.6.1.5 Instrumental analysis

Determination of HAAs was performed using a high-performance anion-exchange chromatography (HPAEC; Dionex™, Thermo Scientific™, ICS-6000, Waltham, USA) coupled to a Triple Quadrupole Mass Spectrometer (Thermo Scientific™, TSQ Altis™, Waltham, USA) using a heated-electrospray source (H-ESI) that operated in negative mode. Chromatographic separation was performed using an anion exchange column Dionex IonPac™ AS24 RFIC™ 2 × 250 mm (Thermo Scientific™) equipped with a guard column Dionex IonPac™ AG24 RFIC™ 2 × 50 mm (Thermo Scientific™).

Instrumental analysis, comprehending chromatographic method, mass spectrometer and source parameters, was conducted as previously described by Feltracco et Al 2024 [4]. Please refer to their publication for a comprehensive description of the method and its validation parameters.

Between each sample in the instrumental sequence of analysis, a washing run was executed, consisting in an ultrapure water analysis where the chromatographic gradient was set at 100 mM potassium hydroxide (KOH) for 30 minutes.

4.6.2 Preliminary investigation of an electrochemical sensor approach for Chloroacetic Acid detection

4.6.2.1 Reagents and Equipment

Silver wire (ϕ = 1 mm), Tricholoroacetic acid (TCAA), Dichloroacetic acid (DCAA) 99% purity and Chloroacetic acid (MCAA) 99% purity and Hydrochloric acid (HCl, 36%(w/w)) were purchased from Sigma Aldrich. Nitric Acid (65%) (HNO_3) was purchased from VWR Chemicals. Phosphate buffer solution (PBS, pH=6.84, 0.02 $mol \cdot L^{-1}$) was prepared with KH2PO4 and KOH and used as supporting electrolyte throughout electrochemical studies. Potassium dihydrogen phosphate and potassium hydroxide bought from Sigma Aldrich. All measurements were performed using an Metrohm Multi Autolab M204 potentiostat using Nova Software. The data were elaborated using Origin 9.0 software.

4.6.2.2 Electrodes preparation

The silver wire surface is mechanically polished using sandpaper P1000 purchased from Saitac, and subsequently immersed in deionized water and acetone and ultrasonically treated for 5 min. After the pretreatment operation, the etching of the silver wire electrode is carried out, as follows:

i) TCAA etching: 0.50 mol·L^{-1} TCA was used as the etchant, and silver wire, Pt electrode and Ag/AgCl reference electrode were placed in TCA solution to form a three-electrode system. Secondly, the silver wire was etched by cyclic voltammetry at 25 °C with a scan potential from −0.6 V to 1.0 V, scan rate of 50 mV·s^{-1} and 20 cycles. Finally, the silver wire was placed in a PBS solution prepared as reported in **section 4.6.2.1**. and electrochemically cleaned using chronoamperometry performed at E = -0.6V vs Ag/AgCl for t = 200s, in order to remove residual Cl^- on the electrode surface.

ii) HCl etching: same as point *i)* but with 7 cycles of etching cyclic voltammetry.

iii) HNO_3 etching: 0.1 mol·L^{-1} HNO_3 was used as the etchant, and silver wire, Pt electrode and Ag/AgCl reference electrode were placed in TCA solution to form a three-electrode system. Secondly, the silver wire was etched by cyclic voltammetry at 25 °C with a scan potential from −0.6 V to 1.0 V, scan rate of 50 mV·s−1 and 10 cycles.

iv) Control electrode was used as it is after simple mechanical cleaning followed by sonication.

4.6.2.3 Electrochemical measurement

Cyclic voltammetry was performed in PBS solution 0.02 mol L^{-1} pH 6.84 using an Autolab M204 potentiostat on with potential window range from E_1=0 V to E_2= −1.2 V vs Ag/AgCl and scan rate of 20 mV·s^{-1}, using a three-electrode cell with the hp-Ag film electrode as working electrodes, the platinum wire is used as the counter electrode, and the Ag/AgCl electrode is used as the reference electrode. The chronoamperometry was performed at E=−0.6 V. The detection performance analysis was conducted by different concentrations of TCA solutions added to the N_2-saturated 0.02 mol·L^{-1} PBS (6 mL, pH = 6.84).

References

[1] L. Wang, Q. Zhang, B. Chen, Y. Bu, Y. Chen, J. Ma, F.L. Rosario-Ortiz, Photolysis and photocatalysis of haloacetic acids in water: A review of kinetics, influencing factors, products, pathways, and mechanisms, J Hazard Mater 391 (2020). https://doi.org/10.1016/j.jhazmat.2020.122143.

[2] S.D. Richardson, T.A. Ternes, Water Analysis: Emerging Contaminants and Current Issues, Anal Chem 90 (2018) 398–428. https://doi.org/10.1021/acs.analchem.7b04577.

[3] U.S. Environmental Protection Agency (EPA), National Primary Drinking Water Regulations: Disinfectants and Disinfection Byproducts, 2018. https://www.epa.gov/dwreginfo/disinfectants-and-disinfection-byproducts (accessed February 24, 2025).

[4] M. Feltracco, E. Barbaro, G. Formenton, G. Mazzi, S. Striuli, C. Bragato, R. Piazza, C. Barbante, A. Gambaro, The disinfection by-products are in the air: Aerosol measurements in the urban area of Venice, Atmos Environ 318 (2024). https://doi.org/10.1016/j.atmosenv.2023.120224.

[5] C.-Y. Chen, S.-N. Chang, G.-S. Wang, Determination of Ten Haloacetic Acids in Drinking Water Using High-Performance and Ultra-Performance Liquid Chromatography-Tandem Mass Spectrometry, J Chromatogr Sci 47 (2009) 67–74. https://doi.org/10.1093/chromsci/47.1.67.

[6] J. Sanchís, P.E. Redondo-Hasselerharm, C.M. Villanueva, M.J. Farré, Non targeted screening of nitrogen containing disinfection by-products in formation potential tests of river water and subsequent monitoring in tap water samples, Chemosphere 303 (2022). https://doi.org/10.1016/j.chemosphere.2022.135087.

[7] A. Kanan, T. Karanfil, Formation of disinfection by-products in indoor swimming pool water: The contribution from filling water natural organic matter and swimmer body fluids, Water Res 45 (2011) 926–932. https://doi.org/https://doi.org/10.1016/j.watres.2010.09.031.

[8] T. Manasfi, B. Temime-Roussel, B. Coulomb, L. Vassalo, J.-L. Boudenne, Occurrence of brominated disinfection byproducts in the air and water of chlorinated seawater swimming pools, Int J Hyg Environ Health 220 (2017) 583–590. https://doi.org/https://doi.org/10.1016/j.ijheh.2017.01.008.

[9] H. Kausar, M. Abubakar, S. Habib Khan, B. Khalil, Halogenated Compounds and Carcinogenesis: An Integrative Review of Their Role and Therapeutic Options 1 Halogenated Compounds and Carcinogenesis: An Integrative Review of Their Role and Therapeutic Options, 2023.

[10] A. Rodgman, Environmental tobacco smoke, Regulatory Toxicology and Pharmacology 16 (1992) 223–244. https://doi.org/https://doi.org/10.1016/0273-2300(92)90003-R.

[11] M.J. Cardador, M. Gallego, Determination of haloacetic acids in human urine by headspace gas chromatography–mass spectrometry, Journal of Chromatography B 878 (2010) 1824–1830. https://doi.org/https://doi.org/10.1016/j.jchromb.2010.05.022.

[12] O. Kanoun, T. Lazarević-Pašti, I. Pašti, S. Nasraoui, M. Talbi, A. Brahem, A. Adiraju, E. Sheremet, R.D. Rodriguez, M. Ben Ali, A. Al-Hamry, A review of nanocomposite-modified electrochemical sensors for water quality monitoring, Sensors 21 (2021). https://doi.org/10.3390/s21124131.

[13] L. Yuan, L. Jiang, T. Zhang, G. Wang, S. Wang, X. Bao, G. Sun, Electrochemically synthesized freestanding 3D nanoporous silver electrode with high electrocatalytic activity, Catal. Sci. Technol. 6 (2016) 7163–7171. https://doi.org/10.1039/C6CY01174H.

[14] Y. Chu, X. Wang, L. Wang, Z. Chen, Y. Zhu, F. Zhao, Electroanalytical sensing of trichloroacetic acid based on activated self-supported porous silver wire prepared by voltammetric etching

with trichloroacetic acid as etchant, Journal of Electroanalytical Chemistry 921 (2022) 116601. https://doi.org/https://doi.org/10.1016/j.jelechem.2022.116601.

[15] Y. Cai, X. Long, Y.H. Luo, C. Zhou, B.E. Rittmann, Stable dechlorination of Trichloroacetic Acid (TCAA) to acetic acid catalyzed by palladium nanoparticles deposited on H2-transfer membranes, Water Res 192 (2021). https://doi.org/10.1016/j.watres.2021.116841.

[16] Y.H. Xu, H. Zhang, C.P. Chu, C.A. Ma, Dechlorination of chloroacetic acids by electrocatalytic reduction using activated silver electrodes in aqueous solutions of different pH, Journal of Electroanalytical Chemistry 664 (2012) 39–45. https://doi.org/https://doi.org/10.1016/j.jelechem.2011.10.010.

[17] G. Korshin, M. Yan, Electrochemical dehalogenation of disinfection by-products and iodine-containing contrast media: A review, Environmental Engineering Research 23 (2018) 345–353. https://doi.org/10.4491/eer.2018.054.

[18] A.J., Bard, L.R. Faulkner, Electrochemical Methods: Fundamentals and Applications, 2001. https://doi.org/10.1002/9780470727124.

Chapter 5: Conclusions

This thesis explores innovative analytical methodologies for the detection of emerging contaminants in biological fluids, focusing on pesticides and disinfection by-products. The growing concern over environmental pollutants and their potential effects on human health poses the necessity of developing accurate, cost-effective, and widely applicable detection methods. The methodologies proposed in this work address both fundamental analytical challenges and practical applications, contributing to the broader goal of environmental and public health protection.

The introductory chapter provides a comprehensive overview of the challenges associated with environmental contaminants and their impact on human health. The strength and limitations of traditional chromatographic methods in large-scale biomonitoring were highlighted, emphasizing the need to integrate rapid, cost-effective screening tools with high-sensitivity confirmatory techniques. While chromatographic methods remain the gold standard for the analysis of organic contaminants due to their precision and selectivity, their rutinary application is affected by high operational costs, time consuming procedures, and the need for specialized personnel. To overcome these drawbacks, a large number of chemical sensors are actually under study to obtain a more widespread analysis of many samples by portable and user-friendly devices. This notwithstanding, performances of these devices are often not suitable for the application sought, especially concerning the limit of detection that are required for the analysis of contaminants of emerging concern in biological fluids.

Overall, the experimental section of the various chapters highlights the dichotomy between these two analytical approaches: application of robust chromatographic lab techniques versus the use of portable sensor devices. In any case, new sustainable solutions were developed to overcome the issues related to the presence of interfering species present in the matrix, which complicate the transfer of analytical procedures from the analysis of water solutions to biological fluids.

Chapter 2 focused on the development of a low-cost, paper based electrochemical sensor platform for glyphosate detection in human urine. The innovative use of paper as a multifunctional material allowed effective sample pre-treatment to overcome the interference provided by the presence of uric acid in solution which affect the accuracy of the detection. The sensor device developed demonstrated promising results,

offering a practical alternative to conventional chromatographic analysis, although showing a fairly high limit of detection. The advantages of using paper-based platforms, especially concerning biodegradability, affordability, and adaptability for point-of-care applications, were highlighted, contributing to the ongoing efforts to design accessible and environmentally sustainable analytical tools.

The advantages in the use of paper-based devices were also highlighted in Chapter 3, where a novel sample pre-treatment approach for the protein removal was proposed. It is aimed to significantly reduce matrix interference, improving the performance of electrochemical sensors for biomarkers detection in urine samples. The proof-of-concept application of the paper strip for the quantification of free tryptophan demonstrated the effectiveness of the device for the analysis of real biological matrices, paving the way for broader applications in environmental and clinical analysis.

Chapter 4 addressed the issues related to the detection of HAAs in urine and saliva samples, employing both chromatographic and electrochemical techniques. The IC-ESI-MS/MS method developed proved to be a reliable tool for the quantification of these species in samples collected from smokers and swimmers, highlighting the efficiency of this modern hyphenated technique in real analytical problems. Concerning the development of portable devices for the quantification of these contaminants, the preliminary study still reported in this chapter provides new insights into the use of silver-based surfaces for their electrochemical detection. Despite the potential shown by TCAA-etched surfaces, the electrochemical detection still requires further optimization to improve the limit of detection required for a real application of these devices in real-world settings. This notwithstanding, this section provides important information concerning the importance of the study concerning the analyte-surface interaction for the development of an efficient sensor system.

Overall, this work highlights the importance of integrating sensor technologies with advanced sample preparation techniques to develop scalable, efficient, and environmentally friendly biomonitoring tools. The findings contribute to ongoing efforts to enhance pollutant detection and management, offering practical solutions that align with sustainability goals. Future research should focus on refining sensor performance, expanding target analyte detection, and integrating real-time data acquisition

technologies to further improve biomonitoring capabilities. Additionally, interdisciplinary collaborations between analytical chemists, environmental scientists, and healthcare professionals could facilitate the translation of these methodologies into real-world applications. The development of standardized protocols, regulatory frameworks, and field-deployable systems will be crucial for ensuring the long-term impact and adoption of these technologies in environmental and clinical settings.

Appendix A

Table A1 *Main organochlorine pesticides and their biochemical effects.*

Pesticide name	Chemical structure	Use	Intoxication symphtomps	Biochemical Effects on Human	Ref
GLY	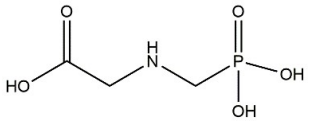	Her	Adominal cramps, anxiety, breathing difficulty, diarrhea, dizziness, headache, low blood pressure, kidney failure, slow heart rate	Genotoxicity, oxidative stress, acute or chrinic inflammatory sundromes, respiratory disease, neurotoxicity, estrogen disruptor,	[1,2]
AMPA	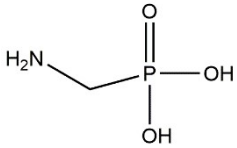	Her			
Malathion	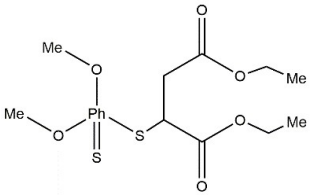	Her	Headache, dizziness, nausea, burning eyes, vomiting, bradycardia, miosis, lethargy	Oxidative stress, citotoxicity, genotoxicity (liver carcinoma), neurotoxicity, metabolic disorders, immunotoxicity, hepatotoxicity	[3,4]
Fenthion	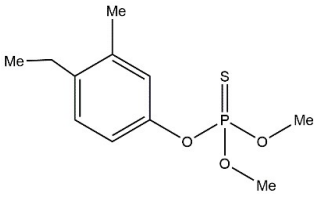	Her	Miosis, headache, nausea, vomiting, dizziness, muscle weakness, drowsiness, lethargy, anxiety, abdominal pain, diarrhea	N/D	[5]

Table A2. *Main Organophosphates pesticides and their biochemical effects*

Pesticide name	Chemical structure	Use	Intoxication symphtomps	Biochemical Effects on Human	Ref
DDE	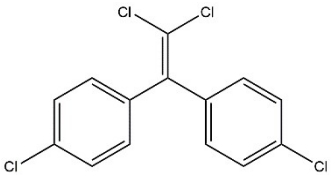	Ins	Tremors, seizures, headache, nausea, vomiting, dizziness	Prickling sensation of the mouth, lethargy, anorexia, anemia, muscular weakness, hyperexcitability, anxiety, and nervous tension	[6]
DDD	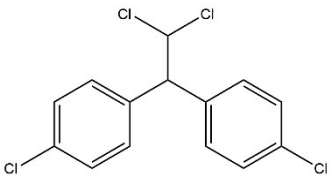	Ins			
DDT	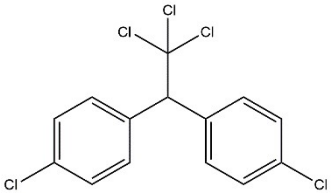	Ins			
Endosulfan	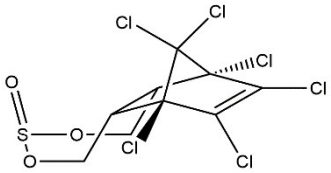	Ins	Excessive perspiration, nausea, vomiting, convulsions, headache, increased salivation, tremors, accelerated heartbeat, cyanosis of the lips	Genotoxic, reproductive, immological, neurotoxic	[7]
Aldrin	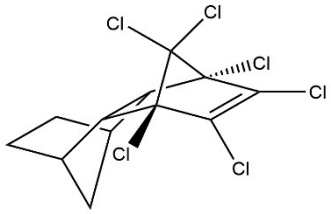	Ins	Nausea, vomiting, drowsiness, dyspnea, sweating, mild jerking, rise in blood pressure and convulsions	Neurotoxic, reproductive, developmental,immunological, genotoxic, tumerogenic effects, aplastic anemia	[8]
Dieldrin	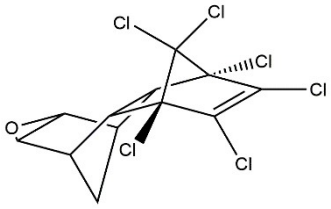	Ins			
Endrin	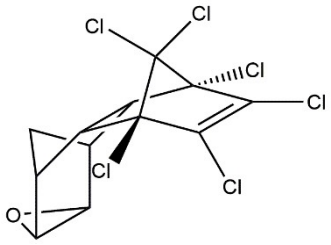	Ins	Jerking of arms and legs, twitching facial muscles, contraction, convulsion, fatty degeneration, lipid peroxidation	Neurological effects, convulsion, hepatic toxicity, diffuse organ damage,	

Table A3. *Main Carbammates pesticides and their biochemical effects.*

Pesticide name	Chemical structure	Use	Intoxication symphtomps	Biochemical Effects on Human	Ref
Carbofuran	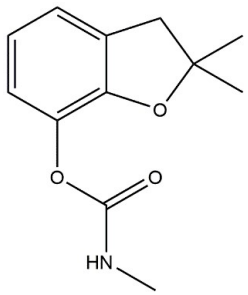	Ins	Profuse salivation, lacrimation, miosis, hypothermia, muscle twitches and fasciculations, body tremors, and convulsions	Neurotoxic, genotoxic, cytotoxic, mutagenic, reproductive, endrocrine disrupting, embryo-toxic and dermal skin problems	[9,10]
Propuxur	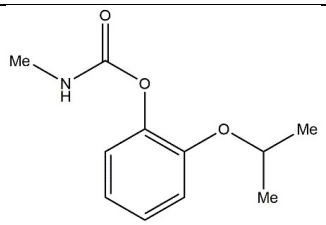	Ins	Headache, sweating, nausea, vomiting, diarrhea, muscle twitching, loss of coordination		
Carbaryl	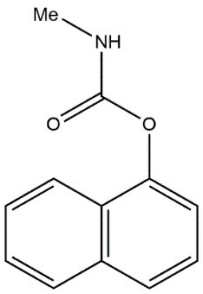	Ins			

Table A4. *Summary of six pesticides classes and their principal biochemical effects.*

Class	Pesticide Name	Principal biochemical effects	Ref
Phenylamides	**Carbanilates**: Barban, Carbetamide, Chlororprofan, Prophan, Phenyl Urea, Fenuron, Monuron, Diuron,Flumeturon, Chloroxuron, Neburon, Bromuron **Acylanalides**: Propanil, Dicryl, Karsil, Propachlor, Alachlor, Butachlor **Toluidines**: Trifluralin, Dipropanil, Benefin, Oryzalin, Isopropanil, Nitralin	Potential endocrine disruptors.	[11]
Pyrethroids	Allethrin, Bonthrin, Dimethrin, Tetramethrin, Ptrethrin, Cyclethrin, Furethrin,Fenevelerate, Alphamethrin, Decamethrin, Cypermethrin	Neurotoxic, temporary paresthesiaa, neurodevelopment, reproductive, immunological effects.	[12]
Triazines	Atrazine, Ametryn, Atratone, Chlorazine, Cynazine, Cyprazine, Metribuzin	Reproductive, developmental effects. Data on carginogenicity inconclusive. Poor data on human health effects in general.	[13]
Benzoic acid	Dicamba, Dichlorobenil, Chloroambin, Tricamba, Neptalan,Bromoxynil	Large oral doses may cause abdominal pain, nausea and vomiting, may cause urticaria, asthma, rhinitis and anaphylactic shock, possible liver, kidney and brain toxicant.	[14,15]
Pthalimides	Captan, Diflotan, Folpet	Not known on human, low toxicity in general	
Dipyrids	Paraquat, Diquat	Correlated to the onset of Parkinsons's disease.	[16]

Table A5 *This table summarizes the chemical formulas, regulatory classification, and known biocemical effects of various haloacetic ac*

HAA Name	Chemical Formula	Regulation Status	Biochemical Effects on Humans	Reference
Monochloroacetic Acid (MCAA)	$C_2H_3ClO_2$	Regulated (HAA5)	Oxidative stress, metabolic disruption, dermal absorption risk	
Dichloroacetic Acid (DCAA)	$C_2H_2Cl_2O_2$	Regulated (HAA5)	Genotoxicity, hepatotoxicity, oxidative stress, potential carcinogenicity	
Trichloroacetic Acid (TCAA)	$C_2HCl_3O_2$	Regulated (HAA5)	Liver toxicity, endocrine disruption, developmental toxicity	[17-19]
Monobromoacetic Acid (MBAA)	$C_2H_3BrO_2$	Regulated (HAA5)	Cytotoxicity, metabolic interference, dermal and inhalation absorption risks	
Dibromoacetic Acid (DBAA)	$C_2H_2Br_2O_2$	Regulated (HAA5)	Mutagenicity, carcinogenicity, increased oxidative damage	
Bromochloroacetic Acid (BCAA)	$C_2H_2BrClO_2$	Unregulated	Higher mutagenicity and toxicity compared to DCAA and TCAA	
Tribromoacetic Acid (TBAA)	$C_2HBr_3O_2$	Unregulated	Suspected carcinogen, potential endocrine disruptor	
Fluoroacetic Acid (FAA)	$C_2H_3FO_2$	Unregulated	Extremely toxic, inhibition of the citric acid cycle	[20-21]
Iodoacetic Acid (IAA)	$C_2H_3IO_2$	Unregulated	Enzyme inhibition, neurotoxicity	
Bromodichloroacetic Acid (BDCAA)	$C_2HBrCl_2O_2$	Unregulated	Potential toxicity, requires further study	
Dibromochloroacetic Acid (DBCAA)	$C_2HBr_2ClO_2$	Unregulated	Potential toxicity, requires further study	

Table A6 *Summary of the different chromatographic methods developed for pesticides analysis in different biological fluids.*

Analytes	Method	ME Evaluation	LOD	LOQ	Linear Range	Pretreatment	Sample	Ref
GLY, GLUF, PQ, DQ	LC-MS/MS	Y	BLOOD: 0.1 µg L^{-1} [PQ]; [GLY] 0.05 µg L^{-1} [DQ]; 0.01 µg L^{-1} [GLUF]; URINE: 0.1 µg L^{-1} [PQ]; [GLY]; [GLUF]; 0.05 µg L^{-1} [DQ]	BLOOD: 0.2 µg L^{-1} [PQ]; 0.1 µg L^{-1} [DQ]; [GLY]; [GLUF]; URINE: 0.2 µg L^{-1} [PQ]; [GLY]; 0.1 µg l^{-1} [DQ]; [GLY]	1-20 µg L^{-1}	Protein precipitation	Blood/Urine	[22]
DML, DEP, DMTP, DETP, DMDTP, DEDTP, GLY**	IC-MS/MS	Y	0.2 µg L^{-1}	0.8 µg L^{-1} [DEDTP]	N/D	Not needed	Urine	[23]
GLY, AMPA	GC-MS-MS	N	-	-	-	Derivatization	Urine	[24]
GLY, AMPA	LC-MS/MS	Y	0.023 µg L^{-1} [GLY]P; 0.038 µg L^{-1} [GLY]S; 0.033 µg L^{-1} [AMPA]P; 0.041 µg L^{-1} [AMPA]S	0.10 µg L^{-1} [GLY]; [AMPA]	0.0012 - 24 µg/mL	Dilution, I.S	Urine	[25]
PQ	UHPLC-HRMS	Y	0.5 ng mL^{-1}	1 ng mL^{-1}	1–1000 ng mL^{-1}	DBS	Blood	[26]
PQ, DQ	UPLC–MS/MS	Y	0.5 ng mL^{-1}	1 ng mL^{-1}	1–3000 ng mL^{-1}	I.S., centrifugation, dilution	Plasma/Urine	[27]

Analytes	Method	ME Evaluation	LOD	LOQ	Linear Range	Pretreatment	Sample	Ref
GLY, GLUF, AMPA, MPPA	LC-MS/MS	Y	0.02 µg L^{-1}	0.05 µg L^{-1}	0.05-5 µL	Diluition and Derivatization	Plasma/Urine	[28]
GLY, GLUF, AMPA, MPPA, BIALAPHOS	UPLC-MS/MS	Y	0.02 mg L^{-1} [GLYF]; [GLUF]; [AMPA], 0.01 mg L^{-1} [BIALAPHOS]; [MPPA]	0.05 µg L^{-1} [GLYF]; [GLUF]; [AMPA]; 0.03 µg L^{-1} [BIALAPHOS]; [MPPA]	0.05-5 mg L^{-1} [GLYF]; [GLUF]; [AMPA]; 0.03-5 mg L^{-1} [BIALAPHOS]; [MPPA]	SPE column (PRiME HLB)	Serum	[29]
GLY, PA*, CHLORATE, ETHEPHON, FOSETYL-Al, HEPA, MPPA	LC-MS/MS	Y	0.025 mg L^{-1} [PA]; [CHLORATE]; [GLY]; 0.01 mg L^{-1} [ETHEPHON]; [FOSETYL-Al]; [HEPA]; [MPPA]	0.05 mg L^{-1} [GLUF]	N/D	Modified QuPPe	Serum	[30]
GLY, AMPA	UHPLC-MS/MS	Y	0.003 mg L^{-1} [GLYF]; 0.001 mg L^{-1} [AMPA]	0.006 mg L^{-1} [GLYF]; 0.0025 mg L^{-1} [AMPA]	0.5-50 µg L^{-1} [GLYF]; 0.2-50 µg L^{-1} [AMPA]	CIPS combined with PTSPE	Urine	[31]
GLY, AMPA, N-Acetyl GLY/AMPA	microLC-MS/MS	Y	-	0.00005 mg L^{-1}	0.0122-50 µg L^{-1}	SPE	Plasma/Serum/Urine	[32]
GLY, AMPA	IC-MS/MS	N	0.0006 µg L^{-1} [GLYF]; 0.012 µg L^{-1} [AMPA]	0.002 µg L^{-1} [GLYF]; 0.004 µg L^{-1} [AMPA]	0.005-0.1 µg L^{-1}	Centrifugation + Eppendorf workup	Serum	[33]
Multiresidue	GC-MS-MS	N	0.01 µg mL^{-1}	0.01 ng mL^{-1}	0.01-2.0 mg L^{-1}	Modified QuEChERS	Blood/Urine	[34]

Table A7 *Summary of the some of the most relevant chromatographic methods developed for HAAs analysis in different biological fluids.*

Analytes	Method	ME Evaluation	LOD	LOQ	Linear Range	Pretreatment	Sample	Ref
TCAA, DCAA, MCAA	LC-MS/MS	Yes	0.5 ng mL^{-1}	N/D	N/D	SPE (Oasis HLB)	Urine	[35]
TCAA	HPLC-MS/MS	Yes	0.5 ng mL^{-1}	N/D	N/D	SPE (Oasis HLB), Isotope Dilution	Urine	[36]
TCAA, HAAs	IC-MS	No	0.6 ng L^{-1} (TCAA)	2 ng L^{-1} (TCAA)	5-100 ng L^{-1}	Centrifugation, Filtration	Plasma Serum	[20]
HAAs (9 species)	HS-GC-MS	Yes	0.01-0.1 µg L^{-1}	N/D	N/D	Liquid-liquid microextraction, derivatization	Urine	[37]
TCAA, HAAs	GC-MS (EPA 552.2)	Yes	2 µg L^{-1} (TCAA)	N/D	N/D	Methylation, Liquid-liquid extraction	Urine	[38]

Appendix A References

[1] G. Tóth, J. Háhn, J. Radó, D.A. Szalai, B. Kriszt, S. Szoboszlay, Cytotoxicity and hormonal activity of glyphosate-based herbicides, Environmental Pollution 265 (2020). https://doi.org/10.1016/j.envpol.2020.115027.

[2] C. Peillex, M. Pelletier, The impact and toxicity of glyphosate and glyphosate-based herbicides on health and immunity, J Immunotoxicol 17 (2020) 163–174. https://doi.org/10.1080/1547691X.2020.1804492.

[3] P.D. Moore, C.G. Yedjou, P.B. Tchounwou, Malathion-induced oxidative stress, cytotoxicity, and genotoxicity in human liver carcinoma (HepG2) cells, Environ Toxicol 25 (2010) 221–226. https://doi.org/10.1002/tox.20492.

[4] P.B. Tchounwou, A.K. Patlolla, C.G. Yedjou, P.D. Moore, Environmental Exposure and Health Effects Associated with Malathion Toxicity, in: Toxicity and Hazard of Agrochemicals, InTech, 2015. https://doi.org/10.5772/60911.

[5] P. Mahieu, A. Hassoun, R. van Binst, R. Lauwerys, Y. Deheneffe, Severe and prolonged poisoning by fenthion. Significance of the determination of the anticholinesterase capacity of plasma, Clin Toxicol 19 (1982) 425–432. https://doi.org/10.3109/15563658208992497.

[6] Klassen, Curtis D., Casarett and Doull's Toxicology: The Basic Science of Poisons , Ninth Edition, Ninth, 2019.

[7] R. Jayaraj, P. Megha, P. Sreedev, Review Article. Organochlorine pesticides, their toxic effects on living organisms and their fate in the environment, Interdiscip Toxicol 9 (2016) 90–100. https://doi.org/10.1515/intox-2016-0012.

[8] N. Sharma, D. Garg, R. Deb, R. Samtani, Toxicological profile of organochlorines aldrin and dieldrin: An Indian perspective, Rev Environ Health 32 (2017) 361–372. https://doi.org/10.1515/reveh-2017-0013.

[9] S. Mishra, W. Zhang, Z. Lin, S. Pang, Y. Huang, P. Bhatt, S. Chen, Carbofuran toxicity and its microbial degradation in contaminated environments, Chemosphere 259 (2020). https://doi.org/10.1016/j.chemosphere.2020.127419.

[10] C. Gupta, Invited review: Carbofuran toxicity ramesh, J Toxicol Environ Health 43 (1994) 383–418. https://doi.org/10.1080/15287399409531931.

[11] Y. Song, L. Li, C. Li, Z. Lu, X. Men, F. Chen, Evaluating the sensitivity and efficacy of fungicides with different modes of action against botryosphaeria dothidea, Plant Dis 102 (2018) 1785–1793. https://doi.org/10.1094/PDIS-01-18-0118-RE.

[12] S. Ferland, J. Côté, M. Ratelle, R. Thuot, M. Bouchard, Detailed Urinary Excretion Time Courses of Biomarkers of Exposure to Permethrin and Estimated Exposure in Workers of a Corn Production Farm in Quebec, Canada, Annals of Occupational Hygiene 59 (2014) 1152–1167. https://doi.org/10.1093/annhyg/mev059.

[13] S. Zhu, T. Zhang, Y. Wang, X. Zhou, S. Wang, Z. Wang, Meta-analysis and experimental validation identified atrazine as a toxicant in the male reproductive system, Environmental Science and Pollution Research 28 (2021) 37482–37497. https://doi.org/10.1007/s11356-021-13396-6/Published.

[14] A. Jabłońska-Trypuć, U. Wydro, L. Serra-Majem, E. Wołejko, A. Butarewicz, The analysis of bifenox and dichlobenil toxicity in selected microorganisms and human cancer cells, Int J Environ Res Public Health 16 (2019). https://doi.org/10.3390/ijerph16214137.

[15] E. Björklund, B. Styrishave, G.G. Anskjær, M. Hansen, B. Halling-Sørensen, Dichlobenil and 2,6-dichlorobenzamide (BAM) in the environment: What are the risks to humans and biota?, Science of the Total Environment 409 (2011) 3732–3739. https://doi.org/10.1016/j.scitotenv.2011.06.004.

[16] A. Safaei Asl, P. Dadashzadeh, Acute kidney injury in patients with paraquat intoxication; a case report and review of the literature, J Renal Inj Prev 5 (2016) 203–206. https://doi.org/10.15171/jrip.2016.43.

[17] U.S. Environmental Protection Agency, National Primary Drinking Water Regulations, (2024). https://www.epa.gov/ground-water-and-drinking-water/national-primary-drinking-water-regulations (accessed March 9, 2025).

[18] U.S. Environmental Protection Agency (EPA), National Primary Drinking Water Regulations: Disinfectants and Disinfection Byproducts, 2018. https://www.epa.gov/dwreginfo/disinfectants-and-disinfection-byproducts (accessed February 24, 2025).

[19] F.H. Frimmel, J.B. Jahnel, Formation of Haloforms in Drinking Water, in: A.D. Nikolaou (Ed.), Haloforms and Related Compounds in Drinking Water, Springer Berlin Heidelberg, Berlin, Heidelberg, 2003: pp. 1–19. https://doi.org/10.1007/978-3-540-44997-3_1.

[20] S. Parvez, J.L. Ashby, S.Y. Kimura, S.D. Richardson, Exposure characterization of haloacetic acids in humans for exposure and risk assessment applications: An exploratory study, Int J Environ Res Public Health 16 (2019). https://doi.org/10.3390/ijerph16030471.

[21] I.R. Schultz, J.L. Merdink, A. Gonza-Lez-Leon, R.J. Bull, Comparative Toxicokinetics of Chlorinated and Brominated Haloacetates in F344 Rats, 1999. http://www.idealibrary.com.

[22] Y.C. Tsao, Y.C. Lai, H.C. Liu, R.H. Liu, D.L. Lin, Simultaneous determination and quantitation of paraquat, diquat, glufosinate and glyphosate in postmortem blood and urine by LC-MS-MS, J Anal Toxicol 40 (2016) 427–436. https://doi.org/10.1093/jat/bkw042.

[23] A. Schütze, P. Morales-Agudelo, M. Vidal, A.M. Calafat, M. Ospina, Quantification of glyphosate and other organophosphorus compounds in human urine via ion chromatography isotope dilution tandem mass spectrometry, Chemosphere 274 (2021). https://doi.org/10.1016/j.chemosphere.2020.129427.

[24] A. Connolly, S. Koslitz, D. Bury, T. Brüning, A. Conrad, M. Kolossa-Gehring, M.A. Coggins, H.M. Koch, Sensitive and selective quantification of glyphosate and aminomethylphosphonic acid (AMPA) in urine of the general population by gas chromatography-tandem mass spectrometry, J Chromatogr B Analyt Technol Biomed Life Sci 1158 (2020). https://doi.org/10.1016/j.jchromb.2020.122348.

[25] P.K. Jensen, C.E. Wujcik, M.K. McGuire, M.A. McGuire, Validation of reliable and selective methods for direct determination of glyphosate and aminomethylphosphonic acid in milk and urine using LC-MS/MS, J Environ Sci Health B 51 (2016) 254–259. https://doi.org/10.1080/03601234.2015.1120619.

[26] D. Wen, Y. Yang, P. Xiang, F. Yu, F. Zheng, T. Liu, Y. Shi, X. Zhang, M. Dong, B. Cong, C. Ma, A novel approach for determination of paraquat based on dried blood spot (DBS) extraction and UHPLC-HRMS analysis, J Pharm Biomed Anal 159 (2018) 11–17. https://doi.org/10.1016/j.jpba.2018.06.040.

[27] Z. Mao, Y. Yu, H. Sun, W. Xie, H. Zhao, Q. Jiang, Y. Sun, Y. Cao, F. Chen, Development and validation of a sensitive and high throughput UPLC–MS/MS method for determination of paraquat and diquat in human plasma and urine: application to poisoning cases at emergency departments of hospitals, Forensic Toxicol 40 (2022) 102–110. https://doi.org/10.1007/s11419-021-00603-9.

[28] T. Ohara, T. Yoshimoto, Y. Natori, A. Ishii, A simple method for the determination of glyphosate, glufosinate and their metabolites in biological specimen by liquid chromatography/tandem mass spectrometry: an application for forensic toxicology, Nagoya J Med Sci 83 (2021) 567–587. https://doi.org/10.18999/nagjms.83.3.567.

[29] H. Guo, H. Wang, J. Zheng, W. Liu, J. Zhong, Q. Zhao, Sensitive and rapid determination of glyphosate, glufosinate, bialaphos and metabolites by UPLC–MS/MS using a modified Quick Polar Pesticides Extraction method, Forensic Sci Int 283 (2018) 111–117. https://doi.org/10.1016/j.forsciint.2017.12.016.

[30] R. López-Ruiz, R. Romero-González, A. Garrido Frenich, Simultaneous determination of polar pesticides in human blood serum by liquid chromatography coupled to triple quadrupole mass spectrometer, J Pharm Biomed Anal 190 (2020). https://doi.org/10.1016/j.jpba.2020.113492.

[31] D. Chen, H. Miao, Y. Zhao, Y. Wu, A simple liquid chromatography-high resolution mass spectrometry method for the determination of glyphosate and aminomethylphosphonic acid in human urine using cold-induced phase separation and hydrophilic pipette tip solid-phase extraction, J Chromatogr A 1587 (2019) 73–78. https://doi.org/10.1016/j.chroma.2018.11.030.

[32] N.P. Nørskov, S.K. Jensen, M.T. Sørensen, Robust and highly sensitive micro liquid chromatography–tandem mass spectrometry method for analyses of polar pesticides (glyphosate, aminomethylphosfonic acid, N-acetyl glyphosate and N-acetyl aminomethylphosfonic acid) in multiple biological matrices, J Chromatogr A 1605 (2019). https://doi.org/10.1016/j.chroma.2019.06.064.

[33] H. Zhang, X. Liu, Z. Huo, H. Sun, F. Zhang, B. Zhu, An ion chromatography tandem mass spectrometry (IC-MS/MS) method for glyphosate and amino methyl phosphoric acid in serum of occupational workers, Microchemical Journal 170 (2021). https://doi.org/10.1016/j.microc.2021.106614.

[34] S. Iqbal, M.M. Iqbal, M. Javed, A. Bahadur, S. Yasien, Najam-ud-din, A. Hurr, N. Ahmad, M. Raheel, G. Liu, Modified QuEChERS extraction method followed by simultaneous quantitation of nine multi-class pesticides in human blood and urine by using GC-MS, Journal of Chromatography B 1152 (2020) 122227. https://doi.org/https://doi.org/10.1016/j.jchromb.2020.122227.

[35] K. van Veldhoven, P. Keski-Rahkonen, D.K. Barupal, C.M. Villanueva, L. Font-Ribera, A. Scalbert, B. Bodinier, J.O. Grimalt, C. Zwiener, J. Vlaanderen, L. Portengen, R. Vermeulen, P. Vineis, M. Chadeau-

Hyam, M. Kogevinas, Effects of exposure to water disinfection by-products in a swimming pool: A metabolome-wide association study, Environ Int 111 (2018) 60–70. https://doi.org/10.1016/j.envint.2017.11.017.

[36] Z. Kuklenyik, D.L. Ashley, A.M. Calafat, Quantitative detection of trichloroacetic acid in human urine using isotope dilution high-performance liquid chromatography - Electrospray ionization tandem mass spectrometry, Anal Chem 74 (2002) 2058–2063. https://doi.org/10.1021/ac011250g.

[37] Y. Sun, Y.X. Wang, C. Liu, Y.J. Chen, W.Q. Lu, C. Messerlian, Trimester-specific blood trihalomethane and urinary haloacetic acid concentrations and adverse birth outcomes: Identifying windows of vulnerability during pregnancy, Environ Health Perspect 128 (2020) 1–10. https://doi.org/10.1289/EHP7195.

[38] W.-S. Zhou, L. Xu, S.-H. Xie, Y.-L. Li, L. Li, Q. Zeng, Y.-K. Du, W.-Q. Lu, Decreased birth weight in relation to maternal urinary trichloroacetic acid levels, Science of The Total Environment 416 (2012) 105–110. https://doi.org/https://doi.org/10.1016/j.scitotenv.2011.10.073.

Appendix B

Table B1: Chromatographic gradient for Ultimate 3000 Dionex.

Time (minutes)	Phase A%	Phase B%
0	100%	0%
5	100%	0%
10	50%	50%
12	0%	100%
19	0%	100%
21	100%	0%
28	100%	0%

Table B2 *Source parameters tested in the orbitrap. Final parameters are highlighted with an asterisk.*

Parameter	Values
Spray Voltage (kV)	2,5; 3,5; 4*
Sheet Gas Flow (mL/min)	30; 40; 50*;60
Aux Gas (mL/min)	5*;10
Sweep Gas (mL/min)	0*
In Column Flow (µl/min)	200*
Post Column MeOH Flow (µl/min)	0; 50*; 100
Ionization Temperature	180; 200*; 220; 350

Table B3 *Comparison of performance from different SPE tested*

Eluted Solution				
SPE	MBAA-ISTD	MCAA-ISTD	DCAA-ISTD	TCAA-ISTD
Strata	59000	209000	205000	12000
HLB	**56000**	**232000**	**189000**	**20000**
WAX	n/d	48000	n/d	n/d
C18	32000	47000	93000	12000
Loaded Solution				
SPE	MBAA-ISTD	MCAA-ISTD	DCAA-ISTD	TCAA-ISTD
Strata	n/d	37000	n/d	n/d
HLB	**18000**	**87000**	**6000**	**n/d**
WAX	n/d	48000	n/d	n/d
C18	164000	248000	495000	15000

MBAA-ISTD: mono bromo acetic acid internal standard; MCAA-ISTD: monochloro acetic acid internal standard; DCAA-ISTD: dichloro acetic acid internal standard; TCAA-ISTD: trichloro acetic acid internal standard

Glossary of Abbreviations and Acronyms

AChE = Acetylcholinesterase

AMPA = Methylphosphonic Acid, Glycine, Sarcosine

AgNPs = Silver Nanoparticles

Au-NPs = Gold Nanoparticles

BCAA = Bromochloroacetic Acid

BSA = Bovine Serum Albumin

CECs = Contaminants Of Emerging Concerns

CNTs = Carbon Nanotubes

CPE = Carbon Paste Electrodes

DBAA = Dibromoacetic Acid

DBPs = Disinfection By-Products

DCAA = Dichloroacetic Acid

DDT = Dichlorodiphenyltrichloroethane

DQ = Diquat

ECD = Electron Capture Detection

EEA = European Environment Agency

EIS = Electrochemical Impedance Spectroscopy

EPA = Environmental Protection Agency

ESI = Electrospray Ionization Process

EU = European Union

GC = Gas Chromatography

GLY = Glyphosate

GO = Graphite Oxide

HAAs = Haloacetic Acid

HILIC = Hydrophilic Interaction Liquid Chromatography

HPLC = High-Performance Liquid Chromatography

HRMS = High-Resolution Mass Spectrometry

HRP = Horse Radish Peroxidase

HS-GC-MS = Static Headspace Gas Chromatography-Mass Spectrometry

Hb = Hemoglobin

IC = Ion Chromatography

IC-ESI-MS/MS = Ion Chromatography-Electrospray Ionization Tandem Mass Spectrometry

ITO = Indium Tin Oxide

LC = Liquid Chromatography

LC-HRMS = LC-High Resolution Mass Spectrometry

LC-MS = Liquid Chromatography-Mass Spectrometry

LLE = Liquid-Liquid Extraction

LLME = Liquid–Liquid Microextraction

LODs = Limits of Detection

LOQ = Limit Of Quantification

MBAA = Monobromoacetic Acid

MCAA = Monochloroacetic Acid

MCL = Maximum Contaminant Level

ME = Matrix Effect

MIP = Molecularly Imprinted Polymer

MIPs = Molecularly Imprinted Polymers

MOFs = Metal-Organic Frameworks

MRLs = Maximum Residue Limits

MRM = Multiple Reaction Monitoring

MS = Mass Spectrometry

Mb = Myoglobin

NOM = Natural Organic Matter

NSA = Non-Specific Adsorption

OCPs = Organochlorines Pesticides

OPPs = Organophosphates Pesticides

PADs = Paper-Based Analytical Devices

PCBs = Polychlorinated Biphenyls

PEG = Polyethylene Glycol

PFAS = Polyfluoroalkyl Substances

POPs = Persistent Organic Pollutants

PPCPs = Pharmaceuticals And Personal Care Products

PQ = Paraquat

QuPPE = Quick Polar Pesticides Extraction

RGB = Red Green Blue

RGO = Graphene Oxide

SAMs = Self-Assembled Monolayers

SERS = Surface-Enhanced Raman Spectroscopy

SPE = Solid-Phase Extraction

SPE-CB = Screen-Printed Electrode modified using Carbon Black

SPEs = Screen-Printed Electrodes

SPME-GC-ECD = Headspace Solid-Phase Microextraction Gas Chromatography

SRM = Selected Reaction Monitoring

TBAA = Tribromoacetic Acid

TCAA = Trichloroacetic Acid

THMs = Trihalomethanes

TMB = 3,3’,5,5’-tetramethylbenzidine

UPLC-MS/MS = Ultra-Performance Liquid Chromatography

USA-DLLME = Ultrasound-Assisted Dispersive Liquid-Liquid Microextraction

WHO = World Health Organization